ISTANBUL TECHNICAL UNIVERSITY ★ GRADUATE SCHOOL OF SCIENCE ENGINEERING AND TECHNOLOGY

CLIMATOLOGIES OF SEVERE CONVECTIVE STORMS IN TURKEY, THEIR ENVIRONMENTS, AND THEIR IMPACTS

Ph.D. THESIS

Şeyda TİLEV TANRIÖVER

Meteorological Engineering Department

Atmospheric Sciences Programme

NOVEMBER 2016

ISTANBUL TECHNICAL UNIVERSITY ★ GRADUATE SCHOOL OF SCIENCE ENGINEERING AND TECHNOLOGY

CLIMATOLOGIES OF SEVERE CONVECTIVE STORMS IN TURKEY, THEIR ENVIRONMENTS, AND THEIR IMPACTS

Ph.D. THESIS

Şeyda TİLEV TANRIÖVER

Meteorological Engineering Department

Atmospheric Sciences Programme

Thesis Advisor: Prof. Dr. Mikdat KADIOĞLU
Thesis Co-advisor: Prof. Dr. David M. SCHULTZ

NOVEMBER 2016

İSTANBUL TEKNİK ÜNİVERSİTESİ ★ FEN BİLİMLERİ ENSTİTÜSÜ

TÜRKİYE ŞİDDETLİ KONVEKTİF FIRTINA KLİMATOLOJİLERİ, ÇEVRE KOŞULLARI VE ETKİLERİ

DOKTORA TEZİ

Şeyda TİLEV TANRIÖVER
(511092007)

Meteoroloji Mühendisliği Anabilim Dalı

Atmosfer Bilimleri Programı

Tez Danışmanı: Prof. Dr. Mikdat KADIOĞLU
Eş Danışman: Prof. Dr. David M. SCHULTZ

KASIM 2016

Şeyda Tilev Tanriöver, a Ph.D. student of İTU Graduate School of Science Engineering and Technology student ID 511092007, successfully defended the dissertation entitled "CLIMATOLOGIES OF SEVERE CONVECTIVE STORMS IN TURKEY, THEIR ENVIRONMENTS, AND THEIR IMPACTS", which she prepared after fulfilling the requirements specified in the associated legislations, before the jury whose signatures are below.

Thesis Advisor :	**Prof. Dr. Mikdat KADIOĞLU** İstanbul Technical University	.....
Co-advisor :	**Prof. Dr. David M. SCHULTZ** The University of Manchester	
Jury Members :	**Prof. Dr. Selahattin İNCECİK** İstanbul Technical University	.....
	Prof. Dr. Zafer ASLAN Istanbul Aydın University	.....
	Prof. Dr. Gürcan ORALTAY Marmara University	.....
	Prof. Dr. Sibel MENTEŞ İstanbul Technical University	.....
	Assoc. Prof. Hüseyin TOROS İstanbul Technical University	.....

Date of Submission : 31 August 2016
Date of Defense : 4 November 2016

To my family,

FOREWORD

This dissertation presents climatologies of severe convective storms in Turkey, their impacts and their environments. This is a comprehensive and up-to-date study and a pioneering effort for severe weather researh in Turkey. Hopefully, it will be followed by further studies, which is a very significant need for our region.

I have been kindly supported by TÜBİTAK 2214/A and İTÜ-BAP programs, and European Meteorological Society and European Severe Storms Laboratory awards during this research.

Along the journey of my Ph.D. I have been encouraged, inspired and supported by many people. Here, I would like to take this oppotunity to acknowledge them. First of all, I would like to express my deep gratitude to Professor Mikdat Kadıoğlu, my research supervisor, for his patient guidance and important support during my whole academic life ever since my undergraduate years. Professor David M. Schultz provided me with valuable and constructive suggestions during the planning and development of this research work. I am particularly grateful for his enthusiastic encouragement and useful critiques. I would like to offer my thanks to my committee members, Professor Selahattin Incecik, Professor Zafer Aslan and Professor Gurcan Oraltay, and Professor Yurdanur Unal, for their time, recommendations and comments. Special thanks should be given to Abdullah Kahraman, my dear colleague, for our improving disscussions and his technical supports. I would also like to extend my thanks to Dr. Abdullah Ceylan, observers working at meteorological stations, volunteers, the Turkish State Meteorological Service and the ESWD for the lightning, severe hail and severe non-tornadic winds related reports; the Turkish State Meteorological Service for thunderstorm days data; and Ronald L. Holle and Vaisala for the cloud-to-ground lightning data.

Finally, I wish to acknowledge the support provided by my family. I am greatly indebted to my parents, Türkan Tilev and Metin Tilev, my precious husband, Doğaç Tanrıöver, my sisters, Hülya Arıkan and Seniye Tilev, and Mahmut Arıkan for all they have done to make my studies possible. And my dear son, Alper Buğra Tanrıöver, thank you very much for enhancing my journey!

August 2016

Şeyda TİLEV TANRIÖVER
(Meteorologist - Lecturer)

TABLE OF CONTENTS

Page

ABBREVIATIONS

APR : April
AUG : August
BWD : Bulk Wind Difference
CAPE : Convective Available Potential Energy
CAPEN : Convective Inhibition Energy
CG : Cloud to Ground
CONUS : Contiguous United States
CIN : Convective Inhibition Energy
DEC : December
DMC : Deep Moist Convection
ECMWF : European Centre for Medium-Range Weather Forecasts
EM-DAT : Centre for Research on the Epidemiology of Disasters's Emergency Events Database
ESWD : European Severe Weather Database
FEB : February
Fig : Figure
GFS : The Global Forecast System
GIS : Geographic Information System
GLD : Global Lightning Dataset
ITCZ : Intertropical Convergence Zone
JAN : January
JUL : July
JUN : June
LCL : Lifting Condensation Level
LFC : Level of Free Convection
LST : Local Standard Time
LR7050 : Mid-tropospheric (700–500-hPa) Lapse Rate
MAR : March
MAY : May
MLCAPE : Mixed-Layer Convective Available Potential Energy
MLCIN : Mixed-Layer Convective Inhibition Energy
MLLCL : Mixed-Layer Lifting Condensation Level
MUCAPE : Most Unstable Convective Available Potential Energy
MUCIN : Most Unstable Convective Inhibition Energy
NARR : North American Regional Reanalysis
NCEP : (United States) National Centers for Environmental Prediction
NCAR : (United States) National Center for Atmospheric Research
NCL : NCAR Command Language
NOV : Novermber
OCT : October
PRWA85 : 1000–850 hPa Precipitable Water
SBCAPE : Surface-Based Convective Available Potential Energy
SBCIN : Surface-Based Convective Inhibition Energy
SBLCL : Surface-Based Lifting Condensation Level

SEP **:** September
SRH35 **:** 1000–350 hPa Storm Relative Helicity
SRH85 **:** 1000–850 hPa Storm Relative Helicity
TEFER **:** Turkey Emergency Flood and Earthquake Recovery
TSMS **:** Turkish State Meteorological Service
UK **:** United Kingdom
USA **:** United States of America
UTC **:** Coordinated Universal Time
WRF **:** Weather Research and Forecasting Model

SYMBOLS

T	**:** Temperature
T_d	**:** Dew point temperature
h	**:** Hour
min	**:** Minute
Γ_{dew}	**:** Dew point lapse rate
Γ_d	**:** Dry adiabiatic lapse rate
h_{LCL}	**:** Height of the LCL

LIST OF TABLES

Page

LIST OF FIGURES

Page

CLIMATOLOGIES OF SEVERE CONVECTIVE STORMS IN TURKEY, THEIR ENVIRONMENTS, AND THEIR IMPACTS

SUMMARY

Severe convection is responsible for many hazardous events such as large hail, tornadoes, severe non-tornadic winds, heavy rainfalls and lightnings. These events cause loss of lives and damage to property in Turkey. Considering their effects on life and property and the global increasing trends of them, both short range probabilistic forecasting and nowcasting of these local storms are significant, however challenging issues. Defining the spatial and temporal distributions of these events is a prerequisite for understanding and predicting the environmental conditions that are favorable for them. In other words, knowledge on geographical, seasonal and daily distribution of severe convective storms is an essential need for improving abilities of forecast society.

This thesis contributes the building of 'Storm Data of Turkey' as its first step. Convective storms are local scale events. Because of their small scales, conventional observational networks are not capable to catch all of them. Therefore, creating a storm database requires too much effort and collaborative working. Many parties, such as meteorological service observers, voluntary observer networks, and general public take part in reporting of these storms. Official records, newspapers and news agency archives, social media are good sources for collecting these reports. This dissertation presents report-based climatologies of severe convection related events, specifically severe hail and severe non-tornadic winds in Turkey.

The severe hail climatology part of the reseach shows that severe hail (≥1.5 cm) is observed to be associated with a variety of thunderstorm types in Turkey and can occur in any season of the year. However, very large (≥4.5 cm) hail is usually associated with supercell storms. All parts of the country are vulnerable. The largest hailstones exceed 5 cm in diameter and approach 1 kg in mass. Severe hail in Turkey is most likely in May and June, especially in interior parts of the country. Severe hail is least likely in the winter, though when it occurs in winter, it is most likely along the southern and western coasts. The afternoon and early evening hours are the most favorable time of the day for severe hail.

Seasonal and monthly distribution of severe nontornadic convective wind events shows that although the big portion of this events (51%) occur in summer they can occur in any time of year. They are most frequent in June, 33% of all events occurred in this month and 15% in September. According to the reports including storm duration information, only two of them were longer than six hours and most of them continued for 1 to 3 hours (42%).

Second outcome of this research is on the impacts of severe convective storms on society. A dataset covering January 1930 to June 2014 on lightning related fatalities and injuries in Turkey is created. There were 745 incidents, resulting in 898 deaths, 150 serious injuries and 536 injuries during this period. The total number of fatalities was 31 in 2012, 26 people in 2013 and 25 people in 2014. With a Turkish population

of around 73.7 million, the number of fatalities were 0.42 per million in 2012, 0.35 per million in 2013 and 0.34 per million in 2014 (January–June). The total number of human injuries was 36 in each of 2012 and 2013, and 62 in 2014. Considering the population, the rate of injuries was 0.49 per million in each of 2012 and 2013, and 0.84 per million in 2014 (January–June). Incidents were most frequent in late spring all around Turkey and were rare during winter. The majority of lightning incidents occurred during the afternoon, with fewer occurring at night. The number of incidents was higher over the highly populated western parts, especially in Istanbul and relatively lower in central and eastern Turkey. Geographical, annual and diurnal distributions of the incidents were comparable to thunderstorm and lightning observations, as well as with the report-based severe weather climatologies for Turkey. The risk of being struck by lightning was highest for the people participating outdoor activities such as farming and shepherding. The number of male victims was nearly twice the number of female victims. Almost all of the incidents occurred in rural areas. The number of victims under trees is a sign of the need for awareness campaigns.

Report-based datasets are primary sources for severe convective storm climatologies. However, they have some disadvantages. Observations of hazardous, convection related local scale phenomena such as severe hail, tornadoes and damaging winds have a subjective nature. They are critically sensitive to some parameters such as population density differences, time of the day of occurrence and reporting issues (e.g., subjective estimation of wind speed by non-expert human observers and alike). Due to subjective nature of their observations, regional climatology, temporal variability and trends of these phenomena have been difficult to be defined properly (e.g., Diffenbaugh et al. 2008). Thus, climate change assessments have avoided from certain judgments about the effects of anthropogenic global warming on current and future variability of these phenomena (e.g., Intergovernmental Panel on Climate Change 2007). Usage of numerical models is an alternative method to get rid of mentioned disadvantages of report-based climatologies. Spatial analysis of environmental controls such as CAPE (convective available potential energy) and vertical wind shear on the global reanalysis data shows that there is a significant similarity between distribution of observed severe convective storms and these environmental controls (Brooks et al., 2003; Romero et al., 2007; Gensini and Ashley, 2011).

In this thesis, an objective climatology of severe convective storm environments is established. Various environmental parameters associated with severe convective storms were calculated for a domain covering Europe, Middle East and North Africa for the 35-year period of 1979–2014 using ERA-interim data. Specifically, surface-based convective available potential energy (SBCAPE), mixed-layer (lowest 500m) convective available potential energy (MLCAPE), most unstable convective available potential energy (MUCAPE), surface-based convective inhibition energy (SBCIN), mixed-layer (lowest 500m) convective inhibition energy (MLCIN), most unstable convective inhibition energy (MUCIN), surface-based lifting condensation level (SBLCL), mixed-layer (lowest 500m) lifting condensation level (MLLCL), 0–6 km wind shear, 0–3 km wind shear, 0–1 km wind shear and mid-tropospheric (700–500-hPa) lapse rate (LR7050) were calculated. Previous research shows that, individual parameters did not discriminate well between severe and non-severe deep moist convection. Considering instability and shear together improves discrimination sharply (e.g., Davies and Johns 1993, Johns et al., 1993, Craven and Brooks 2004, Gensini and Ashley 2011). Therefore, proxy distribution of severe convective storms is enquired with the help of a parameter based on product of MLCAPE and deep layer shear. Results shows that the ITCZ, Mediterranean Sea, Red Sea and Arabian clearly

exerts a dominating influence on the CAPE distribution patterns over the domain. Influence is not limited to directly over the seas but is noted over the coasts of these seas. Seasonal cycle of CAPE fields is very clearly defined with larger values during summer than in the winter for all over the domain. For the transition seasons, CAPE values are higher in autumn than spring over Mediterranean, Red and Arabian Seas and neighboring countries as expected. After peak summer insolation, these large water bodies remain warm for several weeks and perform as intense heat and moisture sources. This effect is slightly visible over southern parts of Black Sea and Caspian Sea due to lower insolation, related with their higher latitudes. With the strengthening of the jet stream during winter, the highest average 0–6 km wind shear values occur beneath the jet regions. Overlapping of ingredients seems most probable during spring over a zonal belt including southern Europe, northern Africa and Turkey. Another finding is large 0–1 km wind shear values over the Arabian Sea and Somalia from June to September, related to the Somalia low-level jet. This region is notable considering the extreme SBCAPE values available at that time of the year together with these large wind-shear values. Seasonal and geographical distributions of the environments over Turkey are compatible with report-based severe weather climatologies of Turkey. The long-term variations in severe convective storm environments are worthy of future study.

TÜRKİYE ŞİDDETLİ KONVEKTİF FIRTINA KLİMATOLOJİLERİ, ÇEVRE KOŞULLARI VE ETKİLERİ

ÖZET

Şiddetli konvektif fırtınalar, iri taneli dolu, hortum, şiddetli doğrusal rüzgârlar, şiddetli yağışlar ve yıldırımlar gibi pek çok zarar verici hadisenin kaynağıdır. Bu hava olayları dünyanın pek çok yerinde olduğu gibi ülkemizde de can ve mal kayıplarına neden olmaktadırlar. Küresel ölçekte artış gösteren sayıları ve neden oldukları can ve mal kayıpları nedeniyle şiddetli konvektif fırtınaların hem kısa vadeli olasılıksal tahminleri, hem de anlık tahminleri (nowcasting) oldukça önemlidir. Bu hadiselerin mevsimsel ve coğrafi dağılımlarının belirlenmesi, onları oluşturan çevre koşullarının anlaşılması ve tahmin edilebilmeleri için gerek şarttır. Başka bir deyişle, bu hadiselerin tahminlerinin iyileştirilebilmesi için öncelikle coğrafi, mevsimsel ve günlük dağılımlarını içeren veri setleri oluşturulmalıdır.

Bu tez, öncelikli olarak "Türkiye Şiddetli Konvektif Fırtına Veri Tabanı"nın oluşturulmasına katkı sağlamaktır. Konvektif fırtınalar lokal ölçekleri nedeniyle genellikle geleneksel gözlem ağları tarafından yakalanamamaktadırlar. Bu nedenle hadiselerin oluşumlarının hangi bölgelerde yoğunlaştığını, hangi sıklıkta, hangi şiddette meydana geldiklerini, günlük ve mevsimlik dağılımlılarını belirlemek oldukça zordur. Dünyada şiddetli konvektif fırtına veri tabanlarının ve klimatolojilerin oluşturulmasının çok bileşenli ve kapsamlı çalışmalar olduğu görülmektedir. Bu hadiselere ait raporların tutulmasında başta meteoroloji birimlerinde çalışan gözlemciler olmak üzere, gönüllü meteorolojistler, medya muhabirleri gibi birçok bileşen rol oynamaktadır. Bu raporların toplanması için gazete ve haber ajansı arşivleri, sosyal medya gibi pek çok kaynaktan yararlanılabilmektedir. Bu araştırma kapsamında Türkiye iri taneli dolu ve şiddetli doğrusal rüzgâr klimatolojileri oluşturulmuştur. Tükiye'deki iri taneli dolu (≥1,5 cm) hadiselerinin farklı tipteki konvektif fırtınalarla ilişkili olduğu ve yılın her mevsiminde gözlemlenebileceklerini görülmüştür. Çok iri taneli dolu (≥4,5 cm) hadiseleri ise genellikle süperhücre fırtınaları ile ilişkilidirler. Coğrafi dağılımları ele alındığında ülke genelinde her yerde bu hadiselere rastlanabilmekle birlikte bazı küçük bölgesel farklılıklar dikkat çekmektedir. Örneğin, kış aylarında ülke genelinde seyrekleşen dolu hadiselerinin Akdeniz ve Ege kıyılarındaki frekansları nispeten yüksek kalmaya devam ettmektedir. Aylık dağılımlarına bakıldığında ise hadiselerin Mayıs ve Haziran aylarında iç ve özellikle doğu kesimlerde sıklıkla oluştukları görülmektedir. Ayrıca, öğleden sonra ve ikindi vakitleri iri taneli dolu oluşumunun en sık görüldüğü zaman dilimleridir. Şiddetli doğrusal rüzgârların büyük bir kısmı ise, yaz aylarında oluşmakla beraber bu hadiseler yılın her ayında gözlemlenebilmektedirler. En sık oluştukları ay Haziran ayı olarak belirlenmiştir. Fırtına süresi bilgisi içeren raporlar göstermektedir ki şiddetli doğrusal rüzgârların büyük bir kısmı 1 ila 3 saat arasında sürmektedir.

Çalışmanın ikinci kısmı şiddetli konvektif fırtınaların toplum üzerindeki etkisine ilişkindir. Çalışma kapsamında Ocak 1930 ve Haziran 2014 yılları arasında Türkiye'de gerçekleşen yıldırıma bağlı ölüm ve yaralanmalara ait bir veri seti oluşturulmuştur.

Veri seti, 898 ölüm, 150 ağır yaralanma ve 536 yaralanma ile sonuçlanan 745 olay içermektedir. Veri setinin homojen olmaması, geçmiş dönemler ve günümüz için raporlama ve mevcut raporların ulaşılabilirliği gibi farklılıklar nedeniyle uzun dönem ortalamalar anlamlı bilgi verememektedir. Geçmiş dönemdeki hadise sayısının azlığı büyük oranda elde edilebilen rapor sayısındaki azlıktan kaynaklanmaktadır. Son yıllara ait veriler ise şöyledir: 2014 yılı ölü sayısı (Ocak–Haziran) 25, yaralı sayısı 62; 2013 yılı ölü sayısı 26, yaralı sayısı 36; 2012 yılı ölü sayısı 31, yaralı sayısı 36. Yaklaşık nüfusu 73,7 milyon olan Türkiye için yıldırıma bağlı ölüm sayıları 2014 (Ocak- Haziran) için milyonda 0,34; 2013 için milyonda 0,35 ve 2012 için milyonda 0,42 olarak belirlenmiştir. Yaralı sayıları ise sırasıyla milyonda 0,86; milyonda 0,49 ve milyonda 0,49 şeklindedir. Yıldırma bağlı ölüm ve yaralanmaların ülke genelinde en sık görüldüğü dönem bahar sonu ve en az görüldüğü dönem ise kış aylarıdır. Gün içinde gerçekleşme saatlerine bakıldığında olayların büyük çoğunluğunun öğleden sonra, çok küçük bir kısmının da gece gerçekleştiği görülmektedir. Toplumun yıldırımdan en çok etkilenen kesimini tarım ve hayvancılık gibi açık hava faaliyetlerine katılanlar oluşturmaktadır. Olayların çoğu kırsal kesimde gerçekleşmiştir. Ayrıca erkek kurbanların sayısı kadın kurbanların sayısının neredeyse iki katıdır. Ağaç altında gerçekleşen ölüm ve yaralanmaların çokluğu toplumun yıldırımdan korunma yöntemleri konusunda bilinçsiz olduğunu göstermektedir.

Rapora dayalı veri setleri şiddetli konvektif fırtına klimatolojileri için birincil kaynak olmakla birlikte bazı dezavantajlara sahiptirler. Konveksiyon kaynaklı zarar verici, iri dolu, hortum, şiddetli rüzgâr gibi hava hadiselerinin gözlemleri genellikle sübjektiftir. Nüfus dağılımındaki farklılıklar, günün hangi saatinde oluştukları ve raporlanmalarına ilişkin birçok parametreden şiddetle etkilenmektedirler. Bu nedenle bu hadiselerin bölgesel klimatolojilerinin oluşturulması, zaman içindeki değimleri, trendleri hakkında yargıya varmak oldukça güçtür (örn. Diffenbaugh vd. 2008). Bu konularda yorum yapabilmek için objektif yöntemlerle klimatoloji oluşturulması gerekmektedir. Dünyada objektif konvektif fırtına klimatolojilerinin oluşturulmasında reanaliz verilenin kullanıldığı görülmektedir. Daha önce yapılmış olan çalışmalar, şiddetli konvektif fırtınalar ve onlara ilişkin CAPE (Convective Available Potential Energy) ve düşey rüzgâr kayması gibi çevresel parametrelerin dağılımları arasında güçlü bir benzerlik olduğunu göstermektedir (örn. Brooks vd. 2003, Romero vd. 2007, Gensini ve Ashley 2011).

Bu araştırmanın son aşaması olarak objektif bir şiddetli konvektif fırtına çevre koşulları klimatolojisi oluşturulmuştur. Bu klimatolojide 1979–2014 periyodu için mevcut olan ECMWF ERA-interim verisi kullanılmıştır. Klimatoloji yalnız Türkiye için değil, Avrupa, Orta Doğu ve Kuzey Afrika'yı içeren bir domain için üretilmiştir. Surface-based Convective Available Potential Energy (SBCAPE), Mixed-layer Convective Available Potential Energy (MLCAPE), Most Unstable Convective Available Potential Energy (MUCAPE), Surface-based Convective Inhibition Energy (SBCIN), Mixed-layer Convective Inhibition Energy (MLCIN), Most Unstable Convective Inhibition Energy (MUCIN), Surface-based Lifting Condensation Level (SBLCL), Mixed-layer (lowest 500m) Lifting Condensation Level (MLLCL), 0–6 km wind shear, 0–3 km wind shear, 0–1 km wind shear ve orta troposferik (700–500- hPa) lapse rate (LR7050) değerleri domain içerisindeki tüm grid noktalarında 35yıl için hesaplanmıştır. Ayrıca kompozit parametrelerin şiddetli konvektif fırtınaları tespit etmedeki başarısının müstakil parametreler karşındaki üstünlüğü bilindiğinden (örn. Davies ve Johns 1993, Johns vd. 1993, Craven ve Brooks 2004, Gensini ve Ashley 2011) MLCAPE ve 0–6 km wind shear çarpımlarına dayalı bir parametre yardımıyla şiddetli konvektif fırtınalarının bu coğrafyadaki proxy dağılımları incelenmiştir. Bölge

üzerindeki CAPE dağılım paternlerinde ITCZ, Akdeniz, Kızıl Deniz ve Umman Denizi'nin yoğun etkisi görülmektedir. Bu etki sadece denizler üzerinde sınırlı kalmayıp, bu denizlere kıyısı olan karalar üzerinde de gerçekleşmektedir. CAPE değerlerinin mevsimsel salınımı çok belirgin bir döngü sergilemektedir. En yüksek CAPE değerleri yazın, en düşük CAPE değerleri ise kışın mevcuttur. Geçiş mevsimlerine bakıldığında CAPE değerlerinin Akdeniz, Kızıl Deniz, Umman Denizi ve çevrelerinde sonbaharda ilkbahara oranla daha yüksek olduğu görülür. Bu büyük su kütleleri yazın gerçekleşen maksimum seviyedeki güneşlenmenin ardından haftalarca sıcak kalarak sonbaharda bölge için önemli bir ısı ve nem kaynağı teşkil eder ve yüksek CAPE değerlerine neden olurlar. Bu etki, yüksek enlemlerinden dolayı yazın daha az ısınan Karadeniz ve Hazar Denizi'nin güney kesimlerinde de az da olsa görülür. En yüksek 0–6 km rüzgâr kayması değerleri ise kuvvetlenen jet rüzgârlarına bağlı olarak kış aylarında jeti takip eden bir kuşak üzerinde görülür. Domain içerisinde şiddetli konvektif fırtına oluşumu için en önemli bileşenleri teşkil eden yüksek CAPE değerleri ve yüksek rüzgâr kayması değerlerinin kesişiminin gerçekleşmesinin en muhtemel olduğu dönem bahar ayrında ve Güney Avrupa, Kuzey Afrika ve Türkiye'yi içeren zonal bir kuşak üzerindedir. Somali ve Umman Deniz'i üzerinde Haziran'dan Eylül'e kadar gözlemlenen ve Somali aşağı seviye jeti ile ilişkili olan ekstrem 0–1 km rüzgar kayması değerleri aynı aylarda bölgede gözlemlenen yüksek CAPE değerleri düşünüldüğünde oldukça dikkat çekicidir. Ayrıca, konvektif fırtına çevre koşullarının mevsimsel ve coğrafi dağılımlarının Türkiye hortum ve iri taneli dolu klimatolojileri ve mevcut gök gürültülü fırtına gözlemleri ile oldukça uyumlu olduğu görülmektedir.

1. INTRODUCTION

According to the Centre for Research on the Epidemiology of Disasters's Emergency Events Database (EM-DAT, 2012) natural disasters have been increasing in frequency and becoming more hazardous worldwide over the last 50 years. The International Database reports indicate that the number of reported natural disasters was about 30 per year in the 1950s and more than 400 per year since 2000. Furthermore, the number of people affected by such disasters has risen from about 25 million per year in the 1960s to around 300 million per year since 2000 (Figure 1.1).

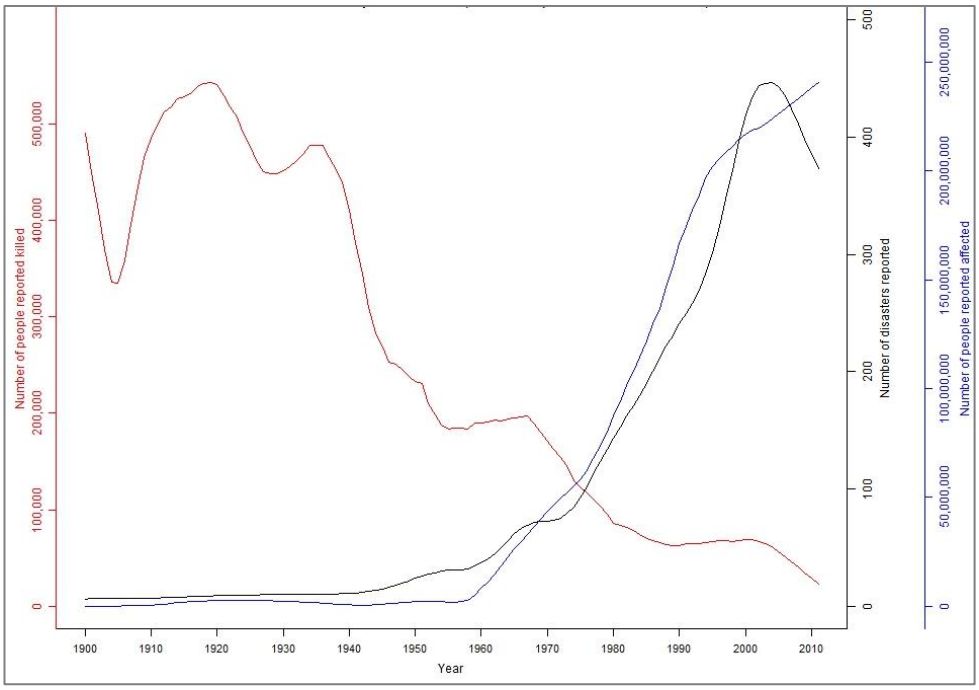

Figure 1.1 : Natural disaster summary 1900-2011 with linear-interpolated smoothed lines (EM-DAT, 2012).

The main cause of this trend is the increasing number of weather-related disasters, (EM-DAT, 2012). Figure 1.2 shows the number of reported disasters with natural disaster groups. As can be seen from the figure weather related disasters have obvious increasing trend since mid 1900s where climatological disasters group includes extreme temperature, drought, wildfire; meteorological disaster group includes storms; hydrological disaster group includes floods and wet mass movements.

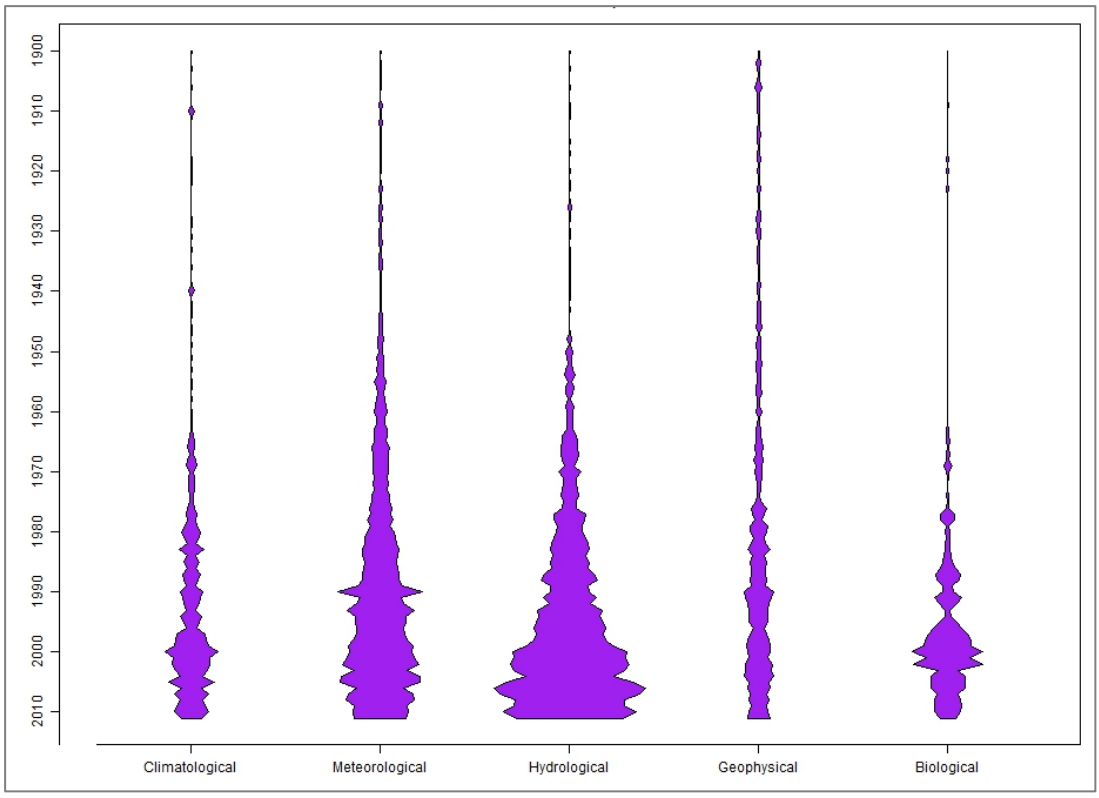

Figure 1.2 : Number of reported natural disaster from 1900 to 2011 with natural disaster groups (EM-DAT, 2012).

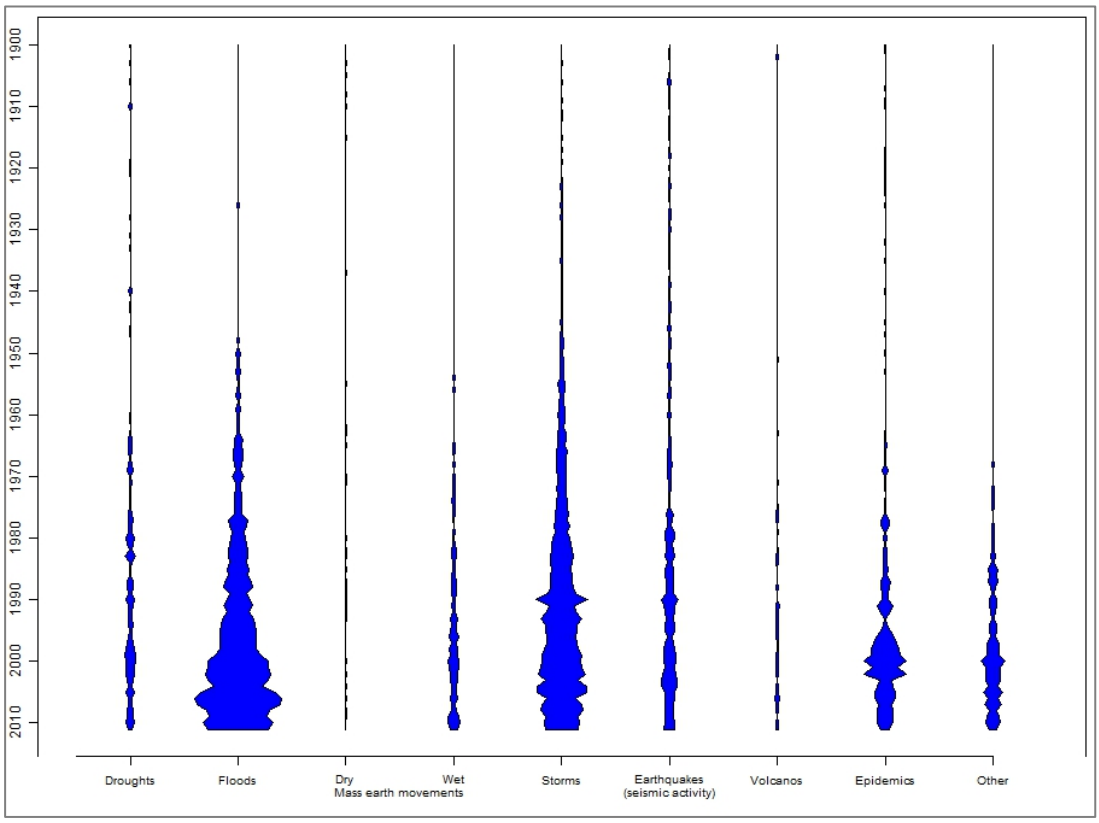

Figure 1.3 : Number of reported natural disaster from 1900 to 2011 with natural disaster main type (EM-DAT, 2012).

In Figure 1.3, the number of reported natural disaster from 1900 to 2011 are shown with the natural disaster main type where storms include tropical storms, extra-tropical cyclones and convective storms; and floods include general river floods, storm surge and flash floods. Flash floods are rapid inland floods caused by intense rainfall usually related to convective stoms. As shown in the figure, floods and storms are distinctly common disasters and have increasing trends (EM-DAT, 2012).

Severe convective storms related severe weather events (e.g., flash floods, tornadoes, lightnings, severe hails, damaging winds) cause loss of lives and damage to property in Turkey (TSMS FEVK records). Considering the effects of severe convective storms both on life and property and the global increasing trends of them, both short range probabilistic forecasting and nowcasting (1-2 hours) of these local storms are significant but unfortunately challenging issues. Because of spatial and temporal scales of severe convective storms, operational numerical weather prediction models are not able to forecast timing, locations and structures of high-impact convective cores properly. Knowledge on geographical, seasonal and daily distribution of severe convective storms is an essential need for improving abilities of forecast society.

Chapter 2 of this dissertation is on storm data of Turkey and presents recent report-based climatologies of severe convection related events, specifiacally severe hail, severe non-tornadic winds and tornadoes. Chapter 3 is on impacts on severe convection related events on society and presents lightning related fatalities and injuries in Turkey. Chapter 4 includes climatology of various environmental parameters associated with severe convective storms for a domain covering Europe, Middle East and North Africa based on 35-year ERA-interim data. Finally Chapter 5 concludes this research.

1.1 Purpose of Thesis

Primary purpose of this thesis is to contribute the building of 'Storm Data of Turkey'. Severe convection is responsible for many hazardous events such as large hail, tornadoes, severe non-tornadic winds, heavy rainfall and lightning. Creating a storm database requires too much effort and collaborative working. Convective storms have small spatial scales, therefore conventinal observational networks are not enough to catch all of them. Consequently, to create their climatologies it is a comman approch for severe weather society to use records of severe event reports from all available

sources. Documenting the occurrence of severe weather events is a necessary first step to understand the environments and processes causing them. And it is not possible to improve their forecasts without this understanding. This research includes collaborative studies on severe hail climatology of Turkey and severe non-tornadic winds in Turkey.

In addition, storm-related damage to property and human life within Turkey are also not well documented. There are a few sources available on some aspects of severe storm events impacts on health and economy of the population (i.e., insured losses owing to hail damage statistics of TARSIM (Turkish Agricultural Insurance Pool)). Many case studies that have been published in meteorological and medical journals prove that lightning causes several number of injuries and fatalities in Turkey, however occurrence of these events, its statistics, geographical distribution was not assesed. In this research lightning related fatalities and injuries in Turkey was enquired using a wide variety of sources.

The final purpose of this dissertation is to produce an objective climatology for severe convective storms. Report-based datasets are the primary sources for severe convection related event climatologies. However, they are not objective. Chance of an event to be reported depends on the availability of an observer. Thus number of reports for a region has a strong relationship with the population of the region. And also occurrence time of an event can effect its reporting. They also have some other disadventages such as subjective estimation of wind speed or hail diameter by non-expert human observers. To be able to make objective conlusions about the regional climatologies, temporal variability and trends of severe convective storms, advanced methods are required. In this research a climatology of severe convective storm environments for a domain covering Europe, Middle East and North Africa for the 35-year period of 1979–2014 from ERA-interim (Dee et al., 2011) is built.

1.2 Background

Report-based datasets are primary sources for severe convective storm climatologies. However, they have some disadvantages. Some of these include: dependence of report frequencies on population density and time of day, subjective estimation of wind speed by non-expert human observers and alike. For this reason other approaches were taken into consideration for creating an objective climatology.

National radar network data would be used to build an objective severe weather climatology. But, unfortunately the Turkish radar network data is not adequate to create a nationwide climatology. Analog meteorological radars were being used in Turkey by Turkish State Meteorological Service which is still responsible for the installation and operation of the radars in the country in the 1970s and 1980s. Modern weather radars have being used in Turkey since mid-2000. The first modern weather radar which was a C-band dual polarization doppler one was installed in Elmadağ, Ankara in June 2000. In 2003, three more C-band doppler weather radars were installed in Istanbul, Zonguldak and Balikesir provinces by Mitsubishi-Hazama Consortium with the Project of TEFER (Turkey Emergency Flood and Earthquake Recovery). Subsequently, a feasibility commision is established which includes experts from relevant disciplines in TSMS to extend the weather radar network. After a long study, the feasibility commision created an inclusive report in June 2007. To cover all parts of the country, installation points for 16 more C-band doppler weather radars were determined with the commision, considering the complex topography of the country which is the major trouble for radar operations in Turkey. In 2008, a contract was signed between TSMS and Vaisala for installation of 6 C-band doppler weather radars. In 2010 in Muğla and İzmir, in 2011 in Adana and Antalya, in 2012 in Trabzon and Samsun installations of these 6 C-band doppler weather radars were completed. In 2013, 10 C-band doppler weather radars were in operation in the country. Doppler mode coverage of these 10 radars are shown in Figure 1.4. In doppler mode, radars have high velocity measuring capability but can not scan long ranges, the radius of the covered area is approximately 120 kms for each radar in this mode. The map also includes the topography information of Turkey, where brighter parts represent higher regions. Figure 1.5. shows the intensity mode coverage analysis of current operational radars. In intensity mode radars can not measure the radial velocity but it can scan longer ranges to detect the location of the targets. Covered area radius for intensity mode is approximately 300 km for each radar. Beam blockage in mid parts of the country is obvious (Figure 1.5).

Figure 1.6 shows the doppler mode and Figure 1.7 shows the intensity mode coverage of 10 operational and 10 planned C-band doppler weather radars together. As can be seen in Figure 1.7 even in intensity mode of 20 radars there are still uncovered regions.

TSMS plans to fill the gaps with short range X-band radars, after installations of these 10 more C-band doppler radars.

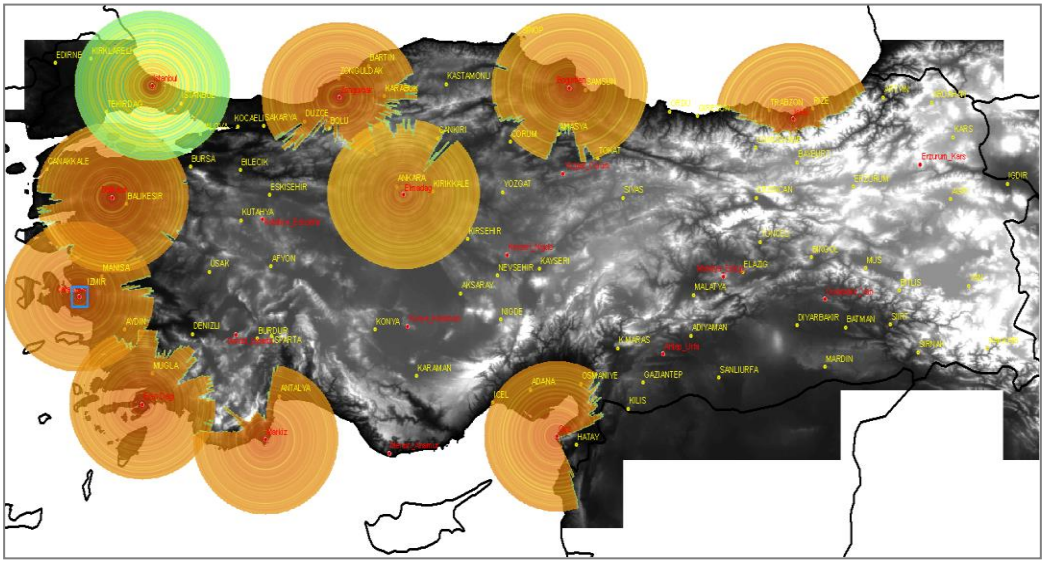

Figure 1.4 : Doppler mode coverage of current operational radars (Bestepe, 2011).

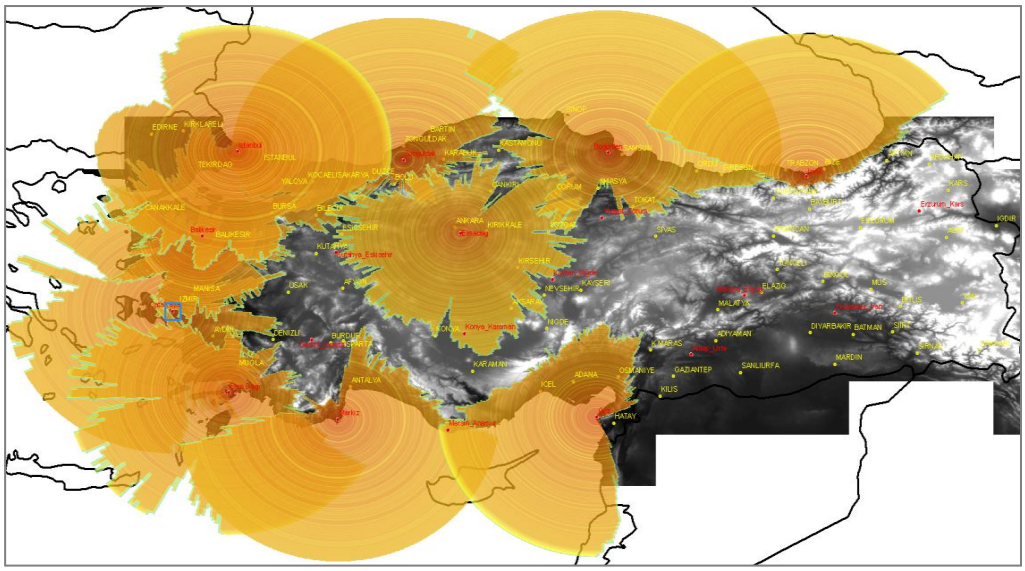

Figure 1.5 : Intensity mode coverage of 10 operational radars (Bestepe, 2011).

Table 1.1 : Radar specifications of TSMS operational radar network in 2013.

	Ankara	İstanbul	Zonguldak	Balıkesir	İzmir	Muğla
Definition	C-Band Dual Polarization Doppler Radar	C-Band Doppler Meteorological Radar	C-Band Doppler Meteorological Radar	C-Band Doppler Meteorological Radar	C-Band Dual Polarization Doppler Radar	C-Band Dual Polarization Doppler Radar
Location	Elmadağ-Ankara	Büyükkuşkaya Hill	Acısu Hill	Akcaldedesi Hill	Çatalkaya-İzmir	Marmaris-Muğla
Operational since	June 2000	March 2003	March 2003	March 2003	May 2010	July 2010
Polarization	Dual (Switch Mode)	Single	Single	Single	Dual (STAR Mode)	Dual (STAR Mode)
Transmitter	Klystron	Klystron	Klystron	Klystron	Klystron	Klystron
Height	1807 meter	378 meter	1108 meter	642 meter	973 meter	960 meter
Latitude	39°47’53” N	41°20’ 30”N	41°10’55”N	39°44’26”N	38°18’41”N	36°53’24”N
Longtitude	32°58’15” E	28°21’30”E	31° 47’54” E	27° 37’10” E	27° 00’04” E	28° 19’39” E
Tower	32 meter steal Construction	20 meter steal Construction	25 meter steal Construction	25 meter steal Construction	40 meter steal Construction	30 meter steal Construction
Firm	AMS-Gematronik	Mitsubishi	Mitsubishi	Mitsubishi	Vaisala	Vaisala

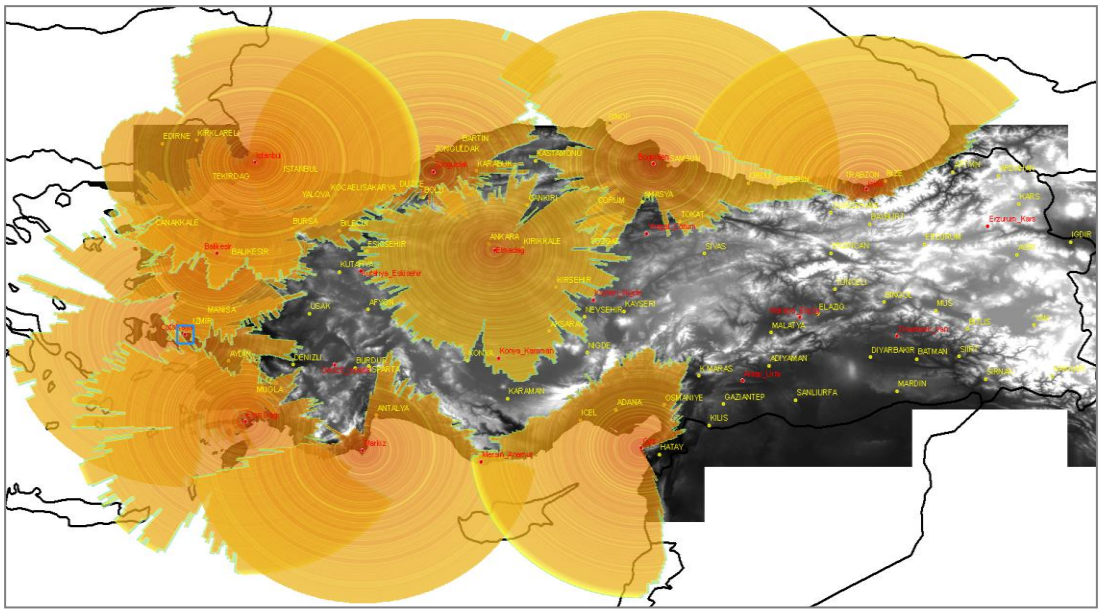

Figure 1.6 : Doppler mode coverage of 20 radars (10 operational and 10 planned) (Bestepe, 2011).

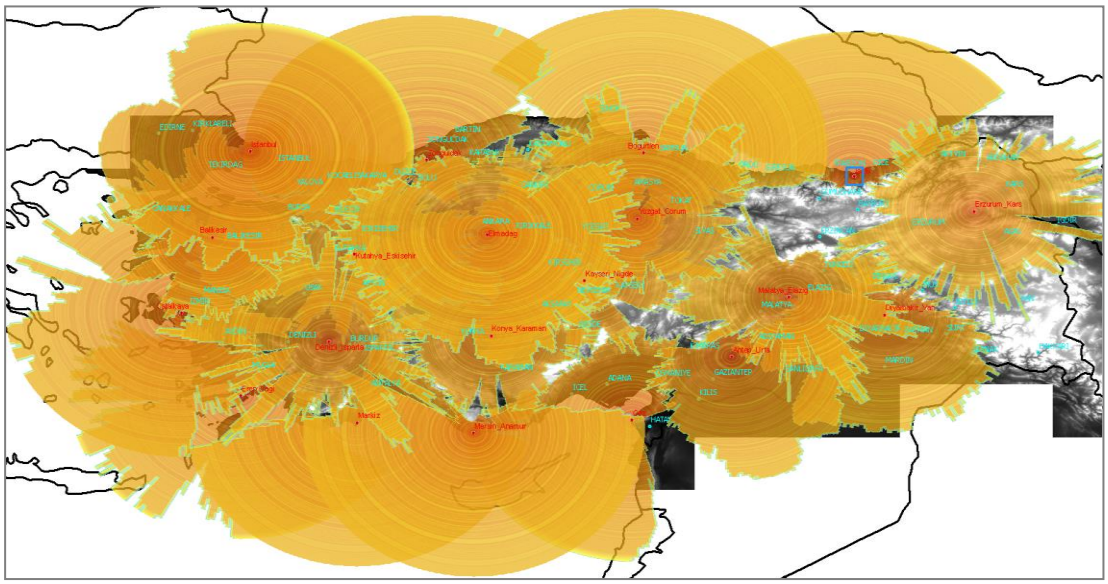

Figure 1.7 : Intensity mode coverage of 20 radars (10 operational and 10 planned) (Bestepe, 2011).

To summarize, the first modern C-band doppler radar was installed in Ankara in 2000 and three years later in 2003, three more radars were installed in İstanbul, Zonguldak and Balikesir provinces; it took seven years to have the fifth and sixth radars of the network. In 2010 İzmir and Muğla radars were installed. Afterwards, in 2011 Adana and Antalya, in 2012 Trabzon and Samsun radars were installed. Unfortunately, the usage of 6 of 10 current operational radars do not go too far in the history. Besides,

there may be some data absence due to technical problems. Table 1.1 shows the radar specifications of TSMS operational radar network in 2013.

The second problem related with radar network of Turkey is the spatial coverage of the existing radars. Even when 10 radars operate together, eastern part of Turkey is not covered. And because of the beam blockage there are uncovered regions in the west and mid parts of the country.

Consequently, Turkish radar network data were not adequate to analyse the geographical distribution and frequency of the severe convective storms over the country. Therefore, other approaches were necessary to create an objective severe convective storm climatology. Another method to analyse the geographical distribution and frequency of the severe convective storms is the investigation of global model reanalysis data in terms of convection related environments. ECMWF or NCEP reanalysis data could be used for that kind of study. Spatial resolutions of these models are not high enough to solve convective storms dynamically. However, environmental conditions like vertical wind shear and CAPE can give information on convective initiation, thus the spatial and temporal distributions of convective storms. It must be kept in mind that, with the information of environmental conditions we can have an idea only on the possibility of a convective storm occurrence. In this research, ERA-Interim data is used for building a severe convective storm environment climatology.

Table 1.2 : Server specifications.

Processors	2 x Intel® Xeon Eight Core E5-2650 (2.00 Ghz, 8.0 GT/s, 20 MB, Turbo, 8 Core)
RAM	32 GB DDR3 1600 Mhz LV RDIMM (4 x 8 GB)
Maximum RAM	768 GB
HDD	3 x 300 GB SAS 15.000 rpm Hot Plug 3.5" (RAID 5)
Maximum HDD	8 x 3,5” Hot Plug
Form Factor	2 U Rack
Optical Driver	16x DVD +/- RW SATA
Power Supply	2 x 750 Watt Hot Plug
Ethernet	1 x Broadcom® NetXtreme 5720 Quad Port Gigabit Ethernet (on board)
Ports	5 USB, Seri, 2 VGA, iDRAC7 Enterprise

A rack server was used for the computation. Specifications of the server are shown in Table 1.2. Additional memory devices (4 TB Dell Nearline-SAS 7.200 rpm 3,5” Hot

Plug) were also used for storage of the outputs. WRF model installed for case studies. For post processing and other applications numerious sofwares were used such as NCL (NCAR Command Language), ArcGIS and Microsoft Excel.

1.3 Literature Review

There are a lot of studies that aim to demonstrate the climatology of severe weather events over a portion of the globe. Some of them are tornado climatologies of Germany (Dotzek, 2001), Lithuania (Marcinoniene, 2003), Austria (Holzer, 2001), Balearic Islands (Gayaa et al., 2001), Italy (Giaiotti et al, 2007) and hail climatologies of Finland, (Tuovinen et al., 2009), Britain and Ireland (Webb et al., 2009).

Creating reasonably accurate climatologies of severe convective storms is challenging. They are relatively small-scale events and rare at any particular location. Their reporting is contingent on the presence of an observer or an observation system available at their location. Reporting processes and population biases are concerns for report-based climatologies (Doswell and Burgess 1988; Brooks and Doswell 2001, 2002; Verbout et al., 2006; Doswell 2007). Due to subjective nature of their observations, regional climatologies, temporal variability and trends of these phenomena have been difficult to be defined properly (e.g., Diffenbaugh et al., 2008)

Usage of numerical models is an alternative method for get rid of mentioned disadvantages of report-based climatologies. There is a significant similarity between distribution of observed severe convective storms and storm environmental parameters (e.g., Brooks et al., 2003; Romero et al., 2007; Gensini and Ashley 2011).

In 2003, Brooks et al., used United States National Centers for Environmental Prediction (NCEP) reanalysis data (with spatial grid spacing on the order of 200 km) proximity soundings to find environmental conditions, related to significant severe convective storms (which cause hail at least 5 cm in diameter, wind gusts at least 120 km per hour, or a tornado of at least F2 damage). Then they searched for these environments in reanalysis data. They constructed maps that show spatial distributions and frequencies of these convective storm favoring environmental parameters. Figure 1.8 shows days per year with favorable severe parameters for CONUS (Contiguous United States) over the period of 1977 to 1999. They applied the relationships between environmental conditions and severe weather events, from CONUS to Europe and

made estimates of the frequency of significant severe convective storms favoring conditions. Figure 1.9 shows days per year with favorable severe parameters for Europe over the period of 1977 to 1999.

Their method for understanding the global distribution of severe deep moist convection (DMC) environments using an ingredients-based approach was away from the before mentioned disadvantages of report based climatologies.

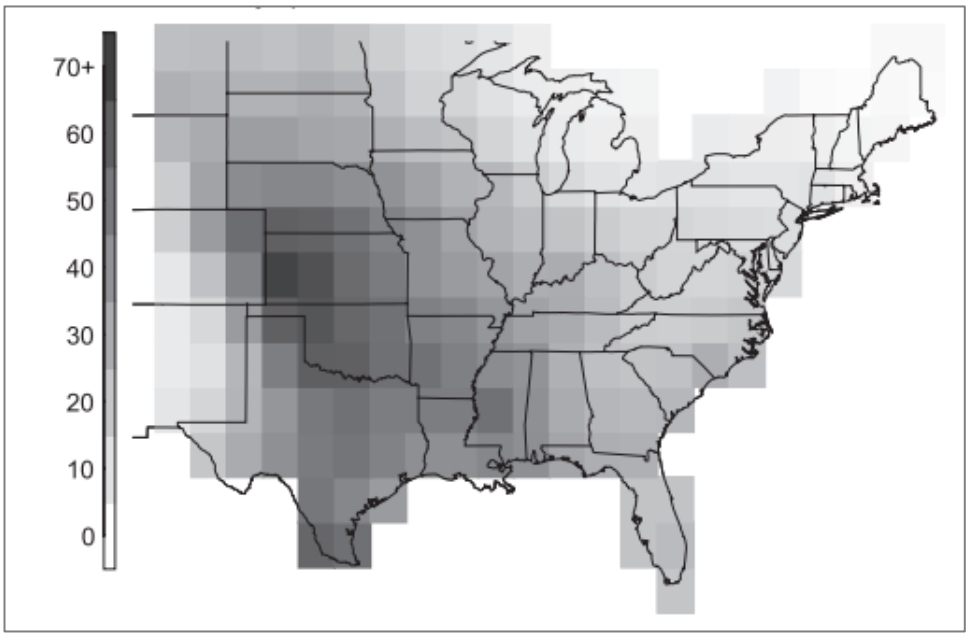

Figure 1.8 : Days per year with favorable severe parameters for CONUS over the period of 1977 to 1999 (Brooks et al., 2003).

Figure 1.9 : Days per year with favorable severe parameters for some part of Europe over the period of 1977 to 1999 (Brooks et al., 2003).

In 2007, Romero et al., made a similar study using ECMWF ERA-40 dataset (with a grid spacing of about 125 km). Their domain was covering Europe. They calculated the following set of diagnostic variables: convective available potential energy for the 1000 hPa "surface" parcel (CAPE), convective inhibition energy for the 1000 hPa "surface" parcel (CAPEN), mid-tropospheric (700–500-hPa) lapse rate (LR7050), low-tropospheric (1000–850 hPa) moisture content, as measured by the precipitable water in that layer (PRWA85), deep layer (1000–350 hPa) storm relative helicity, (SRH35), shallow layer (1000–850 hPa) storm relative helicity (SRH85). They have created a climatology of each diagnostic variable for 1971–2000 at 12 UTC by computing monthly series of the mean value, 25% percentile value, 75% percentile value and inter-quartile range. Their results are available at http://ecss.uib.es. According to this synthetic climatology, areas for severe thunderstorms occurrence in Europe extends along a zonal belt over the south-central regions due to helicity associated with the extratropical storm tracks and thermodynamically-favourable profiles established over the southern Atlantic and Mediterranean Sea.

Gensini and Ashley (2011) established a climatology of potentially severe convective environments for U.S. for the 30-y period of 1980–2009 from the North American Regional Reanalysis (NARR) dataset. NARR data has a relatively higher resolution compering NCEP reanalysis data.

2. STORM DATA OF TURKEY

2.1 Thunderstorms and Lightning in Turkey

Station observations of the Turkish State Meteorological Service indicate that thunderstorms occur in Turkey throughout the year. Monthly-average numbers of thunderstorm days at 277 Turkish State Meteorological Service stations between 1960–2013 were bilinearly interpolated with an inverse distance weighting method (variable radius, 2nd power) on a grid of 263x100 points to produce a gridded analysis of thunderstorm frequency (Fig. 2.1). Thunderstorms were most frequent in May and June all around Turkey, especially over the inland and northeastern parts. The maximum thunderstorm frequency shifts to the Aegean and Mediterranean coasts from late autumn to early spring, while the rest of Turkey has relatively infrequent thunderstorms.

Geographical distribution map (Fig. 2.2) shows that average stroke density is lowest in southern parts of the central Turkey and is highest along the coasts with maxima around Muğla, Hatay, and Adana (see Fig. 3.5 for locations). GLD360 (Global Lightning Dataset 360) lightning observation data provided by Vaisala over a two-year period (1 October 2011 to 30 September 2013) are used to display annual (Fig. 2.3a) and diurnal (Fig. 2.3b) distributions of lightning over Turkey. The annual distribution of lightning was consistent with the annual distribution of thunderstorm observations as expected (cf. Figures 2.1 and 2.3a). Both lightning and thunderstorms were most frequent in May and June. Figure 2.3b shows that most of the lightning strikes occurred in the afternoon.

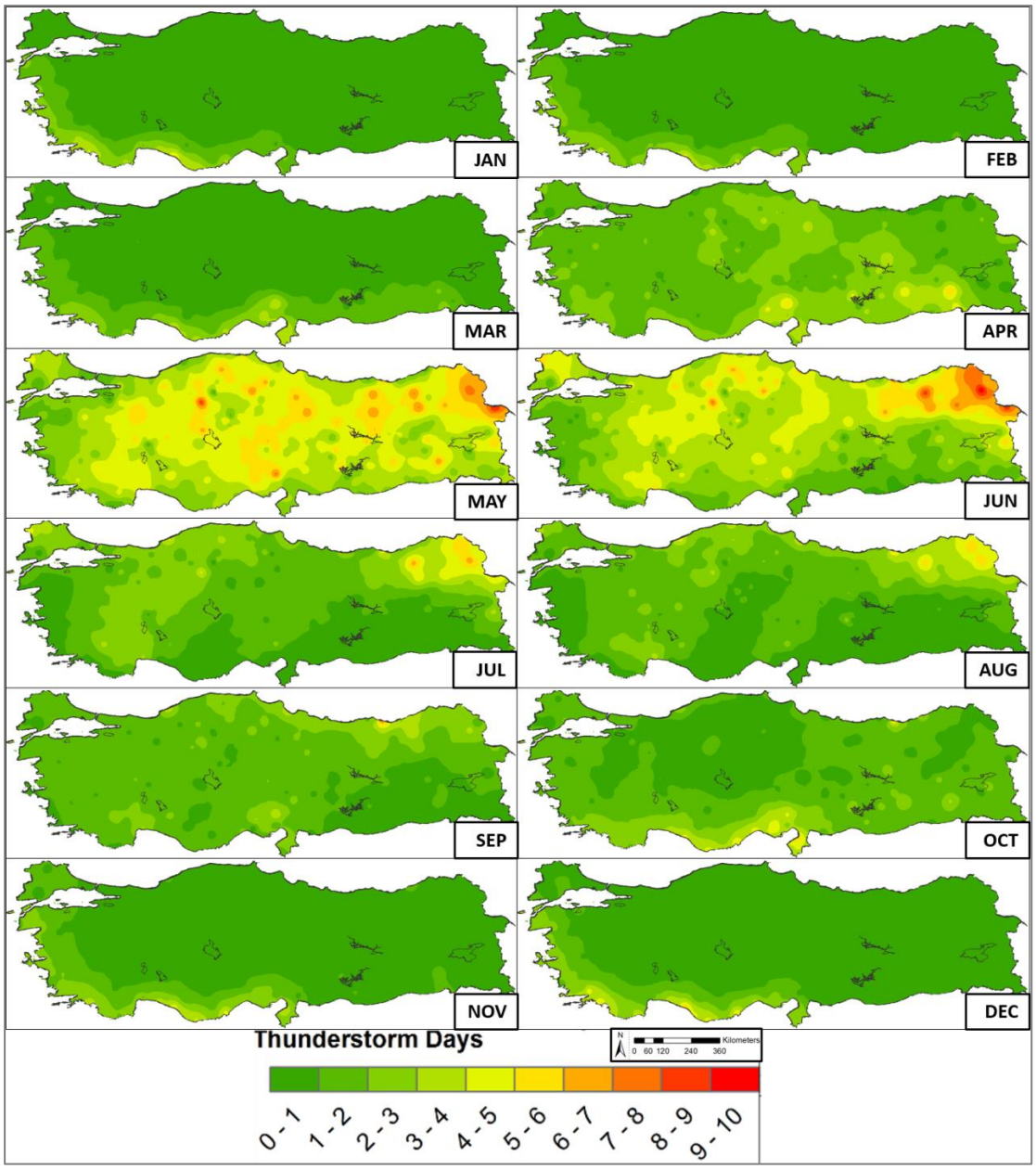

Figure 2.1 : Average number of thunderstorm days in Turkey for each month. Data were provided by the Turkish State Meteorological Service.

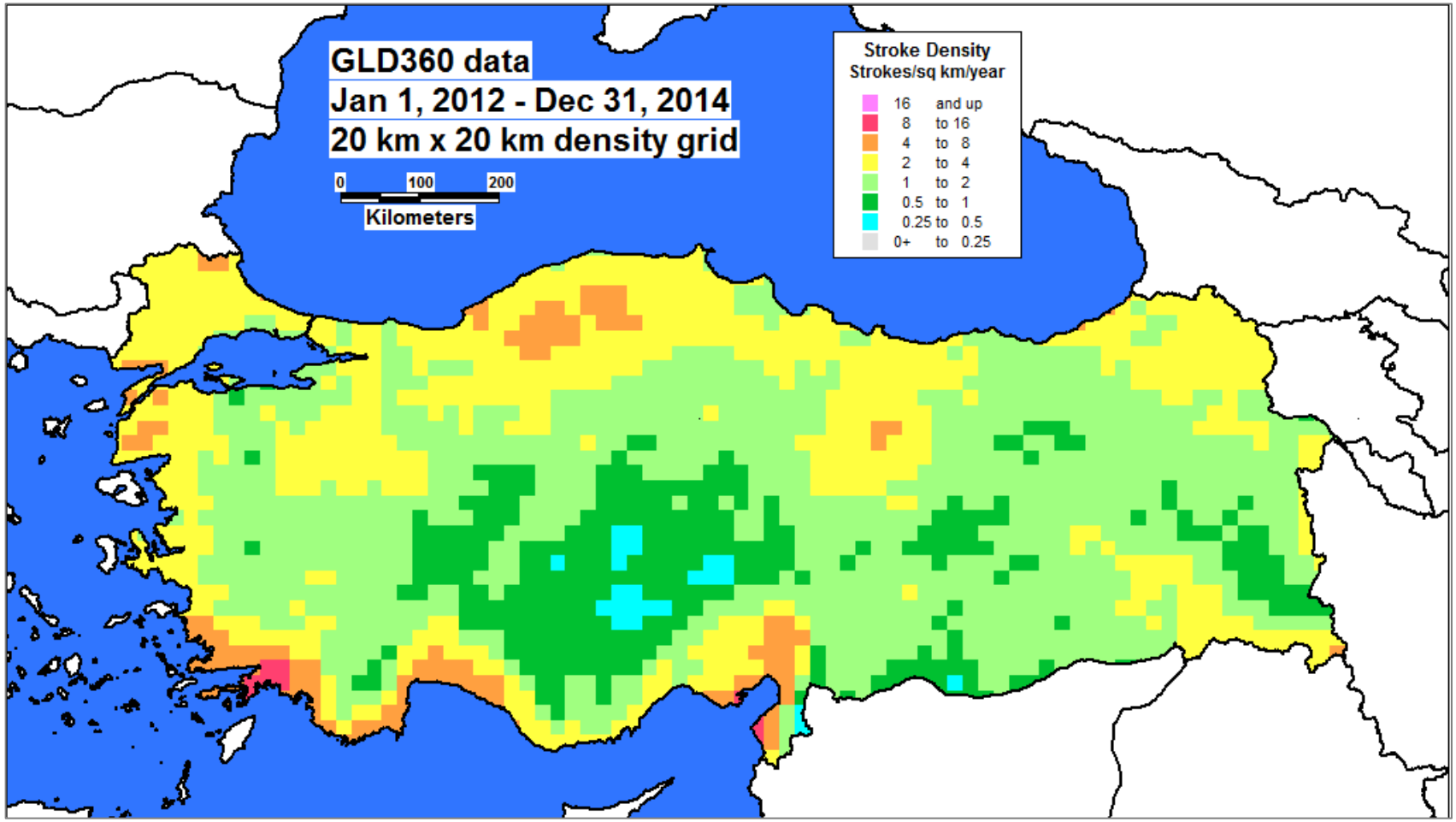

Figure 2.2 : Geographical distribution of lightning over Turkey between 1 January 2012 and 31 December 2014 in strokes km–2 year–1 (provided by Vaisala).

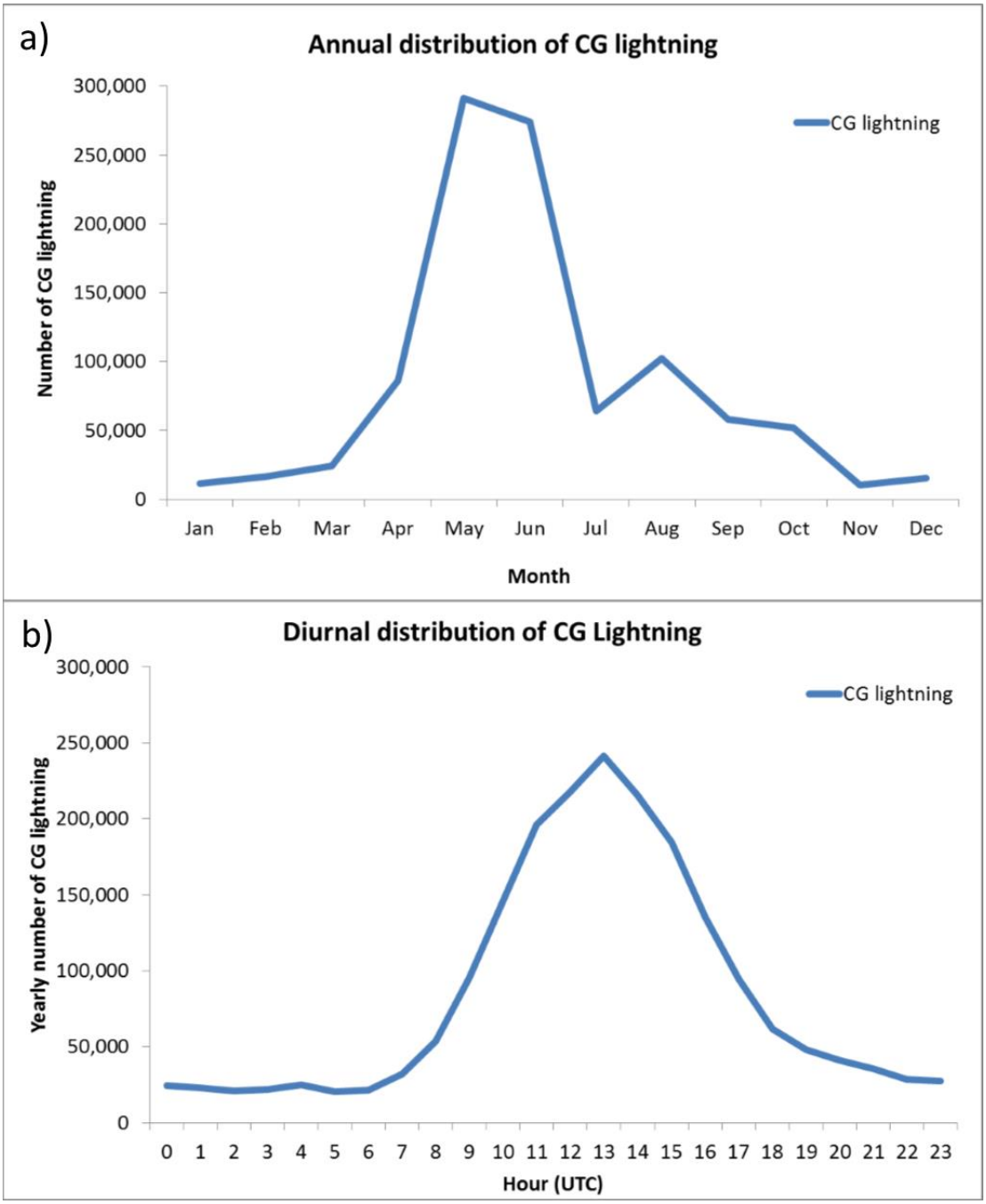

Figure 2.3 : (a) Annual and (b) diurnal distribution of cloud to ground lightning over Turkey between 1 October 2011 and 30 September 2013. Local time in Turkey is UTC+2 from October to March and UTC+3 from April to September due to daylight savings time. Data were provided by Vaisala.

2.2 Severe Hail in Turkey

This section includes data, methods and results on the severe hail climatology part of this research. In this part, the term "case" or "event" implies a specific severe hail occurrence on the ground, which is observed by one or more people, supposedly from

a single storm cell. The term "report" indicates the observation of one or more severe hail case. Although rare, one report may include more than one case, and one case maybe reported more than once. The numbers given in the paper pertain to cases rather than reports.

2.2.1 Data and Methods

Before developing a climatology of severe hail, careful consideration must be given to how severe hail will be defined. Hail severity usually is defined by hail diameter, even though not all of wide-ranging impacts of hailstorms are dependent on hailstone diameter only. A number of previous studies discussed this issue and mentioned other factors such as the wind speed during a hailstorm and quantity of the hail on the ground (Webb et al., 2001, 2009; Sioutas et al., 2009). In addition to these, some studies have defined hail severity in terms of the kinetic energy of the hailstones (e.g., Vinet 2001; Eccel et al., 2012), which increases rapidly with hailstone diameter given that both mass and terminal fall speed increase with hailstone diameter. Another measure of severity can be the depth of the hail accumulation. For example, the European Severe Weather Database (ESWD; Brooks and Dotzek 2008; Dotzek et al., 2009) includes hailstones "having a diameter (in the longest direction) of 2.0 cm or more and/or smaller hailstones that form a layer of 2.0 cm thickness or more on flat parts of the earth's surface." In the United States, the National Weather Service, since 2010, has defined severe hail to have a diameter equal to or exceeding 1 inch (about 2.5 cm) [prior to 2010, the threshold was a diameter of 0.75 inch (1.9 cm)]. Some prior studies have analyzed all hail regardless of severity. For example, Giaiotti et al., (2003) used data from a special hailpad network in the Friuli–Venezia–Giulia region of Italy, and Etkin and Brun (1999), Zhang et al., (2008), Suwala and Bednorz (2013), and Mezher et al., (2012) have documented hail statistics obtained from surface meteorological stations in Canada, China, central Europe, and Argentina, respectively.

Ideally, the present study would adopt a 2-cm diameter threshold for severe hail to facilitate comparison to other hail climatologies in Europe. However, the available hail reports from Turkey rarely include quantitative size information. Instead, 98% (1465) of the 1489 severe-hail cases compare hail sizes to familiar objects such as hazelnuts, chestnuts, olives, walnuts, and eggs, which obviously have a range of diameters. "Hazelnut-sized hail" represents the most commonly reported severe-hail size (721 out of 1489 cases) in the Turkish records. Even though most hazelnut diameters fall short

of 2 cm (hazelnut diameters are more typically about 1.5 cm), in the TSMS data, severe damage (especially to crops) is commonly reported with this size. Moreover, the reports also sometimes merely document average rather than maximum hailstone diameter. After considerable deliberation, hazelnut-sized hail is included in the climatology given the reported damage, uncertainity of maximum/average size during the events, and number of hail reports of that size. A walnut-sized hail threshold also was considered—"walnut-sized hail" also is commonly referenced in Turkey (436 out of 1489 cases), and walnuts would logically be the next size increment up from hazelnuts—but was dismissed because walnuts tend to have diameters considerably larger than 2 cm. Such quantized reports of severe-hail size is not an issue only for Turkey; Schaefer et al., (2004) show that more than 75% of large-hail reports (defined as 0.75 inches before 2010) in the United States dataset describes hail size with three objects (dime/penny, quarter and golf ball).

A subset of severe hail is classified in this study as very large hail, nominally equal to or larger than 4.5 cm in diameter. This category includes hail sizes compared to an egg (this is among the most common descriptions with 75 occasions), tangerine, fist, goose egg, and cigarette pack, among others. The determination of the 4.5-cm–egg-size threshold followed a similar approach to that of 1.5-cm–hazelnut-size threshold mentioned above. Large hail is classified as hail with diameters equal to or greater than 1.5 cm and less than or equal to 4.4 cm. Thus, the severe-hail classification scheme presented in this paper is sum of the two classes: large hail and very large hail. Whenever the term hail is used in this article without qualifier, it is intended to mean all hail regardless of size (the sum of severe hail and nonsevere hail).

Table 2.1 : Hail classification scheme for the Turkish severe hail climatology.

Class	Non-severe	Severe			
Size	Small	Large		Very Large	
Diameter (d) (cm)	$d < 1.5$	$1.5 \leq d < 3.0$	$3.0 \leq d < 4.5$	$4.5 \leq d < 6.0$	$d \geq 6.0$
Sample keywords	Pea	hazelnut, grape	walnut, chestnut	Egg	orange, fist

Table 2.1 summarizes the severity criteria used in the study. No matter how severe the reported hail damage, hail reports without any accompanying size description almost always are excluded from the climatology [the lone exceptions are reports of hailstones

breaking windows and hailstones having “sizes not seen before” (5 of 1489 cases), which are placed in the 3.0–4.4 cm bin]. Moreover, as in any hail study, a reported hailstone diameter probably should be regarded as a typical or maximum observed hail diameter, though larger (and smaller) than observed hailstones might exist from a specific storm.

Considering the relatively small spatial and temporal scale of hailstorms, any climatology based on observations will be limited by underreporting, especially in less-populated regions (e.g., the mountains in eastern Turkey). The higher number of reports around metropolitan areas such as Istanbul, Ankara, Izmir and Bursa can be partially attributed to the high population density. The population of Turkey has risen from 13.6 million in 1927 to 76.7 million in 2013 (based on data from Turkish Statistical Institute), with an impressive shift between rural and urban populations, as 24% of people in 1927 were living in urban areas and 76% were living in urban areas in 2010. Population density in the Istanbul province is 2725 people km^{-2} (slightly lower than Washington D.C.), whereas it is only 11 people km^{-2} in the Tunceli province (like Nevada or Utah).

Underreporting may also be significant in areas without agriculture or other vulnerability to hail. According to Turkish Statistical Institute data, as of 2013, 26.5% of Turkey is arable/cultivated (in 2004, the figure was 23.1%). Reporting biases are further complicated by the fact that agricultural vulnerability to hail varies seasonally and as a function of crop type. Although there is no way to ensure that all severe weather occurrences have been captured, the climatology presented herein has been derived from hail reports obtained from a diverse mix of sources in order to capture as many events as possible, similar to the approach used by Tuovinen et al., (2009).

The most important source for the severe hail reports was the TSMS archive. The TSMS has maintained 459 different meteorological stations throughout Turkey since 1930, though fewer are operational at any given time (243 are in operation at the present time). In addition to making routine climatological observations, the TSMS meteorological stations report hazardous weather phenomena such as hail in their local areas. These reports include a written description (usually just a sentence or two, but occasionally longer entries are made) of the event and any injuries and property damage. Severe hail cases were obtained from a manual search of this archive from 1939–2012 by the two lead authors. The search produced 1083 severe hail cases.

Furthermore, the TSMS database contains hail frequency (all hail, not just severe hail) statistics by month from 1960–2013. These data were used to provide context for the locations of severe hail reports. Another 142 severe hail cases (from 2001–2014) were obtained from the ESWD.

Digital archives of two national mainstream newspapers, Cumhuriyet and Milliyet were also combed for hail records. Currently, these are the only two national newspapers that maintain digitized archives. The keywords used for searching were "dolu yağdı" (hail fallen), "dolu yağışı" (hail precipitation), "büyüklüğünde dolu" (hail with size of), rather than only "dolu", which is the literal translation of "hail" in Turkish (only searching for "dolu" was problematic because the word has popular alternative meanings such as "full"). The Cumhuriyet archive, which is accessible via a paid membership, goes back as far as 1 January 1930 and was the source of 98 additional severe-hail cases. A search of the Milliyet archive, which is freely accessible and contains articles from 3 May 1950 to 30 June 2004, yielded 20 more severe-hail cases. Online records of Hürriyet and Sabah, two other national mainstream newspapers, were also searched. Although these searches were limited to roughly the last decade (the archives extend back to 8 July 1997, and 1 January 1997, respectively), these sources provided 40 and 12 new cases, respectively. Hardcopy archives of Cumhuriyet and another periodical, Akşam, also were searched manually starting in 1929, which is the first year the Latin alphabet was used in Turkey. This search added 2 additional severe hail cases to the climatology.

A search of additional internet news websites in Turkey, with the Google.com.tr search engine, yielded 92 additional severe hail cases. Obviously, the credibility of Internet reports is often questionable. When available, satellite and radar images were used to verify the presence of a convective cloud or high reflectivity at the location of a severe hail report. It was also possible to investigate the reliability of the information via interactions with eyewitnesses using social media (Twitter and Facebook) in 17 cases. In some other cases, the municipality or local administration offices were called (since 2010) to verify the information found on the Internet. All these efforts yielded 1489 severe-hail cases, of which 320 (21%) had multiple sources (cases mostly from recent years in which Internet reports abound).

The term severe-hail day is used in this study to refer to a day with at least one severe-hail report, as in Tuovinen et al., (2009). When multiple severe-hail reports are within

20 km of each other on a single day, they are merged into a single case. Some single severe hail cases might be the result of multiple storms, but the number of such instances is likely small. A storm with a long hail swath might be responsible for multiple severe-hail cases if there are gaps in the severe-hail reports along the storm's path that exceed 20 km. We suspect that a few such storms have been responsible for multiple severe-hail cases in the climatology. Because the exact times of the severe-hail reports are generally unknown (times are available for only 587 out of 1489 cases, or 39%), a time criterion like those used in previous studies could not be applied in this study. For example, hail studies in the United States (Schaefer et al., 2004) and Finland (Tuovinen et al., 2009) attributed a report to a new event if 15 min elapsed since the previous report, with 16 km and 20 km distance criteria, respectively.

2.2.2 Results

The climatology includes 1489 severe hail cases on 1107 severe hail days (days with at least one severe hail case) in Turkey from 1925–2014, of which 124 (8.3%) were classified as very large. These numbers correspond to 16.5 cases per year or 0.21 cases per 10,000 km2 per year, and 12.3 days per year or 0.17 days per 10,000 km2 per year. The actual frequency must be higher given the large number of hail-damage reports without size information and other severe-hail events that may not have been reported at all. However, the annual average of the last five years (2009–2013), which may be more representative of the true frequency given the much greater availability of Internet reports, is 42 cases, or 0.54 cases per 10,000 km2 per year, and 29 days, or 0.37 days per 10,000 km2 per year.

2.2.2.1 Severe-hail cases by year

Between 0 and 74 severe-hail cases per year were documented from 1925–2014 (Fig. 2.4). Severe-hail cases were most numerous in the 1960s, during which every year had at least 29 severe-hail events (74 severe-hail cases were reported in 1963). The 1970s and 1980s generally featured a decline in cases to pre-1960s levels. Curiously, a similar trend in the long-term precipitation records of Turkey exists, as they also show a peak in 1960s and decrease afterwards (Türkeş 1996; Toros 2012). Although the underlying reasons for more frequent severe-hail environments are not yet known, the track of extratropical cyclones might play a role. A shift of the North Atlantic jet stream's latitude in spring from about 45°N (during roughly 1960–1980) to about 48°N

(during roughly 1980–2000), with 1 m s–1 faster speeds in the 1960s on average (Woollings et al., 2014), may be related to the precipitation and severe-hail frequency trends. Since 2005, there has been an increase in the frequency of severe hail reports.

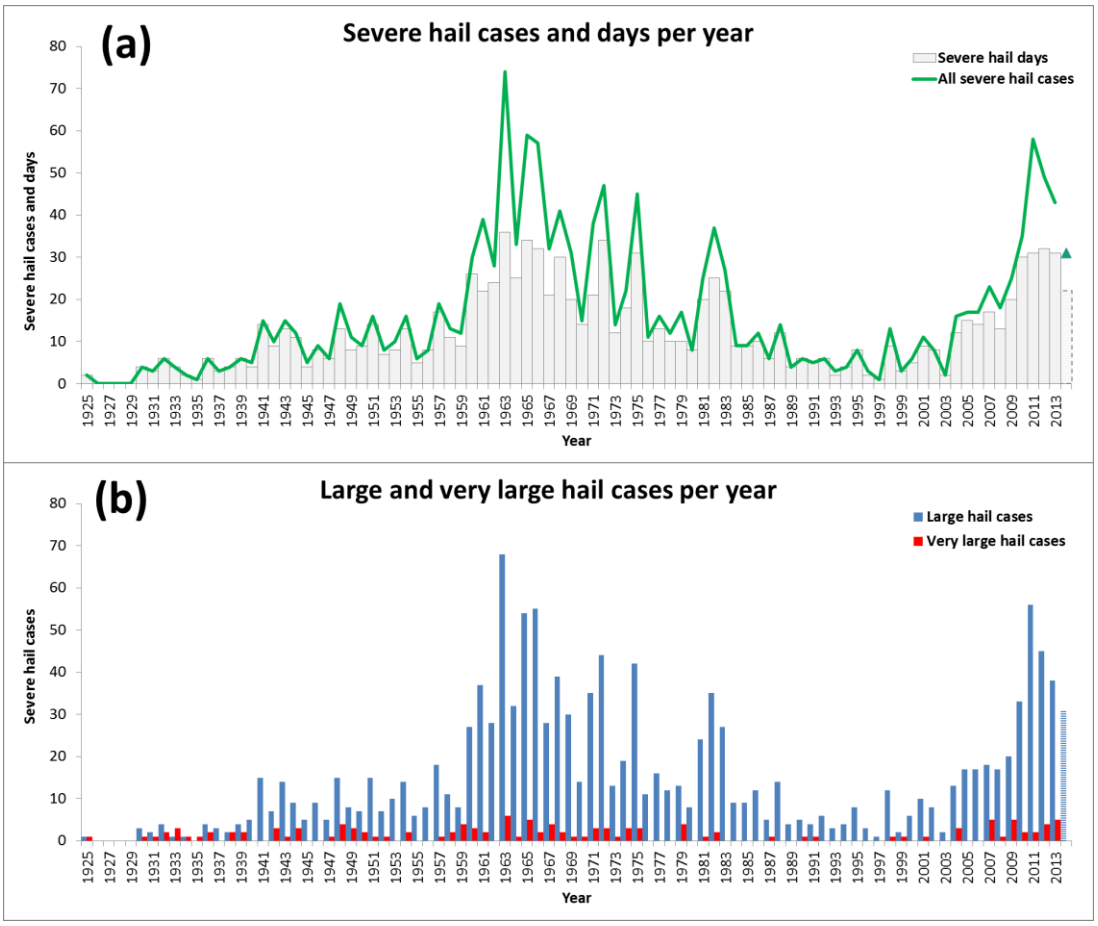

Figure 2.4 : (a) Severe hail cases and days, (b) Large and very large hail cases in Turkey per year, 1925–2014 (the 2014 data are through May 27).

From 2005 to 2013, the annual number of severe-hail cases has increased from 17 to 43, and the annual number of severe-hail days has increased from 12 to 32. Though we cannot rule out that meteorological factors partly contributed to the recent increase in the frequency of the cases, the trends likely also have been heavily influenced by changes in the availability of hail reports. For example, the availability of cases has greatly increased in the last decade owing to the Internet; 249 of 301 cases (83%) during 2004–2013 originate from online sources (search engines, social media, newspaper archives, and the ESWD), whereas there are none before 1998.

The trend in severe-hail days roughly follows that of the severe-hail cases, with a correlation coefficient of 0.9677 (Fig. 2.4a). However, days with more than one case increase in peak periods (e.g., during the 1960s and 2010s), which can be attributed to

regional outbreaks or wider sources of information (especially for the recent years). The leading year is 1963 with 36 severe-hail days, followed by 1965 and 1972 (34 severe-hail days occurred in both of these years).

The trend in the frequency of very large hail cases compared to large-hail cases over the period of the climatology (Fig. 2.4b) indicates a possible underreporting of severe-hail before 1960. Though the frequency of very large hail is roughly steady throughout the climatology, the frequency of large hail is lower prior to roughly 1960 (we might naively expect that very large hail is unlikely to be unreported owing to its likelihood of having an impact). A similar argument has been made for the underreporting of F0/EF0 tornadoes (the F and EF ratings refer to the Fujita and Enhanced Fujita scales, respectively), in that the number of tornadoes rated F1/EF1 or higher has exhibited little upward trend since the 1950s, whereas the number of F0/EF0 tornadoes has dramatically risen (Kelly et al., 1978; Feuerstein et al., 2005; Verbout et al., 2006). The peak year is 1963 with 6 very large hail cases; 55 (62%) of the years in the climatology have very large hail cases.

2.2.2.2 Hail size distribution

The frequency of occurrence of many rare events, such as tornadoes, extreme precipitation, and severe winds, are known to approximately follow a log-linear decline with increasing intensity (Brooks and Doswell 2001; Brooks and Stensrud 2000). Following the approach described by Brooks and Doswell (2001) for tornadoes, the percentages of hail sizes are plotted on a log–linear plot (Fig. 2.5). The near-constant slope of the line in Fig. 2.5 indicates that the distribution of hail sizes equal to or exceeding 3 cm is not biased by size. The slightly smaller slope for the smallest hail sizes likely indicates an underreporting bias.

Of the severe hail cases in Turkey, 55% (821 cases) involve hailstone diameters smaller than 3.0 cm, and 36% (542 cases) are associated with hailstone diameters between 3.0 and 4.4 cm, inclusive (Fig. 2.5). There are 24 very large hail cases involving hailstone diameters equal to or larger than 6.0 cm (1.6% of all severe hail cases). The ratio of very large hail to severe hail in Turkey (defined as 4.5 cm or larger and 1.5 cm or larger, respectively) is 0.083, comparable to 0.082 for the United States (with 2.00 in and 0.75 in thresholds) as suggested by Schaefer et al (2004), and far lower than Finland's 0.36 (5 cm or larger hail cases within 2 cm or larger hail cases, Tuovinen et al., 2009).

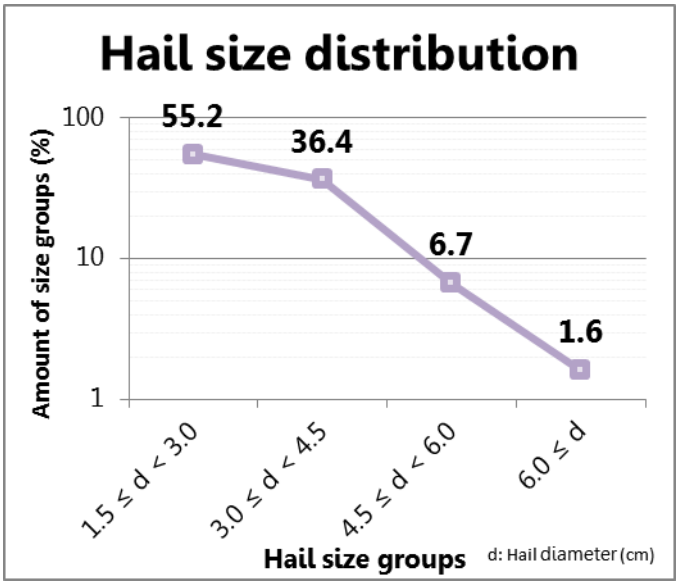

Figure 2.5 : Size distribution of severe-hail cases in Turkey.

The largest hailstone in Turkey is not exactly known owing to the rarity of objective size information in the hail reports. However, some extreme cases have been reported. These include a hailstone in Kadirli on 3 November 1936 estimated to weigh somewhere between 300 and 1000 g, a 750-g hailstone in İznik on 1 July 1947, and roughly a half-dozen other reports of hailstones exceeding 400 g since the 1930s.

2.2.2.3 Annual cycle

Severe hail in Turkey is most frequent in spring and summer. June is the peak month, followed by May (Fig. 2.6), with 864 events (58% of all cases) being reported in these two months. Moreover, very large hail also is most frequent in June (34 events) and May (28 events), followed by July and August (13 and 12 events, respectively). Hailstones with diameters larger than 6 cm have the same peak months, with 6 occurrences in June and 4 in May. Severe hail is least likely in December. The peak season is comparable to other parts of southern Europe. For example, the peak season for severe hail is late May to early July for Bulgaria (Simeonov 1996), May–June for northern Greece (Sioutas et al., 2009), June for northeastern Italy (Giaiotti et al., 2003), May through September for France (Vinet 2001), and May through July for northern Spain (Sanchez et al., 1996). On the other hand, Cyprus experiences severe hail more frequently in December, compared to other months (Michaelides et al., 2008), which is consistent with our results regarding southern coasts of Turkey (discussed below).

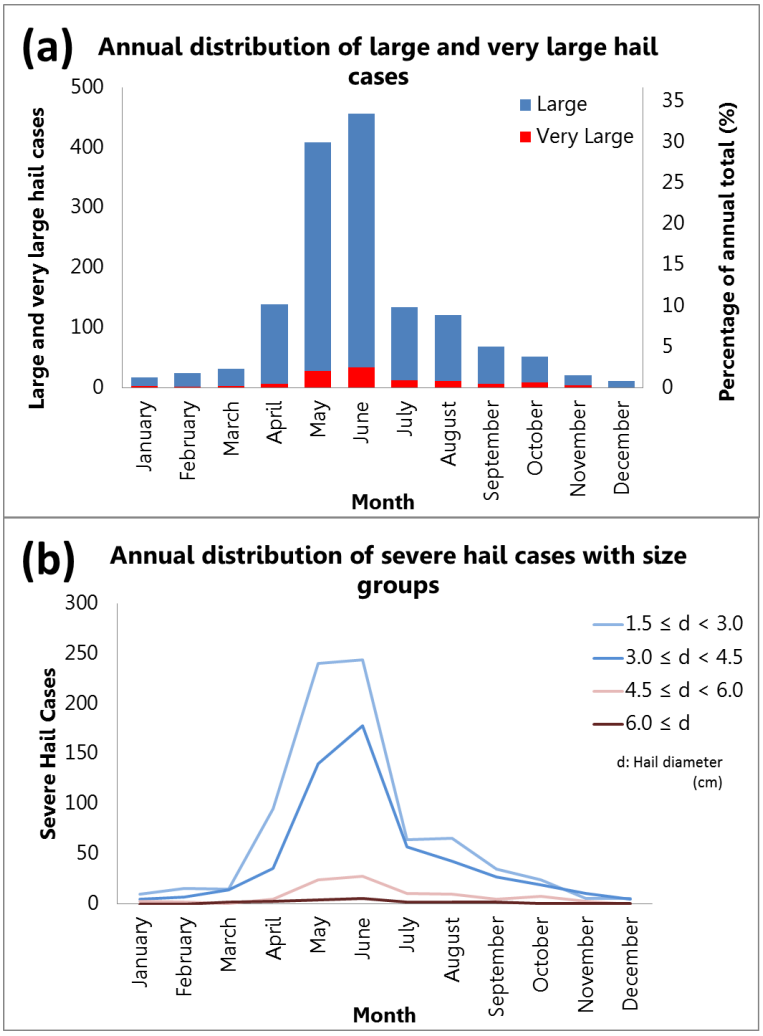

Figure 2.6 : Annual distribution of (a) large and very large hail cases, and (b) size groups for severe hail cases in Turkey.

The geographical distribution of severe hail cases is relatively uniform in Turkey when compared to tornadoes (Kahraman and Markowski 2014). Severe hail has been reported in all of Turkey despite considerable topographic variability (Fig. 2.7).

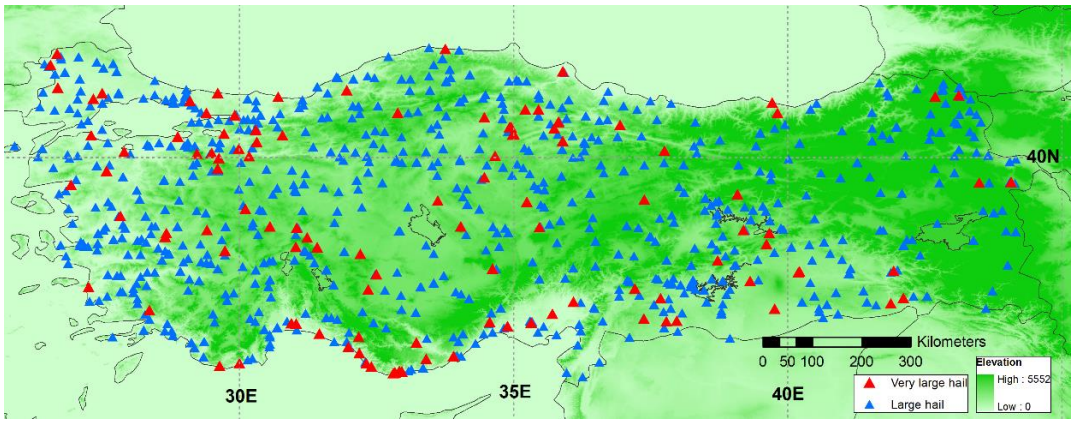

Figure 2.7 : Locations of large and very large hail cases in Turkey, and topography.

However, regional differences in severe-hail occurrences, as well as hail frequency overall (i.e., non-severe and severe hail), are evident in monthly distributions (Fig. 2.8). For example, in the winter, when hail frequency is a minimum nationwide, hail still poses a threat along the Mediterranean (southern) and Aegean (western) coasts, where the proximity to the relatively warm water presumably provides the instability required for hail. In March, the region of higher hail frequency begins expanding into the interior regions, and by April the inlands generally have a higher hail likelihood (especially severe hail) than the coastal regions, particularly southeastern Turkey, where there is a maximum in both severe-hail cases as well as hail days (e.g., at the Siirt observing station, hail is observed an average of 1.5 days in April). In May and June, the peak season for severe hail, severe hail is most likely in interior Turkey, although the maximum for hail days lies in northeastern Turkey, where peak frequencies approach 2 hail days per month. As hail frequencies decline in late summer and fall toward the winter minimum, hail probabilities decline most slowly in extreme northeastern Turkey.

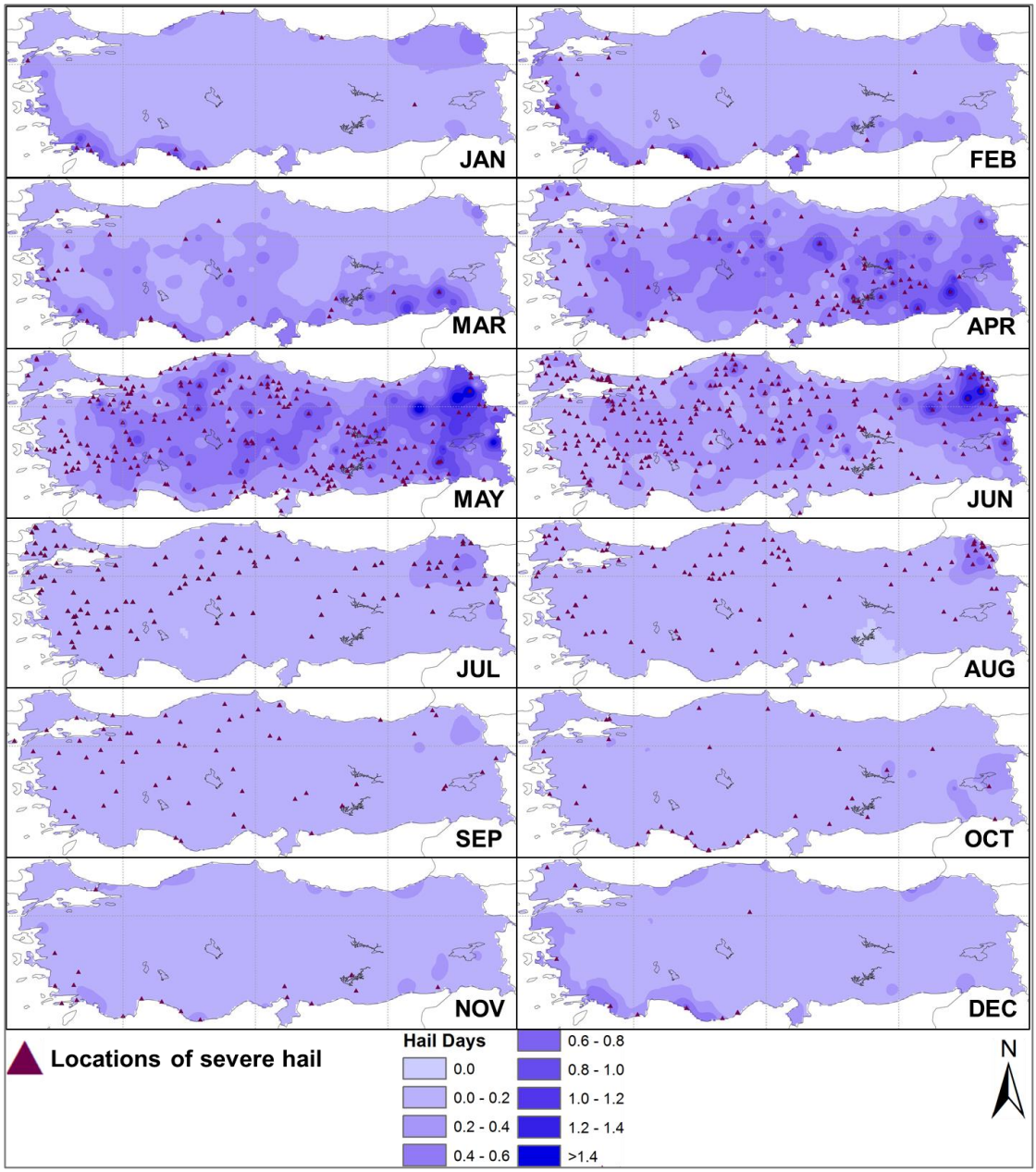

Figure 2.8 : Geographical distribution of (all) hail days (shaded) and locations of severe hail (red triangles) per month. (All) hail days data are from 277 stations of TSMS, 1960–2013. Data are bilinearly interpolated with Inverse Distance Weighting method (variable radius, 2nd power), on 263x100 grids.

2.2.2.4 Diurnal cycle

Severe hail is most frequently observed from 1200–1459 UTC (1400–1659 LST), with 230 cases, followed by 0900–1159 UTC (1100–1359 UTC), with 150 cases (Fig. 2.9). The peak is similar for very large hail; 19 of 45 very large hail events occur between 1200 and 1459 UTC. Severe hail with a diameter of 3.0–4.4 cm more frequently occurs than 1.5–2.9-cm diameter hail in evening hours (between 1500–1759 UTC and 1800–

2059 UTC). Of the cases with diameter of 6.0 cm or larger, the peak time interval is 1500–1759 UTC. However, severe-hail cases have a nighttime minimum, presumably owing to a combination of less frequent nighttime thunderstorms (Fig. 2.10) and underreporting.

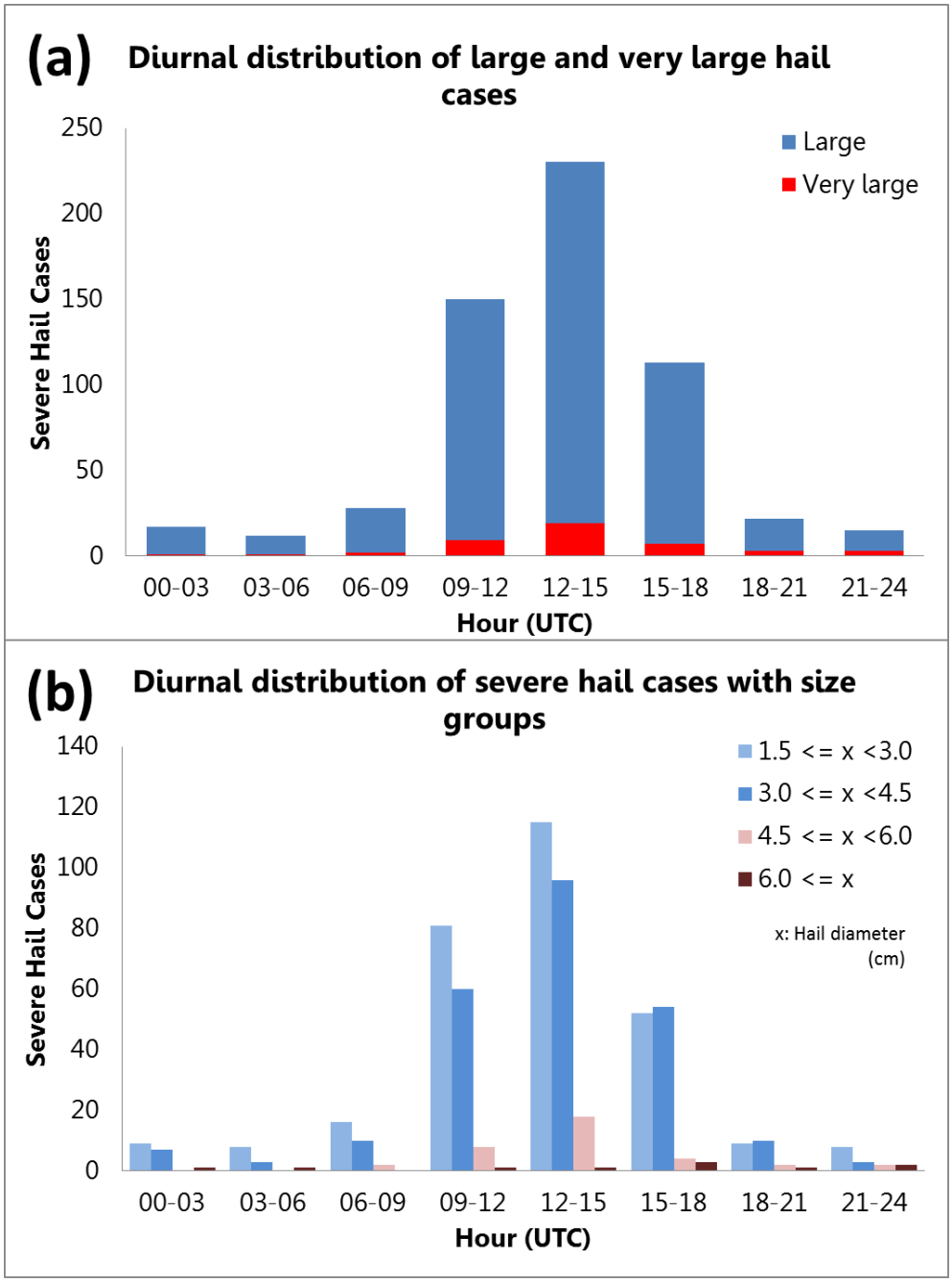

Figure 2.9 : Diurnal distribution of (a) large and very large hail cases, and (b) size groups for severe hail cases in Turkey.

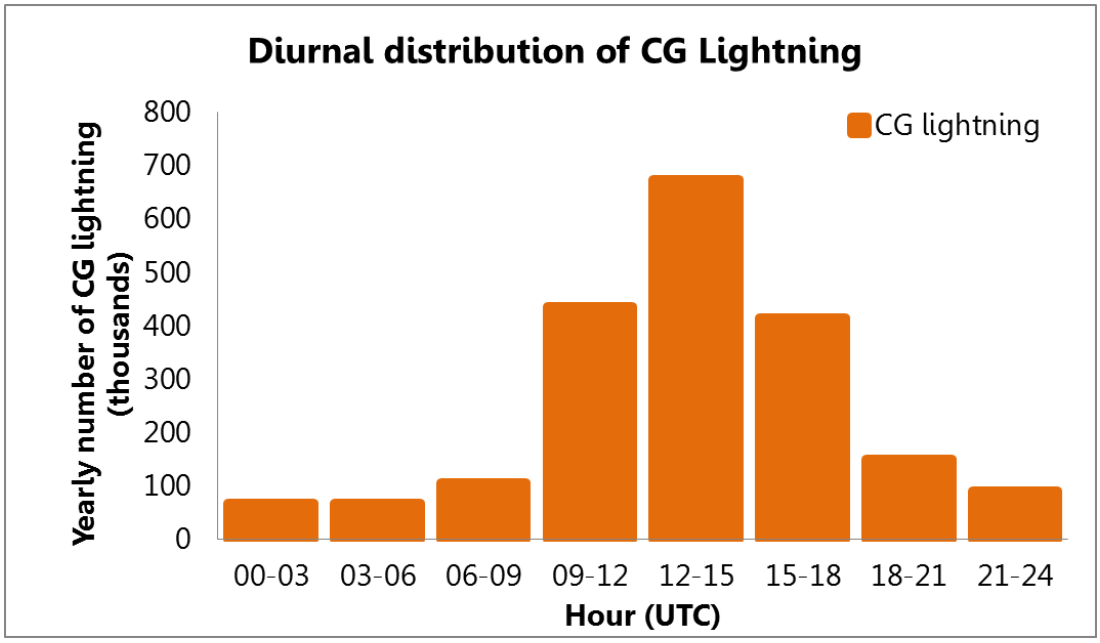

Figure 2.10 : Diurnal distributions of cloud-to-ground (CG) lightning in Turkey (yearly average with the data from 1 October 2011 to 30 September 2013 provided by Vaisala).

2.3 Severe Non-tornadic Winds in Turkey

2.3.1 Data and Methods

Archives of Cumhuriyet and Milliyet newspapers were scanned for the terms of 'fırtına', 'lodos' and 'şiddetli rüzgar'. Results were added to the previous dataset that had been obtained from Turkish State Meteorological Service archive. After elimination of duplicated ones 761 records gained in total for the events related with severe nontornadic winds. Afterwards, each record evaluated individually to determine whether it is related with convection or not. For this purpose, synoptic cards of GFS model reanalysis data for the time of each record were analyzed in terms of synoptic scale high pressure gradiant occurrence. The Lifted Index and the CAPE values are also considered when they are available. Furthermore, information that can be evidence for the presence of convection was taken into account, means that the duration of the event, width of the affected area, presence of convection related accompanying events (e.g., hail, lightning) were examined to prove if the event is convective or not. As a result 145 severe nontornadic wind events were assign as convcetive. Statistical analysis of the composed severe convective nontornadic wind dataset is given in the next section.

2.3.2 Results

Seasonal and monthly distributions of severe nontornadic convective wind events are shown in Fig. 2.11. Although the big portion of this events (51%) occur in summer they can occur in any time of year. They are most frequent in June, %33 of all events occured in this month and 15% in September.

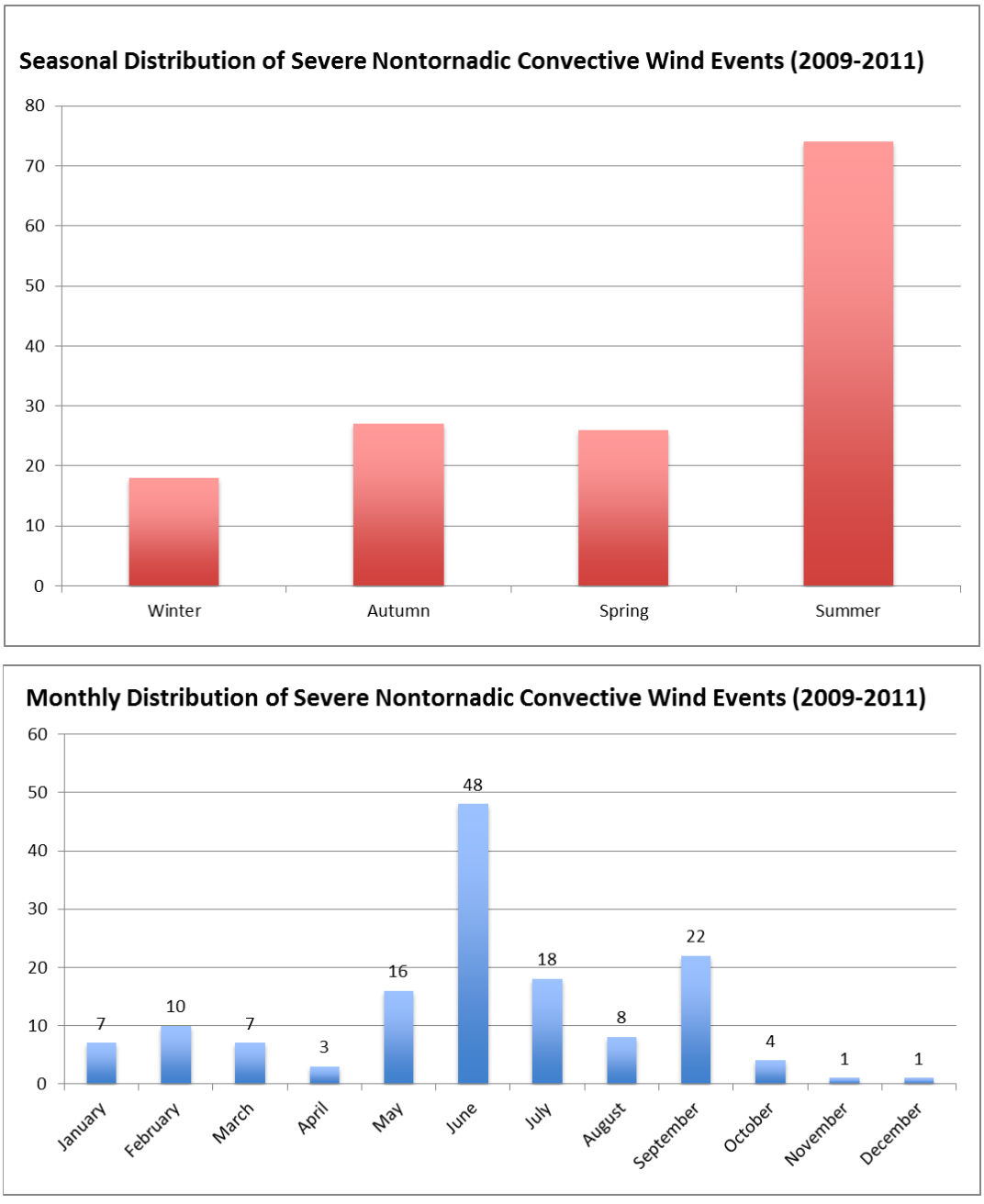

Figure 2.11 : Seasonal and monthly distribution of severe nontornadic convective wind events between January 2009–December 2011.

102 (70% of the all reports) reports were including storm duration information. Figure 2.12 shows durations of severe nontornadic wind events. Only two of them were longer than six hours and most of them continued for 1 to 3 hours (42%).

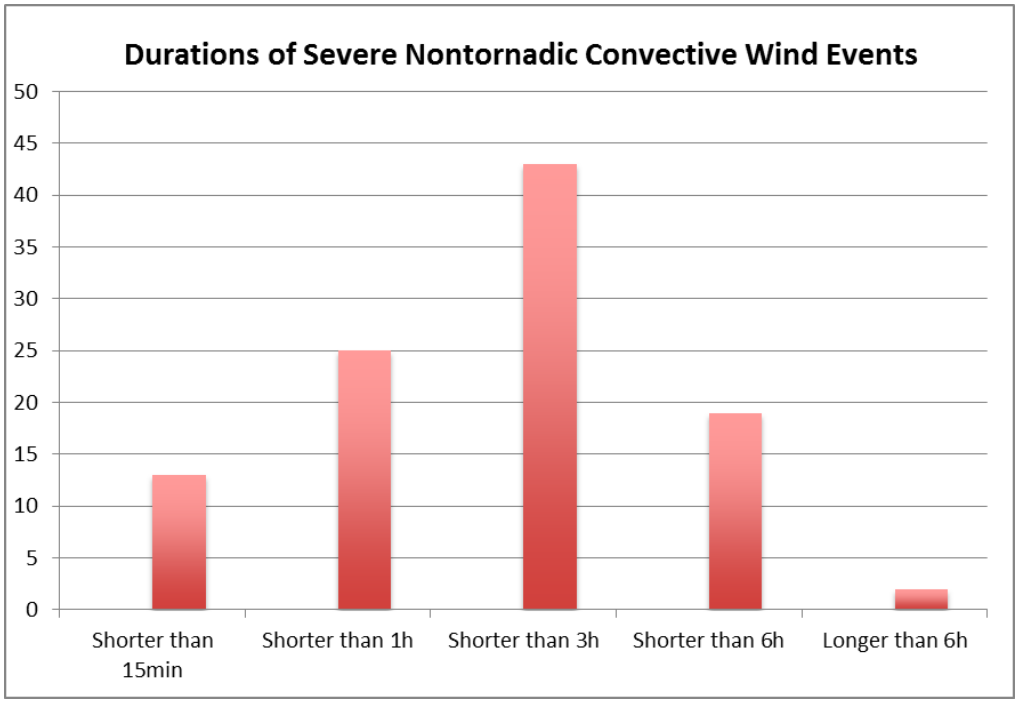

Figure 2.12 : Durations of severe nontornadic convective wind events.

3. IMPACTS OF SEVERE CONVECTIVE STORMS

3.1 Lightning Related Fatalities and Injuries in Turkey

Lightning is responsible for an estimated 24,000 fatalities and 240,000 injuries every year globally (Holle and Lopez 2003). In the USA (1959–2006) 101.2 people per year on average die due to lightning, a number that has decreased over time to about 45 per year by 2006 (Ashley and Gilson 2009). In Canada, 9–10 lightning-related deaths and 92–164 injuries occur every year (Mills et al., 2008). In the UK there were 2 fatalities per year on average for the period of 1988–2012 (Elsom and Webb, 2014). Average fatality per year was 230 in Mexico for the period of 1979–2011 (Raga et al, 2014). Table 3.1 shows average number of fatalities during a year per 1,000,000 population for some countries. Africa has the deadliest statistics. Although there are numerous difficulties that affect the compilation of such report-based datasets (e.g., data collection, population density distributions, socio-economic factors, telecommunication facilities), having these databases and related statistics is a necessity for each country for risk assessment.

Table 3.1 : Average fatality rates per million people per year for some countries.

Country	Average fatality rate per million people per year
USA (1959–2006)	0.44 (Ashley and Gilson 2009)
Canada	0.32 (Mills et al., 2008)
China (1997–2009)	0.31 (Zhang et al., 2011)
UK (1993–1999)	0.05 (Elsom, 2001)
Mexico (1979–2011)	2.72 (Raga et al., 2014)
Malawi	84 (Salerno et al., 2012)
Swaziland (2000–2007)	15.5 (Dlamini, 2009)

As in other parts of the world, Turkey experiences a large number of deaths and injuries due to convective storms, particularly with lightning. Over a 23-year period (November 1975 to October 1998) at the Ankara Numune Teaching and Research Hospital, 22 patients were treated for lightning burns (Aslar et al., 2001). Also, case studies in Turkey have been published in medical journals on the effects of lightning strikes on the human body (e.g., Alyan et al., 2006, Celiköz et al., 1996, Aslan et al.,

2004). Despite these studies, nationwide statistics on lightning deaths and injuries have not been compiled. The purpose of this paper is to compile a database on lightning-strike incidences that have killed or injured people in Turkey. The data is gathered from various sources from January 1930 to June 2014. Although finding all incidents throughout history and creating a complete database is not possible, existing records can be used to determine how frequent such lightning-strike incidences are, what their geographical distribution is, and what season or time of the day is most dangerous for people. Furthermore, some specific information (e.g., percentage of victims under trees) can help to create public awareness. Section 2 of this paper describes the data and the methods used. In particular, the sources of the records, how these sources were searched, and the characteristics of the records are described. Some observations on thunderstorms and lightning in Turkey are given in section 3. In section 4, statistics of the lightning incidents are presented. Section 5 summarizes the findings of this study.

3.1.1 Data Methods

Any lightning-strike event resulting in human injuries or fatalities is defined as an incident in this paper. Five sources were used to create a database of incidents: archives of the Turkish State Meteorological Service, electronic archives of two mainstream national newspapers (Cumhuriyet and Milliyet), European Severe Weather Database, and the internet (Fig. 3.1). These five data sources are presently described.

The first source was the Turkish State Meteorological Service climatological station dataset, which routinely report exceptional weather events, known as FEVK observations. FEVK is an abbreviation for the word fevkalade, which means "exceptional, extraordinary" in Turkish. These observations – which include the information on weather-related exceptional phenomena, human fatalities and injuries, and property damage – are stored in the headquarters as hardcopies since 1939. Scanned pdf and jpeg-formatted records were obtained and manually searched, yielding 220 lightning incidents. Approximately one third of all incidents (29.6%) were from this official source.

The second source was Cumhuriyet, a national newspaper with the biggest online archive in Turkey (Cumhuriyet archive, 2013). News from 1930 to the present week

is accessible to registered users of the archive who purchase a membership. This archive was searched for the Turkish word yıldırım ("cloud-to-ground lightning"), yielding 333 incidences. The biggest portion (44.9%) of the incidents was from this archive, as it covered the longest time range.

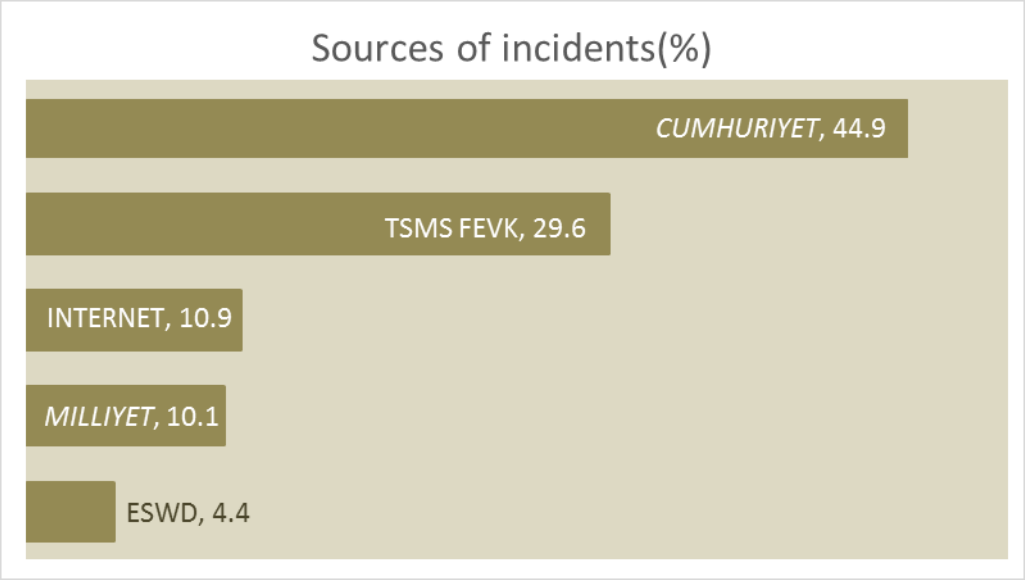

Figure 3.1 : Relative contributions of lightning incident data sources to the total dataset. TSMS is the Turkish State Meteorological Service, and ESWD is the European Severe Weather Database.

The third source was the online archive of Milliyet, another national newspaper, which was also searched for lightning events using the same method (Milliyet archive, 2013). This archive includes news from 1950 to 2004 and is freely available to registered users. Seventy-five incidences (10.1%) were from Milliyet. At the time of writing of this article, there are no other digital archives for old newspapers in Turkey.

A fourth source was the European Severe Weather Database (ESWD; http://www.essl.org/cgi-bin/eswd/eswd.cgi). The ESWD contributed 33 incidences (4.4%), although damaging lightning phenomena was introduced as a separate category in ESWD only in 2011.

A fifth source was the Google.com.tr searches with the keyword yıldırım from 1 January 2012 to 30 June 2014. Eighty-one incidents (10.9%) were found by internet searches. After including the internet searches and ESWD records, 42 incidents in each of 2012 and 2014 (as of June), and 34 incidents in 2013 were counted, which produced far more incidents than all other years in the previous decades.

Comparing all of these five sources led to only 17 duplicate reports. In case of a duplicate report, all available information from both sources was used. Then, the incident was assigned to the source containing the most informative report. After, gathering all records and sifting out the duplicates, a database was built consisting of 742 incidences from 1930 to 2014 in Turkey. These known lightning incidents resulted in 895 fatalities, 149 serious injuries, and 536 other injuries. Injuries mentioned as serious in the reports were classified as serious injury in the database.

One weakness of the newspaper-based records was that the exact date of some incidents may not be known as the occurrence may be listed as "last week" or "the previous day". When there is no precise information about the exact date of the event, but the month is known, the month is used in relevant figures and classifications, but unreliable situations are not included in these statistics. Towns or villages that changed their name were another important problem with old records. Further investigations were done to find the correct geographical locations of the old records that took place in a renamed town or village (e.g., , Issızviran Village is now called Issızören Village, Şeytanbudaklar Village is now called Uluçam Village, Rizok Village is now called Oymak Village).

3.1.2 Results

Because the dataset is not homogeneous throughout the period, it is not possible to talk about the incident trends with confidence. However, an increasing number of lightning causalities and injuries in the 1950s and 1960s, and a decrease in late 1980s and 1990s, are notable (Fig. 3.2). According to the Turkish Statistical Institute, the population of Turkey increased rapidly from 1939 to 2012, from 20 million to over 75 million (see ahead to Figure 3.9) (http://www.turkstat.gov.tr/Start.do). Due to the unrepresentativeness of the historical data and missing records, determining the average mortality rate for a long period was not possible. With the inclusion of incidents from the ESWD and internet, the number of incidents are quite high for the last three years. The total number of fatalities was 31 persons in 2012 (0.42 per million), 26 persons (0.35 per million) in 2013, and 25 persons (0.34 per million) in 2014 (January–June). The total number of injuries was 36 persons (0.49 per million) in each of 2012 and 2013, and 62 persons (0.84 per million) in 2014 (January–June).

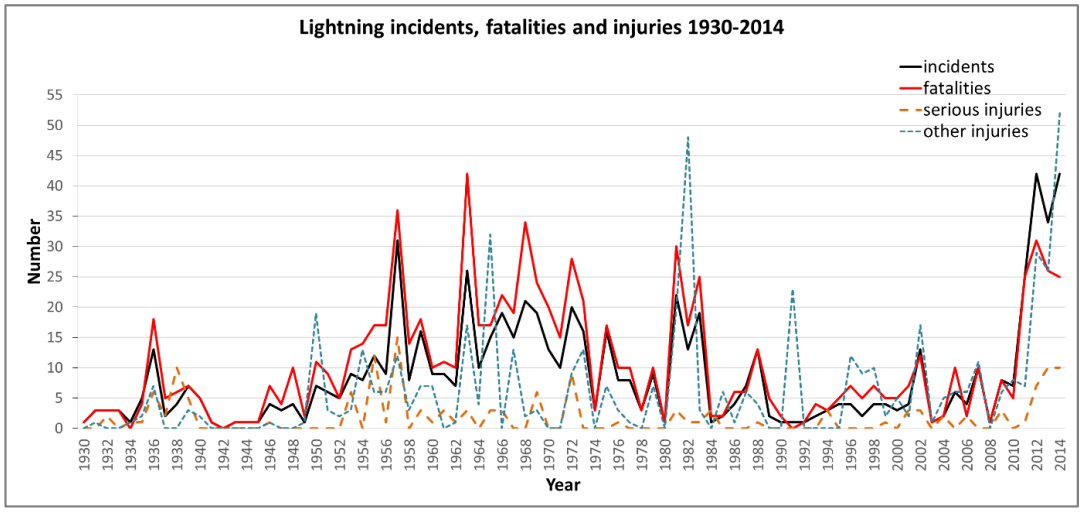

Figure 3.2 : Number of lightning incidents, fatalities and injuries (serious and other) per year (January 1930 to June 2014).

Monthly and diurnal distributions of the incidents and some other aspects of the incidents (e.g., the places of occurrence, the genders of victims) are analysed. Most of the incidents (89%) occurred from April through September with a peak in May and June (26% and 28%), followed by July (14%) (Fig. 3.3). Sixty-seven percent of all incidents occurred in these three months. Incidents peaked in late spring, similar to the peaks in thunderstorm and lightning observations (Figures 2.1 and 2.3a). This peak was also consistent with the Turkish severe storm climate, as the large hail and continental tornado frequencies increase in Turkey around May (Kahraman and Markowski, 2014; Kahraman et al., 2015). Another reason for this peak is the increasing number of human activities that move outside in the spring, particularly during agriculture and shepherding.

There were local or UTC time information in 136 of the reports. Local times were converted into UTC; local time is UTC+2 in Turkey from October to March and UTC+3 from April to September due to daylight savings. More than half of all incidents (54%) occur between 9–15 UTC (Fig. 3.3), which is as expected considering the increasing number of lightning at this time of the day (Fig. 2.3a). Some other severe storm-related phenomena (i.e. severe hail and tornadoes) are also most frequent in the afternoon in Turkey (Kahraman and Markowski, 2014; Kahraman et al., 2015). Incidents are rare during the night.

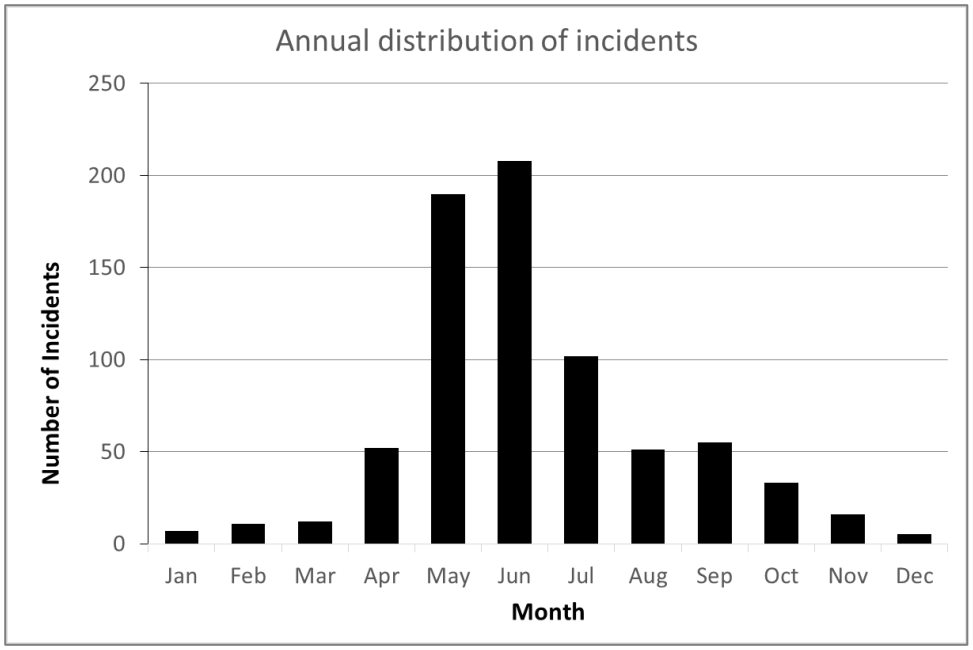

Figure 3.3 : Annual distribution of the total number of lightning incidents by month (January 1930 to June 2014).

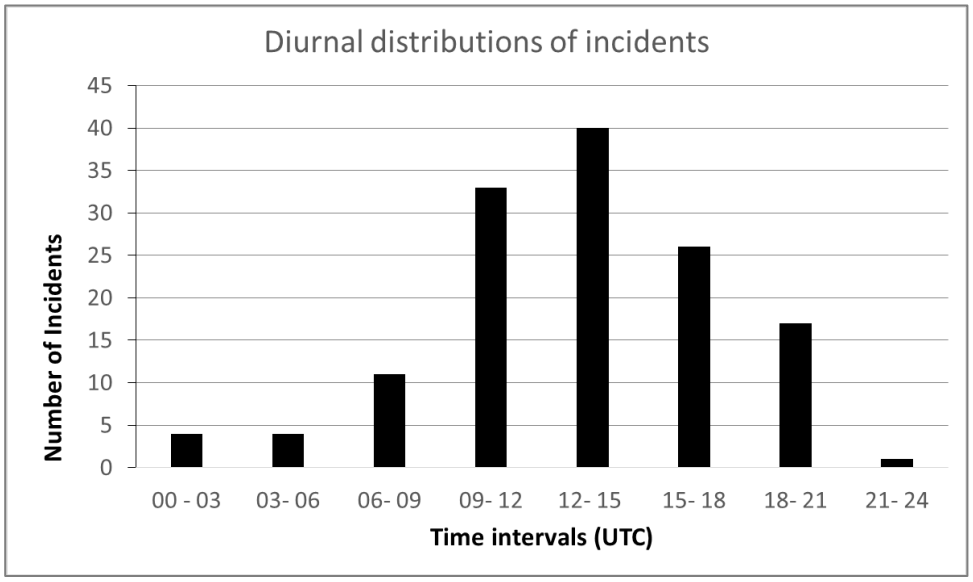

Figure 3.4 : Diurnal distribution of the total number of lightning incidents by 3-h period (January 1930 to June 2014). Local time in Turkey is UTC+2 from October to March and UTC+3 from April to September due to daylight savings time.

There are more incidents near highly populated areas, namely western Turkey and especially Istanbul (Fig. 3.5). There is also a lower density of incidents over central Turkey. The lowest density of lightning over central Turkey and relatively low density over eastern Turkey were similar to the geographical distribution of lightning-related incidents (cf. Fig. 2.2 and 3.5). The number of incidents in Istanbul is higher compared

to the other regions with the same stroke density, because of the massive population of the city (number of the incidents occurred in Istanbul is 40 which is 5.4% of all incidents, whereas stroke density over the city is about 0.5–2 km–2 year–1).

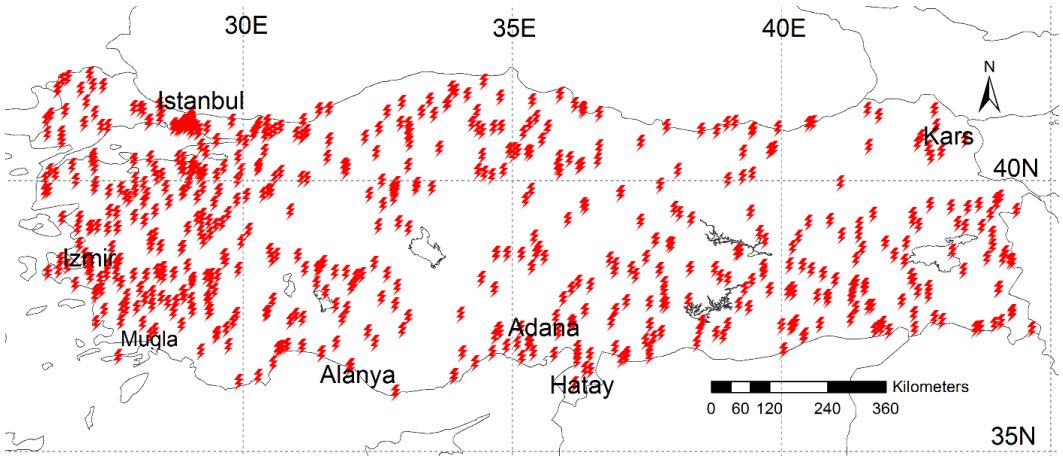

Figure 3.5 : Locations of lightning incidents resulting in fatalities, injuries, or both in Turkey (January 1930 to June 2014). Multiple fatalities and injuries may occur at each red point.

The geographical distribution of lightning incidents for each month (Fig. 3.6) suggests that the relatively rare occurrences in winter months almost always happened along the southern and western coasts, which follows the thunderstorm climate (Fig. 2.1). The number of incidents increased in south-eastern Turkey in April. By May and June, incidents occurred in all parts of Turkey. By July, the number of incidences in the east began to decline, and, after August and September, the number of incidents sharply decreased across most of Turkey.

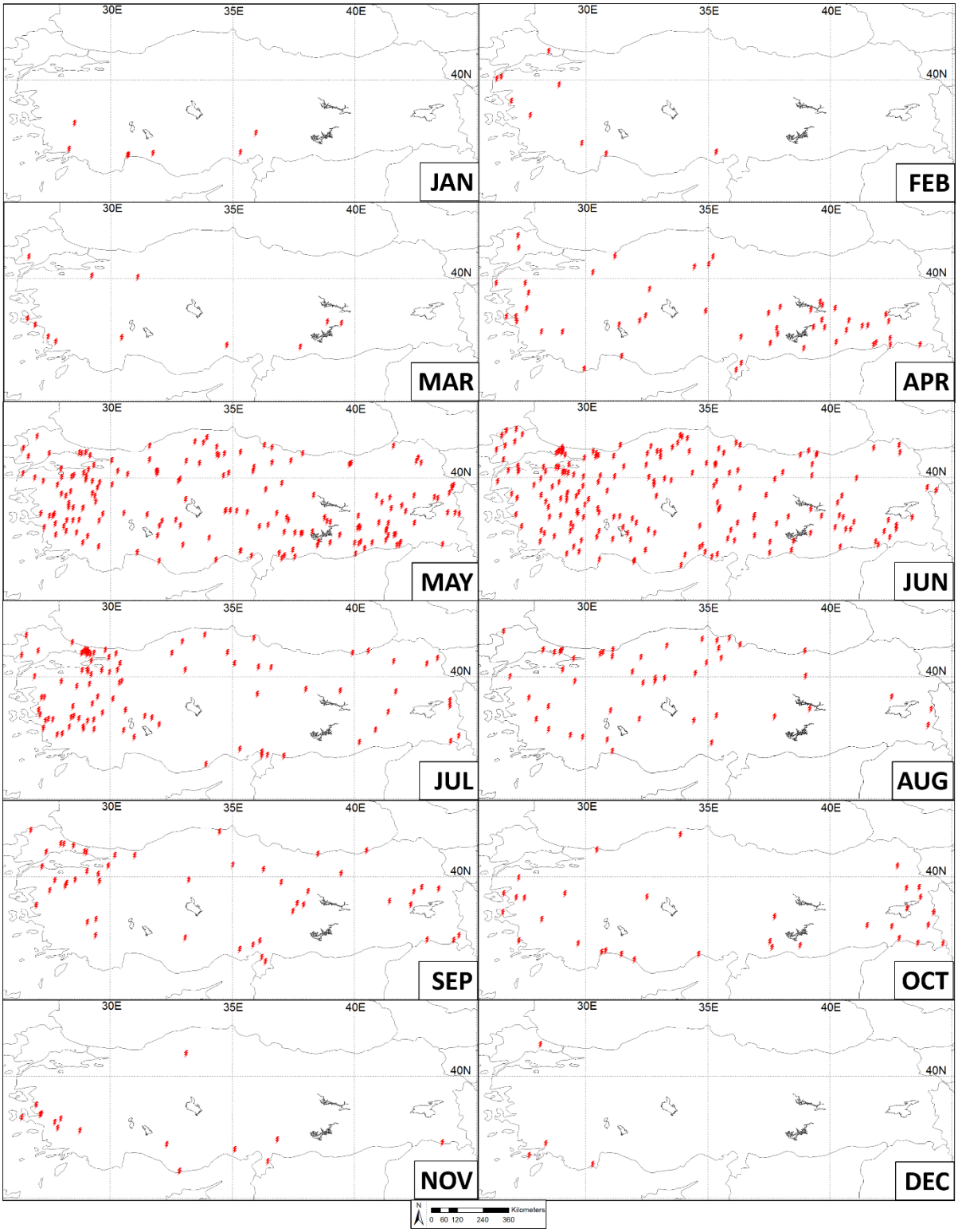

Figure 3.6 : Locations of lightning incidents resulting in fatalities, injuries, or both by month (January 1930 to June 2014). Multiple fatalities and injuries may occur at each red point.

Of the 1580 people in our database who were killed or injured, the gender of 849 (53.7%) was known. For 578 fatalities, 386 (67%) were male and 192 (33%) were female (Fig. 3.7). These values are more balanced than for other countries. For

example, comparing the gender of lightning fatalities in the US from two datasets 100 years apart shows that the percentage of events resulting in only male fatalities was over 70% in the 1890s, but rose to 80% in the 1990s (Holle et al., 2005). In Canada, 84% of all lightning fatalities (1921–2003, excluding 1950–1964) were male (Mills et al., 2008). The percentage of male fatalities is also large in Mexico: 79% (Raga et al, 2014). In contrast, the Turkish data were more comparable to that in the United Kingdom (1993–1999) where 72.7% of deaths were male (Elsom, 2001).

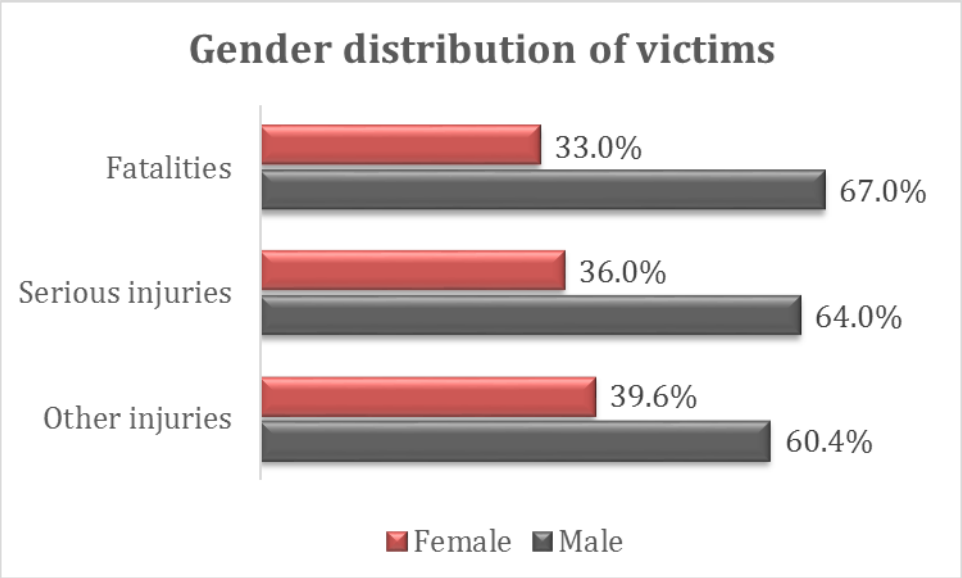

Figure 3.7 : Gender distribution of lightning victims by fatalities, serious injuries, and other injuries (January 1930 to June 2014).

The percentage of men and women with serious or other injuries is not that different from that of the fatalities (Fig. 3.7). Combining all three categories in Fig. 3.7, 553 of 849 people struck by lightning were men (65%) in Turkey, just like the 65% in the UK (Elsom 2001). The reason why men are twice as likely to be struck than women is that men are more likely to be doing outdoor jobs. However, the female fraction is higher compared to the statistics from the other countries, which is presumably because more women work in agriculture in Turkey than the others. The percentage of female employment in agriculture is 37% in Turkey (2012), whereas it is 1% in US (2010), 1% in Canada (2008), 4% in Mexico (2011) and 1% in UK (2012) (Data retrieved from The World Bank website:

http://data.worldbank.org/indicator/SL.AGR.EMPL.FE.ZS/countries/1W-CA-GB-US-MX-TR?display=map).

Age information was available for a small number of events. Out of a total number of 369 incidents where ages were known, ages of 258 (29%) deaths, 47 (32%) seriously injured and 64 (12%) injured victims were known. Most of the victims were young people; 59% of deaths were younger than 30. Similarly, 66% of seriously injured victims and 63% of injured victims were younger than 30 (Fig. 3.8).

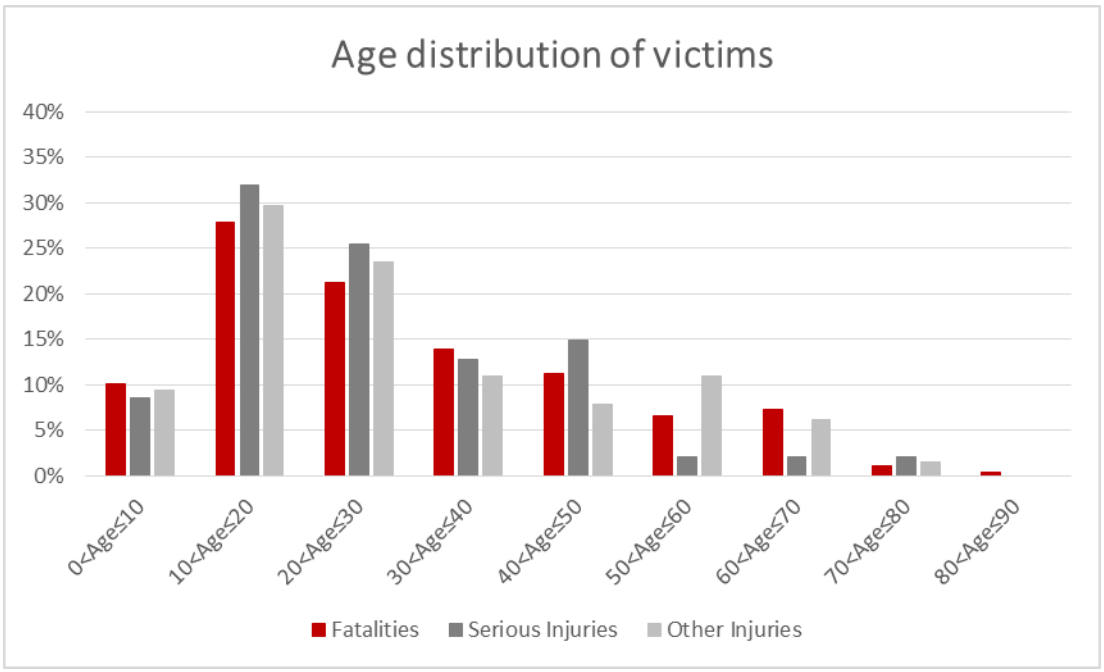

Figure 3.8 : Age distribution of lightning victims by fatalities, serious injuries, and other injuries (January 1930 to June 2014).

If an incident occurred in a province or district centre, then it was categorized as urban. If an incident occurred in a town or village, then it was categorized as rural. Most of the incidents (86%) occurred in rural areas and only 14% in urban areas, with 367 records having this information. In the 1950s, only 25% of the population was living in urban areas, whereas, by the 2000s, 70% of the population was living in urban areas (Fig. 3.9). In each year, the number of incidents was always higher in rural areas during the period (Fig. 3.10). The percentage of urban incidents was relatively higher for the 1920s–1950s and the 1990s. Relative minima are also present in the total number of incidents for the 1940s and 1990s, suggesting that the higher urban incident rates can be result of socioeconomic issues that probably affected the reporting from rural areas. For example, poverty due to World War II can be the reason for underreporting from rural areas for the 1940s.

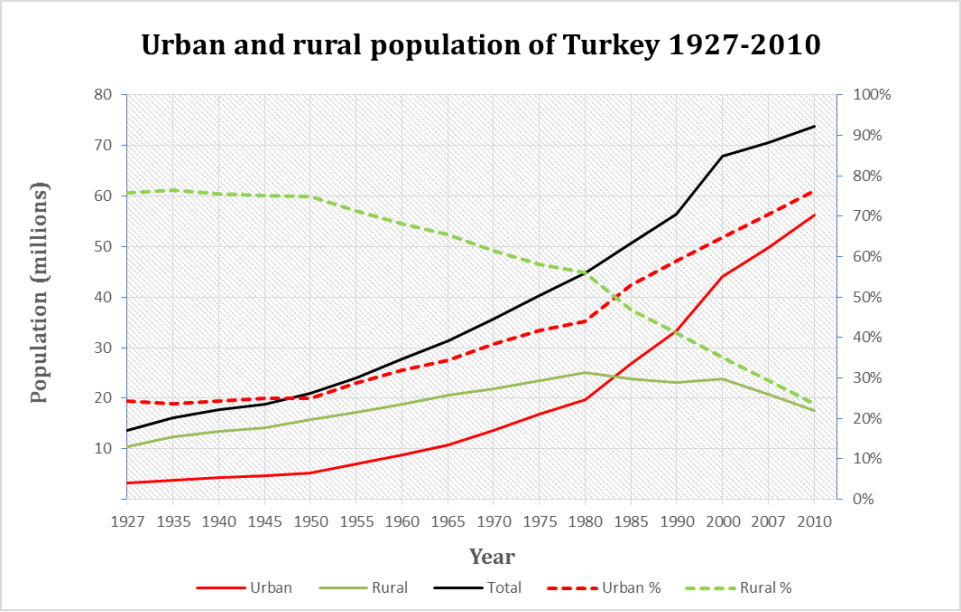

Figure 3.9 : Population distribution of Turkey in rural vs urban areas between 1927 and 2010 and rural vs urban percentage in total population for each survey year. The time interval between survey years varies before 1935 and after 1990 (Turkish Statistical Institute).

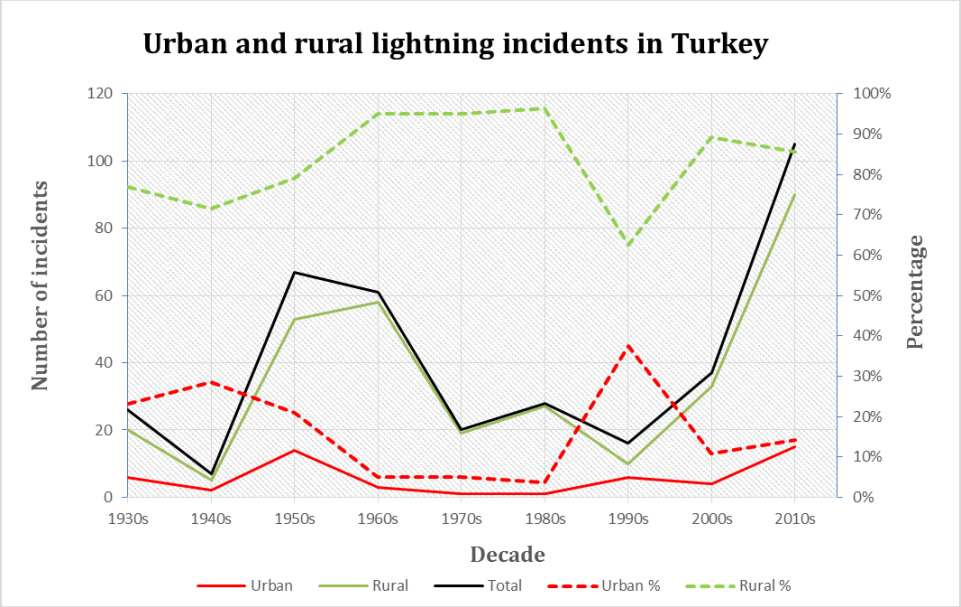

Figure 3.10 : Number and percentage of urban and rural lightning incidents in Turkey by decade between the 1930s and the 2010s ("2010s" include data from January 2010 to the end of June 2014).

Reports show that 71 of the incidents occurred on farms. Victims of 112 incidents were shepherds, which contributed to the rural occurrences. Hiding under a tree, a common behaviour during heavy rain and hail, resulted in 94 fatalities, 25 serious injuries and 85 other injuries due to lightning striking the trees. There were 53 indoor incidents with 53 fatalities, 20 serious injuries and 66 other injuries, usually in farm cottages.

Some of the incidents appeared during transportation. Three people died and one other injured while riding horses. There were 2 incidents with lightning striking cars, causing 5 fatalities and 1 injury. One of the incidents occurred on 5 July 1963 in Kars Province in a rural area in northeastern Turkey (location in Fig. 3.5) while a family was going to their home from the farm. It resulted in 2 deaths and 1 injury. There was no specific information about the event nor the features of the car that would explain why the Faraday cage of the vehicle did not protect the family. The second incident occurred on 22 February 1993 while a car was on its way to Izmir from Alanya. In this case, the lightning strike to the car resulted in a traffic accident, causing 3 fatalities.

4. CLIMATOLOGY OF SEVERE CONVECTIVE STORM ENVIRONMENTS

4.1 Data and Methods

To establish the climatology of severe convective environments for the 35-y period, ECMWF Era-Interim data from 1 January 1979 to 30 December 2014 were interpolated on a limited area domain under a Lambert conformal map projection. Era-Interim data has 0.75° horizontal grid spacing (approximately 80 km), 28 vertical levels, consisting of 1 surface level and 27 pressure levels from 1000 hPa to 100 hPa and available with 6 hours interval (00 UTC, 06 UTC, 12 UTC, 18 UTC). Because 12 UTC is the most active time in terms of convective storms for the selected domain (Fig 4.1), 12 UTC reanalyses data for each day were used.

Figure 4.1 : The areal coverage of used ECMWF Era-interim data (inner box).

Deep moist convection requires conditional instability, enough moisture for the parcel to have a level of free convection (LFC), and lift for the parcel to reach its LFC (Doswell et al., 1996). Vertical wind shear is also a important component in terms of storm organization. Some stability and vertical wind-shear variables were calculated from reanalysis data. The next section explains used environmental parameters and calculation methods in detail.

4.1.1 Convective storm related environmental parameters

Specifically, the climatology consists of surface-based convective available potential energy (SBCAPE), mixed-layer convective available potential energy (MLCAPE), most unstable convective available potential energy (MUCAPE), surface-based convective inhibition energy (SBCIN), mixed-layer convective inhibition energy (MLCIN), most unstable convective inhibition energy (MUCIN), surface-based lifting condensation level (SBLCL), mixed-layer lifting condensation level (MLLCL), 0–6-km wind shear, 0–3-km wind shear, 0–1-km wind shear, and mid-tropospheric lapse rate (LR7050).

Convective Available Potential Energy (CAPE) is a nonlinear combination of the two proper ingredients: moisture and conditionally unstable lapse rates. It is a measure of atmospheric instability and gives information on the strength of thunderstorm updrafts. Comparison between observed convective cloud-base heights and LCL for surface based parcel and mean-layer parcel supports the usage of mean-layer parcel instead of surface-based parcel even in the warm season during the afternoon (Craven et al., 2002). In this study, both SBCAPE and MLCAPE were calculated. For MLCAPE, mean values for the lowest 500 m were used. Additionally, MUCAPE values were also calculated to enquire the elevated convection related environments. Parcel with the highest Theta-E in the layer below 500 mb were used for MUCAPE calculations.

CIN is the "negative" area on a sounding that must be beaten for storm initiation. In this study, SBCIN, MLCIN and MUCIN values were calculated. MUCINs were calculated for the parcel with highest Theta-E in the layer below 500 mb. For MLCIN, the mixed layer depth were specified as 500 m.

All parameters were calculated on each grid point of the domain for the whole period for 12 UTC. For the CAPE and CIN calculations, a Fortran code by George Bryan was

wrapped into NCL (NCAR 2015) with a 100 Pa pressure increment modification (The code is available at http://www2.mmm.ucar.edu/people/bryan/Code/getcape.F).

LCL calculations were done using well-known Espy's equation (Espy, 1841).

$$h_{LCL} = \frac{T - T_d}{\Gamma_d - \Gamma_{dew}} = 125(T - T_d) \quad (4.1)$$

Where Γ_d is dry adiabatic lapse rate, Γ_{dew} is dew point lapse rate, T is temperature, T_d is dew point temperature, and finally $h_{LCL}$is the height of the LCL.

For the shear calculations, horizontal wind components at specific height levels were calculated with linear interpolation between the pressure levels above and below the level using NCL.

Mid-tropospheric (700–500-hPa) lapse rates were also calculated. After calculation of these environmental parameters, averages for each month were calculated for each year and then for long-term.

4.2 Results and Discussion

4.2.1 Longterm monthly means

4.2.1.1 Convective available potential energy

Long-term monthly means show that, in the cold season, there is only small amount of SBCAPE over the Mediterranean Sea and Atlantic Ocean, whereas there is no SBCAPE over Europe, Turkey and Arabian Peninsula in general. Abundant SBCAPE is available over the ITCZ region and Red Sea, even in the cold season (Fig A.1). In early spring, SBCAPE becomes much more widespread around the Mediterranean coasts, southern Europe and interior Turkey (Fig A.2). Highest European average SBCAPE values occur on June, July and August over Iberian Peninsula, Italy and Balkans (Fig A.3). In the same season, averages reach 5000 J kg^{-1} in some parts of Red and Arabian Seas while maximum average SBCAPE values exceed only 100 J kg^{-1} over some regions of the Scandinavian Peninsula and UK, and 200 J kg^{-1} around the Baltic coasts. In September, mean SBCAPE values are still high around Mediterranean coasts with maxima over African coast of central and western Mediterranean Sea and Cyprus. Another remarkable point is higher values around Northeastern Turkey.

During the autumn, values are decreasing gradually with month, mostly keeping geographical distribution pattern. Southerly migration of ITCZ is observable in Fig A.4. In November, values are less compared to the beginning of autumn.

Fig A.5 shows long term monthly means of MLCAPE for the months of December, January and, February. In this season, mean MLCAPE values are below 100 J kg^{-1} almost all over the domain. Around ITCZ region and some parts of Red Sea, values are higher. In February, MLCAPE values reach 300 J kg^{-1} over a small region around southwest hillside of Himalayas around Lahore. In spring, values get higher and widespread (Fig A.6). During March, mean MLCAPEs are still smaller than 100 J kg^{-1} over Europe, Turkey and Northern Africa, with very small regional exemptions. Values get higher than 200 J kg^{-1} over eastern parts of Turkey in April, and finally over southern Europe in May. MLCAPE maxima migrate with ITCZ (Fig A.6 and Fig A.7).

Fig A.7 shows monthly means for summer. European MLCAPE values get higher with month during summer, and in August values are over 100 J kg^{-1} all over Europe except northern Scandinavia and UK. Maxima occur over Italy and Mediterranean coasts of Spain, values reach 600 J kg^{-1} locally. Mediterranean coasts of Africa also experience their highest mean MLCAPE values in August. Extreme values are remarkable around Red Sea and Arabian Sea and southwest hillside of Himalayas during summer, especially in July and August. Siberia has its highest mean MLCAPE values in July.

In September, values are close to the ones in August around the southern parts of the domain. Values get lower gradually with month during the autumn (Fig A.8).

To sum up, MLCAPE field exhibits a similar seasonal cycle to SBCAPE with lower values as expected since 12 UTC reanalysis data used for calculations. The ITCZ, Mediterranean Sea, Red Sea and Arabian Sea clearly exert a dominating influence on the CAPE distribution patterns over the domain. Influence is not limited to directly over the seas but is noted over the coasts of these seas. Seasonal cycle of CAPE fields is very clearly defined with larger values during summer than in the winter for all over the domain. For the transition seasons, CAPE values are higher in autumn than spring over Mediterranean, Red and Arabian Seas and neighboring countries as expected. After peak summer insolation, these large water bodies remain warm for several weeks and perform as intense heat and moisture sources. This effect is visible lessly over

southern parts of Black Sea and Caspian Sea due to lower insolation, related with their higher latitudes.

MUCAPE is useful to assess elevated instability. Difference between mean SBCAPE and mean MUCAPE values over a region can give information on the climate of the region. Higher average MUCAPEs indicate that the climate of the region favours elevated convection more than surface-based convection. Fig A.9– Fig A.12 shows the monthly mean values for MUCAPE.

In the cold season, from December to March, MUCAPE values are slightly higher than SBCAPE values over Red Sea, next to south coasts of Saudi Arabia, and Gulf of Aden. In the warm season, excessiveness of MUCAPE occurs over Southern Adriatic Sea next to coasts of Italy, Eastern Mediterranean Sea around southeast coasts of Turkey, and around southwest foothills of Himalayas. Excessiveness of MUCAPE is visible from June to September over Eastern Mediterranean Sea and June to November over Adriatic Sea. From August to October, MUCAPE values are slightly higher than SBCAPE values over Kyrgyzstan. In September, another excessiveness of MUCAPE occurs over a small area of Southern Caspian Sea.

4.2.1.2 Convective inhibition energy

In general, CIN values are higher in warm season comparing cold season. In all seasons, higher CIN values are found over seas and, peak SBCIN values occur over North African coasts of Atlantic Ocean and Oman coasts of Arabian Sea in July and August. Mean SBCIN values are almost always less than 25 J/kg over lands during year for whole domain. MLCIN values are more widespread and higher comparing SBCINs.

CIN fields exhibit a similar seasonal cycle and geographical distribution pattern with CAPE fields in general. There are some exceptions: North African coasts of Atlantic has highest CIN values during year while CAPE values are not too high due to sparse low level moisture. On the other hand, ITCZ region has high CAPE values whole year with very small CIN values, emphasizing the favourable conditions for deep moist convection in those areas on the average. Lastly, during warm season, when SBCAPE values get higher and widespread over Turkey and continental Europe, SBCIN values are still lower than 25 J/kg.

4.2.1.3 Lifting condensation level

The Lifting Condensation Level (LCL) is the pressure level, at which a lifted parcel reaches saturation when lifted dry adiabatically. During the ascent, the air parcel gets colder, that results in degreasing saturation mixing ratio. The level when the mixing ratio of parcel gets equal to its saturation mixing ratio is called as LCL. It is a proxy for cloud base, and important parameter in terms of tornado forecasts. Many studies have suggested that supercell tornado environments are usually associated with low lifting condensation level heights (e.i., Rasmussen and Blanchard 1998; Thompson et al. 2003). Figure A.25–A.28 show the surface based LCL height distribution, and Figure A.29–A.32 show mixed layer (lowest 500m) LCL height distribution for each month.

4.2.1.4 Wind shear

The vertical wind shear has an important influence on storm type; it tends to promote storm organization and longevity (Markowski and Richardson, 2010). Figure A.33–A.36 show the average 0–6-km wind shear values, Figure A.37–A.40 the average 0–3-km wind shear values, and finally Figure A.37–A.40 the average 0–1-km wind shear values for each season. According to the figures, leading factors for the strength of wind shear are the location and strength of jet streams. With the strengthening of the jet stream during winter, the highest average 0–6-km wind shear values occur beneath the jet regions. Overlapping of ingredients seems most probable during spring over a zonal belt including southern Europe, northern Africa and Turkey. Another finding is large 0–1-km wind shear values over the Arabian Sea and Somalia from June to September, related to the Somalia low-level jet. This region is notable considering the extreme CAPE values available at that time of the year together with these large wind-shear values.

4.2.1.5 Mid-tropospheric lapse rate

Lapse rate is the rate of temperature change with height. When temperature decreases with height faster, lapse rate gets steeper. And steeper lapse rates indicate more unstable atmosphere. Values less than 5.5–6°C/km (moist adiabatic lapse rate) represent stable conditions, while values near 9.5°C/km (dry adiabatic lapse rate) are considered as absolutely unstable. And lapse rate values between these two values are considered as conditionally unstable. In case of conditional instability, stability of the

atmosphere depends on the amount of available moisture. Figure A.45–48 show the distributions of mean mid-tropospheric (700–500-hPa) lapse rates over the domain for each month.

4.2.2 Significant severe parameter (Composite instability/shear parameter)

Previous research shows that, individual parameters did not discriminate well between severe and non-severe deep moist convection. Considering instability and shear together improves discriminaton sharply (e.g., Davies and Johns 1993, Johns et al., 1993, Craven and Brooks 2004, Gensini and Ashley 2011). Craven and Brooks (2004) defined the product of MLCAPE and 0–6-km shear as "significant severe parameter" (m^3 s^{-3}) in the study that they evaluated rawinsonde data (approximately 60,000 soundings) from the lower 48 United States. And they showed that this parameter resulted in a noticable discrimination between thunder events and the significant hail/wind and tornado events. They offered thresholds of 10,000 m^3 s^{-3} (for severe), 20,000 m^3 s^{-3} (for significant hail/wind), and 30,000 m^3 s^{-3} (for significant tornadoes) considering the distributions of this instability/shear parameter. Later, Gensini and Ashley (2011) defined a C composite index using the products of 0–6-km bulk wind difference (BWD) and MUCAPE. They used 20,000 m^3 s^{-3} threshold for determining significant-severe environment in NARR data. Comparisons of the C composite index distribution with reports were satisfying.

In this research, product of MLCAPE and 0–6-km wind shear were calculated over each grid point of the domain using ERA-interim data. Assuming that the environments that produce severe convection in the United States would produce severe convection in our domain, number of days with instability/shear parameter over the same thresholds was enquired. Fig B.1–Fig B.4 show distribution of mean number of days with significant severe parameter over 10,000 m^3 s^{-3}.

In cold season, (from December to February) significant parameter values reach to 10,000 m^3 s^{-3} only for a few days, over small regions of southwest hillside Himalayas, around ITCZ, Red Sea and Gulf of Oman.

During March, enviroments that are favourable for convective storms are still limited over small regions around Red Sea, Gulf of Oman, southwest hillside Himalayas, and Arabian Peninsula for a few days. However values are extremly higher around ITCZ region (i.e., 24−25 days).

By April, storm favouring enviroments get more widespread and reach South Eastern parts of Turkey. Still no occurence over Europe. For Southern Europe, number of days with significant parameter over 10,000 m^3 s^{-3} starts getting higher in summer with a peak at August.

Favourable environments are most widespread over Turkey during May. However, higher number of days occur around the coastal areas in summer, especially over Eastern Black Sea and Eastern Meditteranean coasts. Higher number of days remarkable around these two regions even in September while inlands of country experiencing zero favourable days in average.

After October, number of days gets less all over the domain gradually and finally gets limited only over Seas, ITCZ and around southwest hillside Himalayas in November.

Distributions of mean number of days with significant severe parameter over 20,000 m^3 s^{-3} are shown in Fig B.5–Fig B.8. In cold season, distributions follow a similar pattern with the number of days passing first threshold, however, with lower numbers. During March and April, they are still limited around the same regions. In May, a few number of favourable days (significant parameter>20,000 m^3 s^{-3}) occur over very small regions around nothern coasts of Africa and Georgia, Azerbaijan and Tehran.

For Europe and North African coasts number of favourable days (with significant parameter>20,000 m^3 s^{-3}) is higher during late summer. Peaks occur in August for Southern European coasts and in September for Noth African coasts.

Fig B.9–Fig B.12 show the distribution of number of days with significant severe parameter over 30,000 m^3 s^{-3} for each month. During cold season, number of favourable days (with significant parameter>30,000 m^3 s^{-3}) is zero in average nearly all over the domain. In early spring, there is no significant change. Occurence of higher values starts at late spring around the ITCZ region, particularly over Arabian Sea. During June and July, numbers get higher but still stay limited over the same regions. In August, there are a few favourable days (significant parameter>30,000 m^3 s^{-3}) around south coasts of Europe and north coasts of Africa. In November, no favourable days (significant parameter>30,000 m^3 s^{-3}) available over the domain except Red Sea and Persian Gulf.

No number of favourable days with significant parameter values over 30,000 m^3 s^{-3} occures in Turkey over the course of a year.

The spatial and temporal distributions of significant severe weather environments and severe storm related event reports show strong similarities. For example, May and June is the peak season for severe hail, while the significant severe parameter is most widespread over Turkey during this months. Additionally, similarity of late summer, early fall peak of hail days around northeastern Turkey and high values of significant severe parameter over the region during the same season is remarkable.

Comparisons with thunderstorms days data is also satisfiying. Thunderstorms are most frequent in May and June all around Turkey, especially over the inland and northeastern parts when the significant severe parameter has its higher values over these regions. The maximum thunderstorm frequency shifts to the Aegean and Mediterranean coasts from late autumn to early spring, while the rest of Turkey has relatively infrequent thunderstorms. Accordingly, during late autumn, significant severe parameter has its highest values around the Aegean and Mediterranean coasts while approximately no favourable days are available over the rest of the country in average.

5. CONCLUSIONS AND RECOMMENDATIONS

This dissertation presents report-based climatologies of some severe convective storm related events in Turkey, specifically severe hail and severe nontornadic winds. The severe hail climatology part of the reseach shows that severe hail (≥1.5 cm) is observed to be associated with a variety of thunderstorm types in Turkey and can occur in any season of the year. However, very large (≥4.5 cm) hail is usually associated with supercell storms, which also can produce significant tornadoes in Turkey (Kahraman and Markowski 2014). Investigating the spatial and temporal distribution of severe hail is a prerequisite for understanding and ultimately predicting the environmental conditions that are favorable for severe hail.

Turkey's severe hail climatology reveals that all parts of the country are vulnerable. The largest hailstones exceed 5 cm in diameter and approach 1 kg in mass. Severe hail in Turkey is most likely in May and June, when severe hail is most likely in the interior of the country, especially in the east. Severe hail is least likely in the winter, though when it occurs in winter, it is most likely along the southern and western coasts. The afternoon and early evening hours are the most favorable time of the day for severe hail. The long-term variations in Turkish severe hail events (e.g., the 1960s maximum and early 2000s minimum) are worthy of future study.

Seasonal and monthly distribution of severe nontornadic convective wind events between January 2009–December 2011 shows that although the big portion of this events (51%) occur in summer they can occur in any time of year. They are most frequent in June, 33% of all events occurred in this month and 15% in September. 102 reports (70% of all the reports) included storm duration information. Only two of them were longer than six hours and most of them continued for 1 to 3 hours (42%).

The impact of severe convective storms on society was also investigated in this study. Specifically, lightning-related fatalities and injuries in Turkey were assessed. Lightning-related fatalities and injuries part of the research yielded a dataset covering January 1930 to June 2014. According to the dataset, there were 745 incidents, resulting in 898 deaths, 150 serious injuries and 536 injuries. The total number of

fatalities was 31 in 2012, 26 people in 2013 and 25 people in 2014. With a Turkish population of around 73.7 million, the number of fatalities were 0.42 per million in 2012, 0.35 per million in 2013 and 0.34 per million in 2014 (January–June). The total number of human injuries was 36 in each of 2012 and 2013, and 62 in 2014. Considering the population, the rate of injuries was 0.49 per million in each of 2012 and 2013, and 0.84 per million in 2014 (January–June).

Incidents were most frequent in late spring all around Turkey and were rare during winter. The majority of lightning incidents occurred during the afternoon, with fewer occurring at night. The number of incidents was higher over the highly populated western parts, especially in Istanbul and relatively lower in central and eastern Turkey. Geographical, annual and diurnal distributions of the incidents were comparable to thunderstorm and lightning observations, as well as with the report-based severe weather climatologies for Turkey.

The risk of being struck by lightning was highest for the people participating outdoor activities such as farming and shepherding. The number of male victims was nearly twice the number of female victims. Almost all of the incidents occurred in rural areas. The number of victims under trees is a sign of the need for awareness campaigns.

Report-based datasets are primary sources for severe convective storm climatologies. However, they have some disadvantages. Observations of hazardous, convection related local scale phenomena such as severe hail, tornadoes and damaging winds have a subjective nature. They are critically sensitive to some parameters such as population density differences, time of the day of occurrence and reporting issues (e.g., subjective estimation of wind speed by non-expert human observers and alike). Lastly, an objective climatology of various environmental parameters associated with severe convective storms for a domain covering Europe, Middle East and North Africa, based on 35-year ERA-interim data was created. Specifically, surface-based convective available potential energy (SBCAPE), mixed-layer (lowest 500m) convective available potential energy (MLCAPE), most unstable convective available potential energy (MUCAPE), surface-based convective inhibition energy (SBCIN), mixed-layer (lowest 500m) convective inhibition energy (MLCIN), most unstable convective inhibition energy (MUCIN), surface-based lifting condensation level (SBLCL), mixed-layer (lowest 500m) lifting condensation level (MLLCL), 0–6 km wind shear, 0–3 km wind shear, 0–1 km wind shear and mid-tropospheric (700–500-hPa) lapse

rate (LR7050) were calculated. Previous research shows that, individual parameters did not discriminate well between severe and non-severe deep moist convection. Considering instability and shear together improves discrimination sharply (e.g., Davies and Johns 1993, Johns et al., 1993, Craven and Brooks 2004, Gensini and Ashley 2011). Therefore, proxy distribution of severe convective storms was enquired with the help of a composite parameter. Products of MLCAPE and deep layer shear values were used to calculate this significant severe parameter. Results shows that the ITCZ, Mediterranean Sea, Red Sea and Arabian Sea clearly exert a dominating influence on the CAPE distribution patterns over the domain. Influence is not limited to directly over the seas but is noted over the coasts of these seas. Seasonal cycle of CAPE fields is very clearly defined with larger values during summer than in the winter for all over the domain. For the transition seasons, CAPE values are higher in autumn than spring over Mediterranean, Red and Arabian Seas and neighboring countries as expected. After peak summer insolation, these large water bodies remain warm for several weeks and perform as intense heat and moisture sources. This effect is slightly visible over southern parts of Black Sea and Caspian Sea due to lower insolation, related with their higher latitudes. With the strengthening of the jet stream during winter, the highest average 0–6 km wind shear values occur beneath the jet regions. Overlapping of ingredients seems most probable during spring over a zonal belt including southern Europe, northern Africa and Turkey. Another finding is large 0–1 km wind shear values over the Arabian Sea and Somalia from June to September, related to the Somalian low-level jet. This region is notable considering the extreme SBCAPE values available at that time of the year together with these large wind-shear values.

The spatial and temporal distributions of significant severe weather environments and severe storm related event reports show strong similarities. For example, May and June is the peak season for severe hail, while the significant severe parameter is most widespread over Turkey during this months. Additionally, similarity of late summer, early fall peak of hail days around northeastern Turkey and high values of significant severe parameter over the region during the same season is remarkable.

Comparisons with thunderstorms days data is also satisfiying. Thunderstorms are most frequent in May and June all around Turkey, especially over the inland and northeastern parts when the significant severe parameter has its higher values over

these regions. The maximum thunderstorm frequency shifts to the Aegean and Mediterranean coasts from late autumn to early spring, while the rest of Turkey has relatively infrequent thunderstorms. Accordingly, during late autumn, significant severe parameter has its highest values around the Aegean and Mediterranean coasts while approximately no favourable days are available over the rest of the country in average.

This synthetic climatological dataset is objective and it does not have disadventages like inhomogeneity or sensitivity to population density distributions. Therefore, it can be used to analyze the regional variability and trends of severe convective storm environments in future studies. Moreover using these dataset many other parameters can be created to enquire some specific events distributions (i.e., significant tornado parameter). MLCIN values can be combined with the instability/shear composite or different threshold can be applied to instability/shear composite.

REFERENCES

Alyan O., Ozdemir O., Tufekcioglu O., Geyik B., Aras D., and Demirkan D. (2006). Myocardial injury due to lightning strike: A case report, *Angiology*, 57, 219–223, 2006.

Ashley W. S. and Gilson C. W. (2009). A reassessment of US lightning mortality, *Bulletin of American Meteorological Society*, October 2009, 1501–1518.

Aslan S., Yilmaz S., and Karcioglu O. (2004). Lightning: an unusual cause of cerebellar infarction, *Emergence Medicine Journal*, 21, 750–751.

Aslar A. K., Soran A., Yildiz Y., and Isik Y. (2001). Epidemiology, morbidity, mortality and treatment of lightning injuries in a Turkish burns units, *International Journal of Clinical Practice*, 55, 502–504.

Bestepe, F., (2011). Weather Radar Network in Turkey.

http://www.slidefinder.net/t/tsms_radar_network_firatbestepe/32927670

Brooks HE, Doswell CA III (2001) Normalized damage from major tornadoes in the United States: 1890–1999. *Weather Forecast* 16:168–176.

Brooks HE, Doswell CA III (2002) Deaths in the 3 May 1999 Oklahoma City tornado from a historical perspective. *Weather Forecast* 17:354–361.

Brooks, H.E., Lee, J.W. and Craven, J.P. (2003) The spatial distribution of severe thunderstorm and tornado environments from global reanalysis data. *Atmos Res, **67***:73–94

Brooks, H., and C. A. Doswell (2001) Some aspects of the international climatology of tornadoes by damage classification. Atmos. Res., 56, 191–201.

Brooks, H. E., and D. J. Stensrud (2000) Climatology of heavy rain events in the United States from hourly precipitation observations. *Mon. Wea. Rev.*, 128, 1194–1201. doi: http://dx.doi.org/10.1175/1520-0493(2000)128<1194:COHREI>2.0.CO;2

Brooks, H. E., and N. Dotzek (2008) The spatial distribution of severe convective storms and an analysis of their secular changes. *Climate Extremes and Society*, H. F. Diaz and R. Murnane, Eds., Cambridge University Press, 35–53.

Celiköz, B., Isik, S., Türegün, M., and Selmanpakoğlu, N. (1996). An unusual case of lightning strike: Full-thickness burns of the cranial bones, *Burns*, 22, 417–419.

Cumhuriyet Archive (2014) <http://www.cumhuriyetarsivi.com>, date retrieved 29.06.2015.

Craven, J. P., J. M. Davies, and P. W. Leftwich (1993) Some wind and instabilityparameters associated with strong and violent tornadoes. Part II: Variations in the combinations of wind and instability parameters. The Tornado: Its Structure, Dynamics, Prediction, and Hazards, *Geophys. Monogr.,* No. 79, Amer. Geophys. Union, 583-590.

Craven, J. P., Jewell, R. E. and Brooks, H. E. (2002) Comparison between observed Convective Cloud-Base Heights and Lifting Condensation Level for Two Different Lifted Parcels. *Weather and Forecasting.* 17(4):885-890.

Craven, J. P. and H. E. Brooks (2004) Baseline climatology of sounding derived parameters associated with deep moist convection. *Natl. Wea. Digest*, 28, 13–24.

Davies, J. M., and R. H. Johns (1993). Some wind and instability parameters associated with strong and violent tornadoes. 1: Wind shear and helicity. The Tornado: Its Structure, Dynamics, Prediction, and Hazards, *Geophys. Monogr*., No. 79, Amer. Geophys. Union, 573-582.

Dee, D. P., Uppala, S. M., Simmons, A. J., Berrisford, P., Poli, P., Kobayashi, S., Andrae, U., Balmaseda, M. A., Balsamo, G., Bauer, P., Bechtold, P., Beljaars, A. C. M., van de Berg, L., Bidlot, J., Bormann, N., Delsol, C., Dragani, R., Fuentes, M., Geer, A. J., Haimberger, L., Healy, S. B., Hersbach, H., Hólm, E. V., Isaksen, L., Kållberg, P., Köhler, M., Matricardi, M., McNally, A. P., Monge-Sanz, B. M., Morcrette, J.-J., Park, B.-K., Peubey, C., de Rosnay, P., Tavolato, C., Thépaut, J.-N. and Vitart, F. (2011), The ERA-Interim reanalysis: configuration and performance of the data assimilation system. *Q.J.R. Meteorol. Soc.*, 137: 553–597. doi:10.1002/qj.828.

Diffenbaugh, N. S., Trapp R. J., Brooks H. E. (2008). Challenges in identifying influences of global warming on tornado activity. *Eos Trans.* ***89(53)***:553–554

Dlamini Q. M. (2009). Lightning fatalities in Swaziland: 2000–2007, *Nat Hazards*, 50, 179–191.

Doswell CA III, Burgess DW (1988) On some issues of United States tornado climatology. *Mon. Weather Rev,.* 116:495–501.

Doswell CA III (2007) Small sample size and data quality issues illustrated using tornado occurrence data. *Electron J Sev Storms Meteorol*, 2:1–16.

Dotzek, N. (2001) Tornadoes in Germany. *Atmospheric Research.* Vol ***56***, Pages 233–251

Dotzek, N., P. Groenemeijer, B. Feuerstein, and A. M. Holzer (2009). Overview of ESSL's severe convective storms research using the European Severe Weather Database ESWD. Atmos. Res., 93, 575–586.

Eccel, E., Cau, P., Riemann-Campe, K. and Biasioli, F. (2012). Quantitative hail monitoring in an alpine area: 35-year climatology and links with atmospheric variables. Int. J. Climatol., 32, 503–517.

Elsom D. M. (2001). Deaths and injuries caused by lightning in the United Kingdom: Analyses of two databases, *Atmos. Res.*, 56, 325–334.

Elsom D. M and Webb J. D. C. (2014). Deaths and injuries from lightning in the UK, 1988–2012, *Weather*, 69, 221–226.

EM-DAT, (2012). Trends and Relationships Periods 1900–2011. Emergency Events Database. Centre for Research on the Epidemiology of Disasters, *http://www.emdat.be/disaster-trends*

European Severe Weather Database, (2014). <http://www.essl.org/cgi-bin/eswd/eswd.cgi>, date retrieved 12.06.2014.

Espy, J. P (1841). *Philosophy of Storms*. Boston, Little and Brown, pp 552.

Etkin, D. and Brun, S. E. (1999). A note on Canada's hail climatology: 1977–1993. Int. J. Climatol., 19, 1357–1373.

Feuerstein, B., N. Dotzek and J. Grieser (2005). Assessing a Tornado Climatology from Global Tornado Intensity Distributions. J. Climate, 18, 585–596. doi: http://dx.doi.org/10.1175/JCLI-3285.1

Gayaa, M., V. Homar, R. Romero, C. Ramis (2001) Tornadoes and waterspouts in the Balearic Islands: phenomena and environment characterization. *Atmospheric Research. **56:*** 253–267

Gensini, V. A., and Ashley, W. S. (2011), Climatology of potentially severe convective environments from North American regional reanalysis. *Electronic J. Severe Storms Meteor*, 6 (8), 1–40.**Holle R. L., Lopez R. E. and Navarro B. C.** (2005). Deaths, injuries, and damages from lightning in the United States in the 1890s in comparison with the 1990s, *J. Appl. Meteor.*, 44, 1563–1573.

Giaiotti D., S. Nordio, and F. Stel (2003). The climatology of hail in the plain of Friuli Venezia Giulia, Atmos. Res., 67-68, 247–259.

Giaiotti D.B., Giovannoni, M., Pucillo, A., Stel, F., (2007). The climatology of tornadoes and waterspouts in Italy. *Atmospheric Research*, Vol ***83***, Issues 2–4, Pages 534-541

Holle R. L. and Lopez R. E. (2003). A comparison of current lightning death rates in the US with other locations and times, In International Conference on Lightning and Static Electricity, Blackpool, England, *Royal Aeronautical Society*, paper 103–34 KMS, 7 pp, September 16–18.

Holzer, A.M. (2001). Tornado climatology of Austria. Atmospheric Research, Vol 56, Pages 203-211

Intergovernmental Panel on Climate Change (2007) Climate change 2007: the physical science basis. Cambridge University Press,Cambridge

Kahraman A., and Markowski P. (2014). Tornado climatology of Turkey, *Monthly Weather Review*, 142, 2345–2352. doi:10.1175/MWR-D-13-00364.1.

Kahraman A., Tilev-Tanriover Ş., Kadioğlu M., Schultz D. M. and Markowski P. M. (2016). Severe hail climatology of Turkey, *Monthly Weather Review*, 144, 337–346.

Kelly, D. L., J. T. Schaefer, R. P. McNulty, C. A. Doswell and R. F. Abbey (1978). An Augmented Tornado Climatology. Mon. Wea. Rev., 106, 1172–1183. doi: http://dx.doi.org/10.1175/1520-0493(1978)106<1172:AATC>2.0.CO;2

Marcinoniene, I., (2003). Tornadoes in Lithuania in the period of 1950–2002 including analysis of the strongest tornado of 29 May 1981. Atmospheric Research. Vol 67–68, Pages 475-484

Markowski, P. and Richardson, **Y.** (2010). *Mesoscale Meteorology in Midlatitudes*. West Sussex, UK: Wiley-Blackwell Publication.

Mezher R. N., M. Doyle, and V. Barros (2012). Climatology of hail in Argentina. Atmos. Res., 114-115, 70-82.

Michaelides, S. C., Savvidou, K., Nicolaides, K. A., Orphanou, A., Photiou, G., and Kannaouros, C. (2008). Synoptic, thermodynamic and

agroeconomic aspects of severe hail events in Cyprus, Nat. Hazards Earth Syst. Sci., 8, 461-471, doi:10.5194/nhess-8-461-2008.

Milliyet Archive, <http://gazetearsivi.milliyet.com.tr, 2013>, date retrieved 07.12.2013.

Mills B., Unrau D., Parkinson C., Jones B., Yessis J., Spring K., and Pentelow L. (2008). Assessment of lightning-related fatality and injury risk in Canada, *Natural Hazards*, 47, 157–183.

Raga G. B., Parra M. G., and Kucienska B. (2014). Deaths by lightning in Mexico (1979–2011): Threat or vulnerability? *Wea. Climate Soc.*, 6, 434–444.

Rasmussen, E. N., and Blanchard, D. O. (1998). A baseline climatology of sounding-derived supercell and tornado forecast parameters. *Wea. Forecasting*, 13, 1148–1164.

Romero, R., Gayà, M., and Doswell CA III (2007). European climatology of severe convective storm environmental parameters: A test for significant tornado events. *Atmos. Res*., Volume 83, Issues 2–4, Pages 389–404.

Salerno J., Msalu L., Caro T., and Mulder M. B. (2012). Risk of injury and death from lightning in Northern Malawi, *Natural Hazards*, 62, 853–862.

Sánchez, J. L., R. Fraile, J. L. de la Madrid, M. T. de la Fuente, P. Rodríguez, and A. Castro, (1996). Crop damage: The hail size factor. J. Appl. Meteor., 35, 1535–1541.

Schaefer, J. T., J. J. Levit, S. J. Weiss, and D. W. McCarthy (2004). The frequency of large hail over the contiguous United States. Preprints, 14th Conf. on Applied Climatology, Seattle, WA, Amer. Meteor. Soc., 3.3.

Simeonov, P. (1996). An overview of crop hail damage and evaluation of hail suppression efficiency in Bulgaria. J. Appl. Meteor., 35, 1574–1581.

Sioutas M., T. Meaden, and J.D.C. Webb (2009). Hail frequency, distribution and intensity in Northern Greece, Atmos. Res., 93, 526-533.

Skamarock, W.C., Klemp, J.B., Dudhia, J., Gill, D.O., Barker, D.M., Duda, M.G., Huang, X-Y., Wang, W., Powers, J.G. (2008). A description of the advanced research WRF version 3. *NCAR Tech. Note*. 113 pp

Suwala K., and E. Bednorz, (2013). Climatology of hail in central Europe. Quaestiones Geographicae, 32(3), 99-110.

The NCAR Command Language (Version 6.3.0) [Software]. (2015). Boulder, Colorado: UCAR/NCAR/CISL/TDD. <http://dx.doi.org/10.5065/D6WD3XH5>

Thompson, R. L., R. Edwards, J. A. Hart, K. L. Elmore, and P. Markowski, (2003). Close proximity soundings within supercell environments obtained from the Rapid Update Cycle. *Wea. Forecasting*, 18, 1243–1261.

Toros, H., (2012). Spatio-temporal precipitation change assessments over Turkey. Int. J. Climatol., 32: 1310–1325. doi: 10.1002/joc.2353

Tuovinen J-P., A-J. Punkka, J. Rauhala, H. Hohti, and D. M. Schultz (2009). Climatology of Severe Hail in Finland, Mon. Wea. Rev., 137, 2238-2249.

Turkish State Meteorological Service FEVK records

Türkeş, M., 1996: Spatial and temporal analysis of annual rainfall variations in Turkey, Int. J. Climatol., 16: 1057–1076. doi: 10.1002/(SICI)1097-0088(199609)16:9

Verbout S.M., Brooks H.E., Leslie L.M. and Schultz D.M. (2006), Evolution of the U.S. tornado database: 1954–2003. *Weather Forecast*, 21:86–93.

Vinet, F., 2001: Climatology of hail in France. Atmos. Res., 56, 309–323.

Webb, J. D. C., D. M. Elsom, and D. J. Reynolds (2001) Climatology of severe hailstorms in Great Britain. Atmos. Res., 56, 291–308.

Webb, J.D.C., D.M. Elsom, G.T. Meaden (2009). Severe hailstorms in Britain and Ireland, a climatological survey and hazard assessment. Atmospheric Research, Vol 93, Pages 587-606

Woollings T., C. Czuchnicki, C. Franzke (2014). Twentieth Century North Atlantic jet variability. Q. J. R. Meteorol. Soc., 140, 783–791.

Zhang, C., Q. Zhang, and Y. Wang (2008). Climatology of hail in China: 1961–2005. J. Appl. Meteor. Climatol., 47, 795–804.

Zhang W., Meng Q., Ma M., and Zhang Y. (2011). Lightning causalities and damages in China from 1997 to 2009, *Natural Hazards*, 57, 465–476.

APPENDICES

APPENDIX A: Long-term monthly mean maps for each variable.
APPENDIX B: Mean number of days with MLCAPE × 0–6 km wind shear values over the thresholds (10000 m3/s3, 20000 m3/s3, 30000 m3/s3) for each month.

APPENDIX A

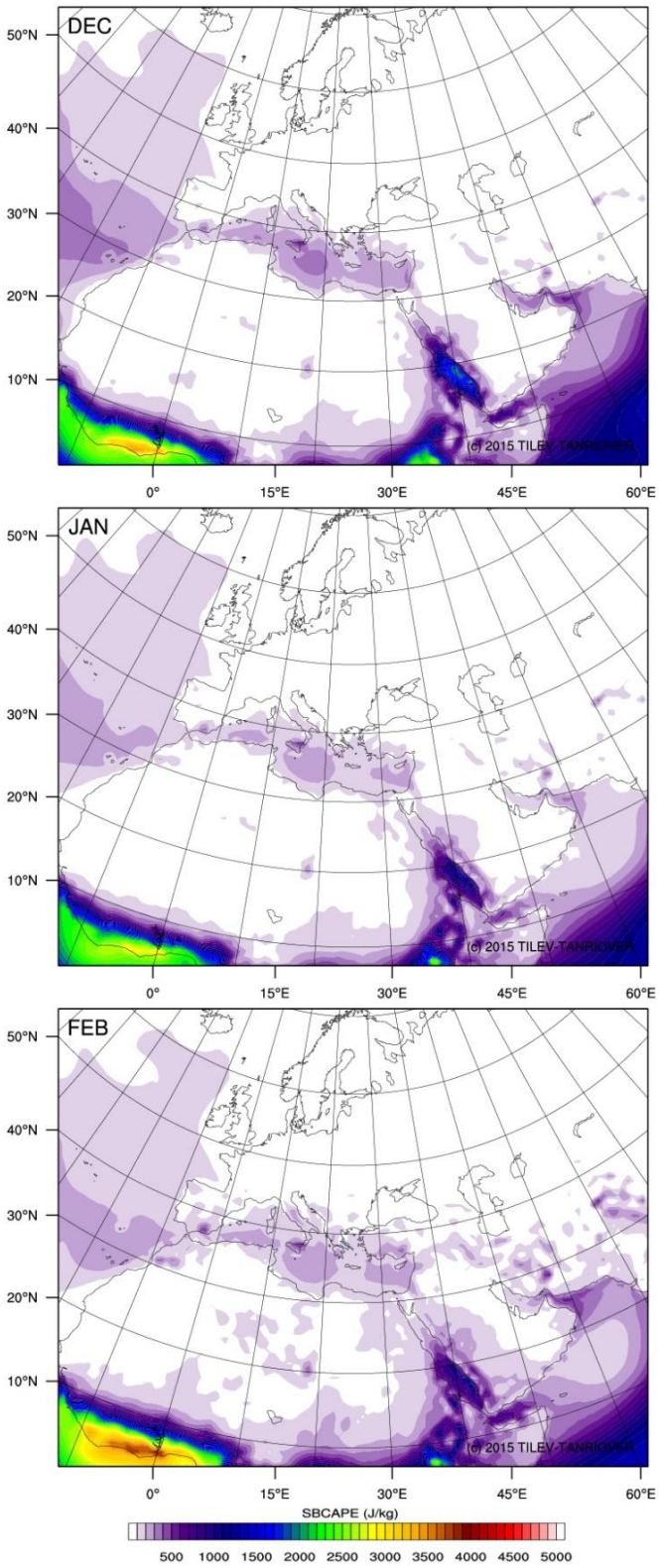

Figure A.1 : Long-term monthly mean maps of SBCAPE for winter: December, January, and February.

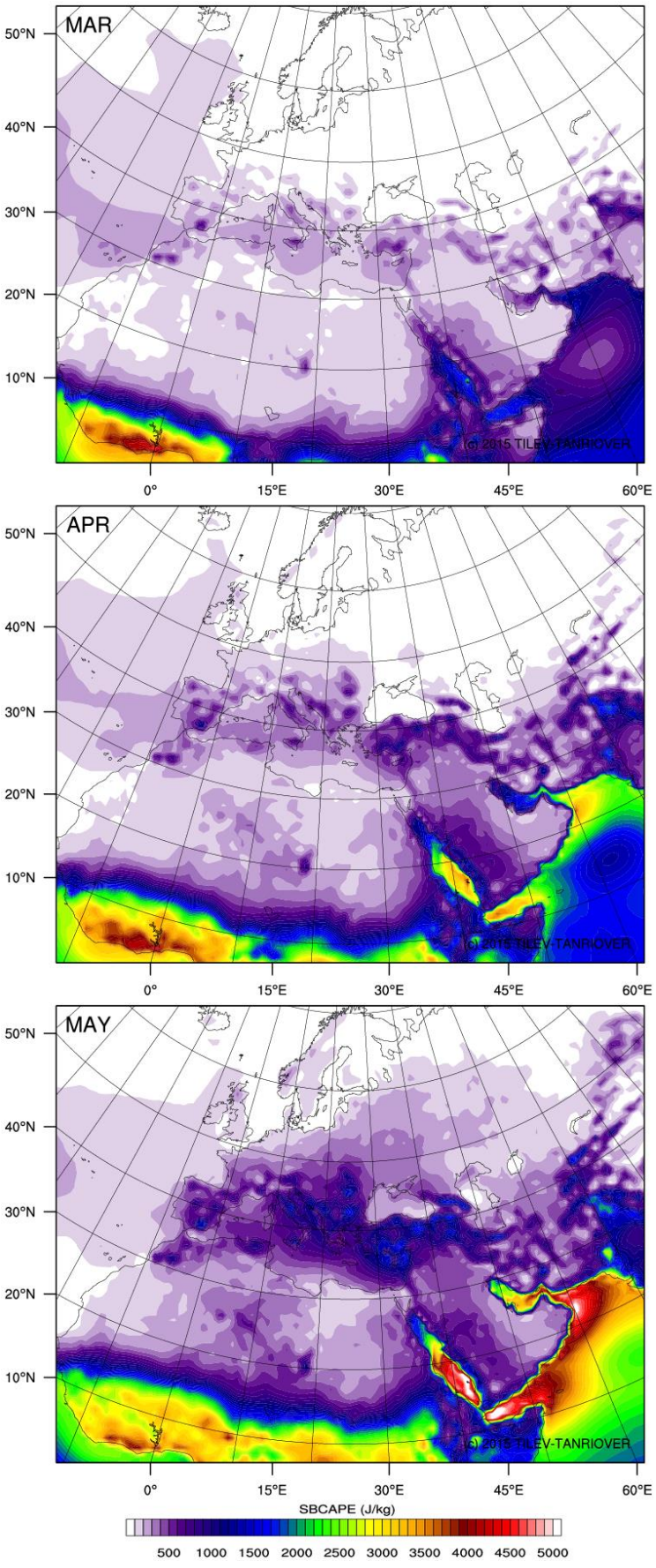

Figure A.2 : Long-term monthly mean maps of SBCAPE for spring: March, April, and May.

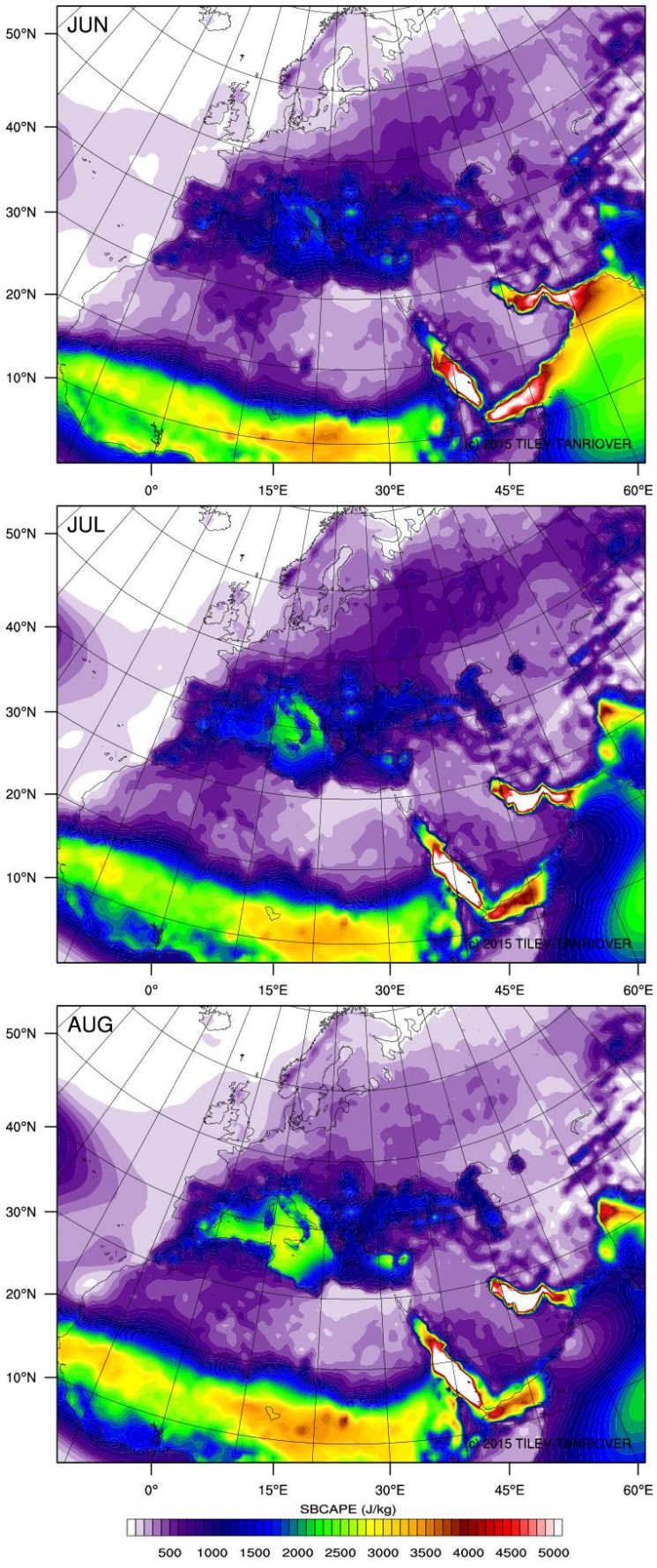

Figure A.3 : Long-term monthly mean maps of SBCAPE for summer: June, July, and August.

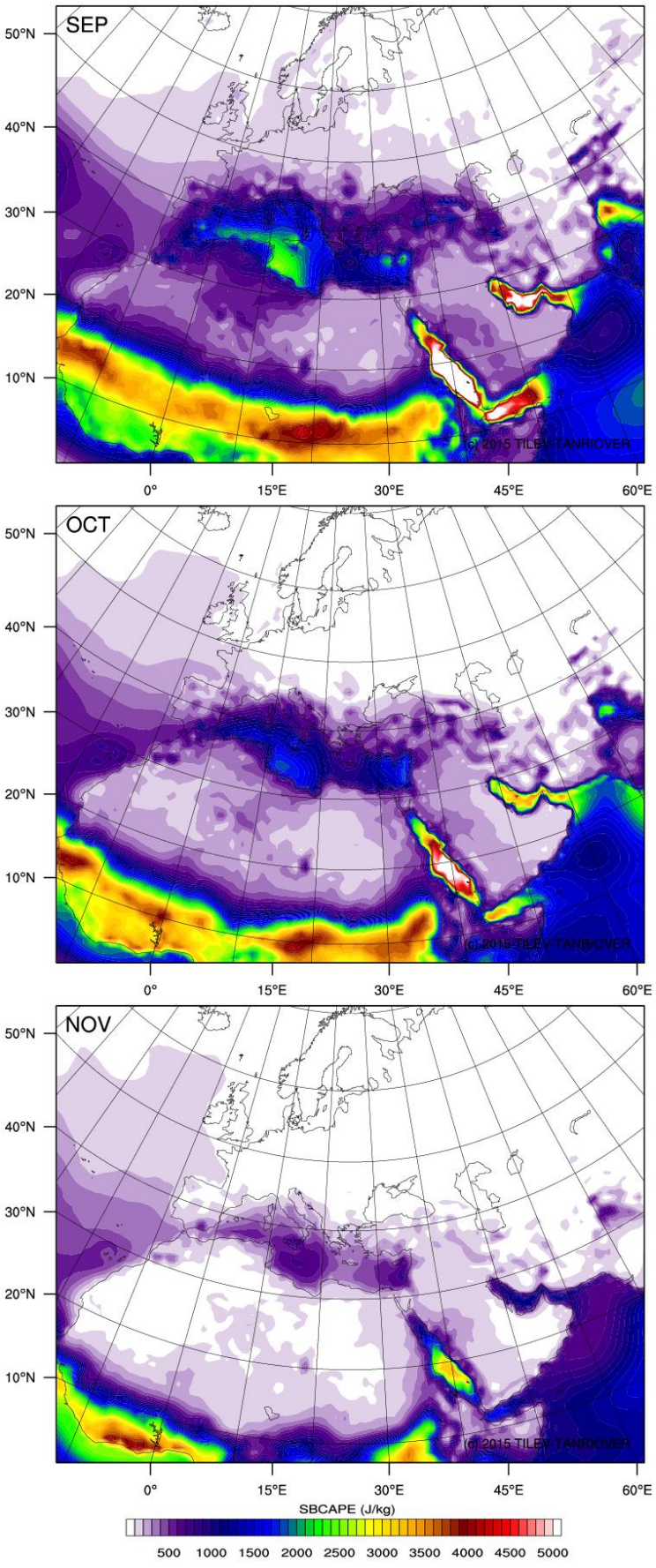

Figure A.4 : Long-term monthly mean maps of SBCAPE for autumn: September, October, and November.

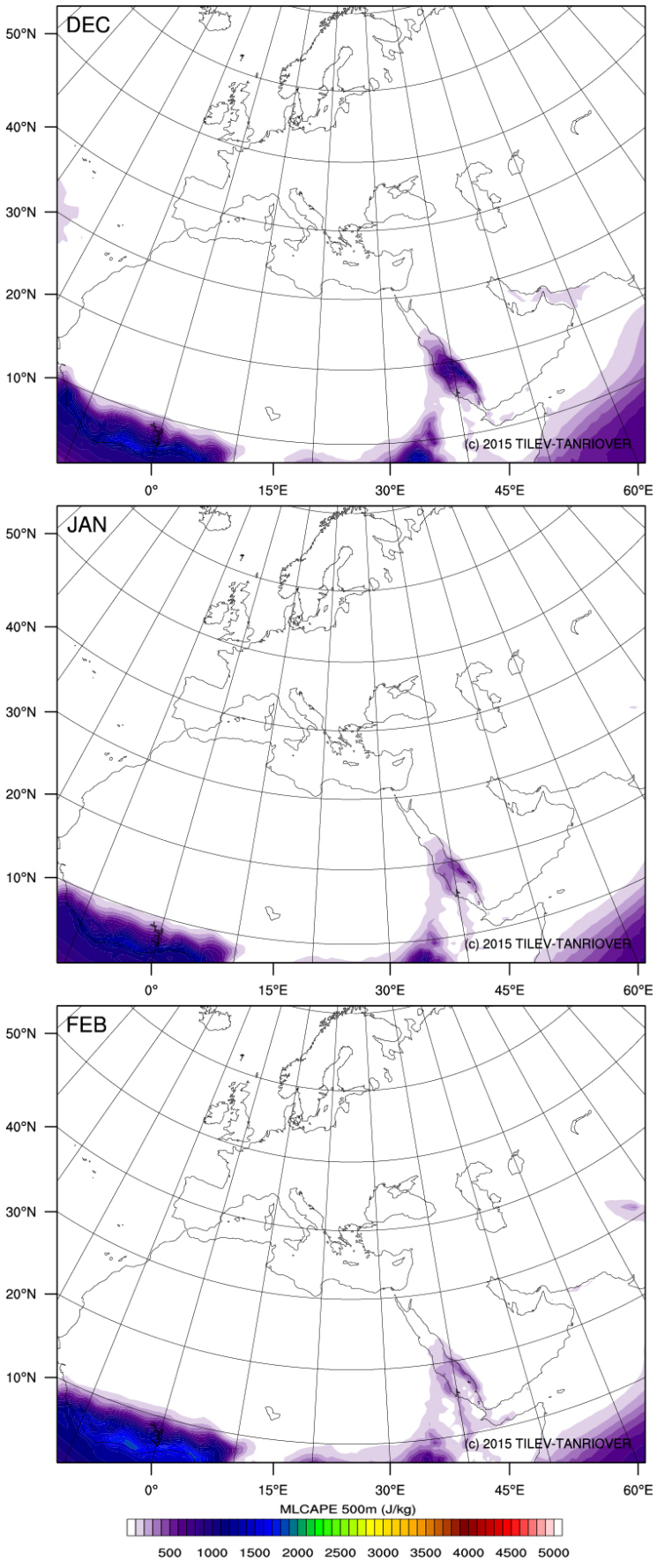

Figure A.5 : Long-term monthly mean maps of MLCAPE for winter: December, January, and February.

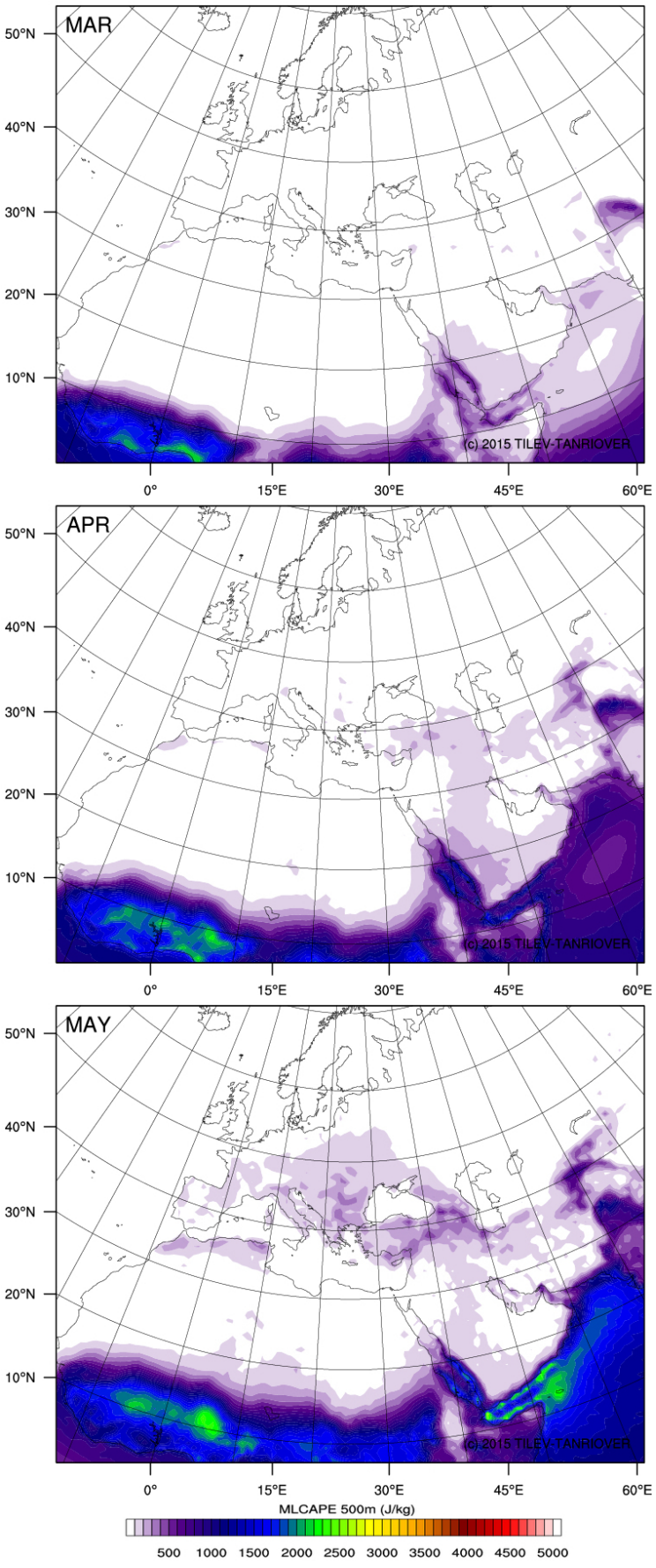

Figure A.6 : Long-term monthly mean maps of MLCAPE for spring: March, April, and May.

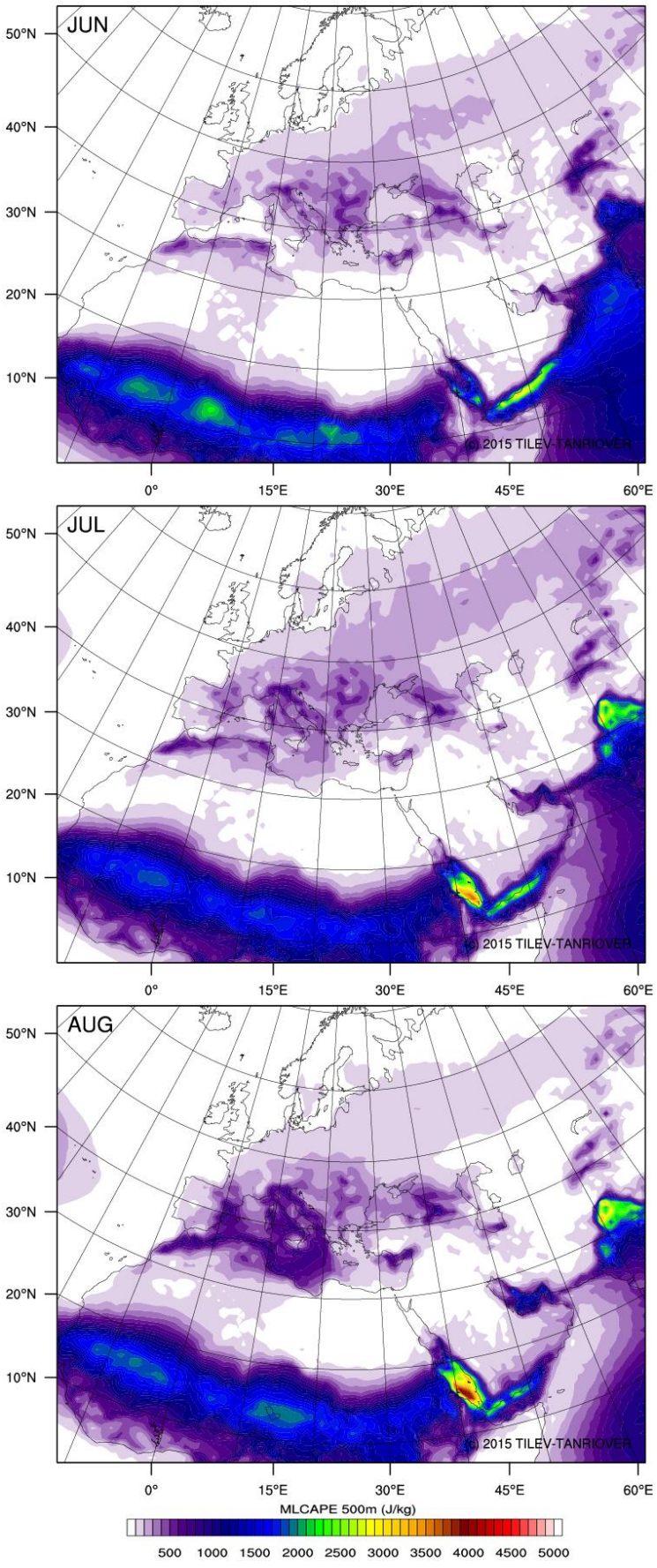

Figure A.7 : Long-term monthly mean maps of MLCAPE for summer: June, July, and August.

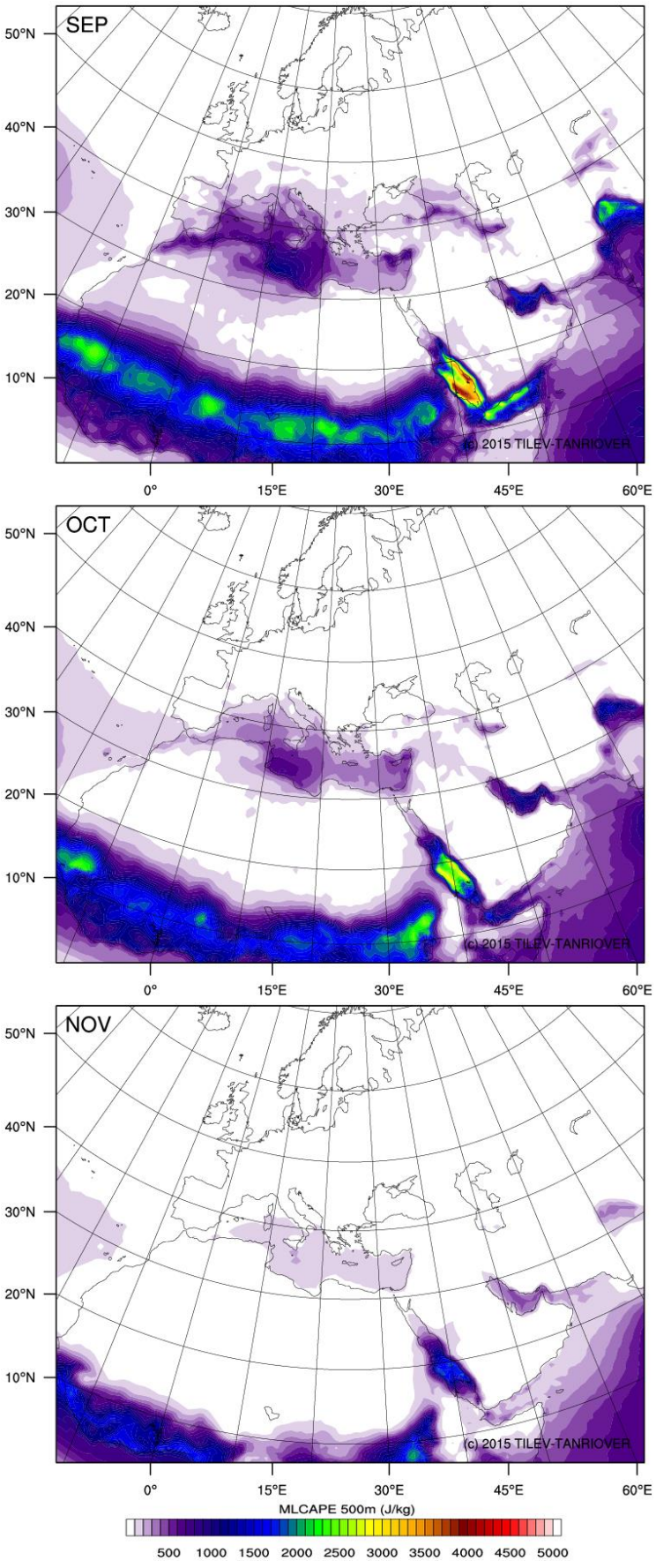

Figure A.8 : Long-term monthly mean maps of MLCAPE for autumn: September, October, and November.

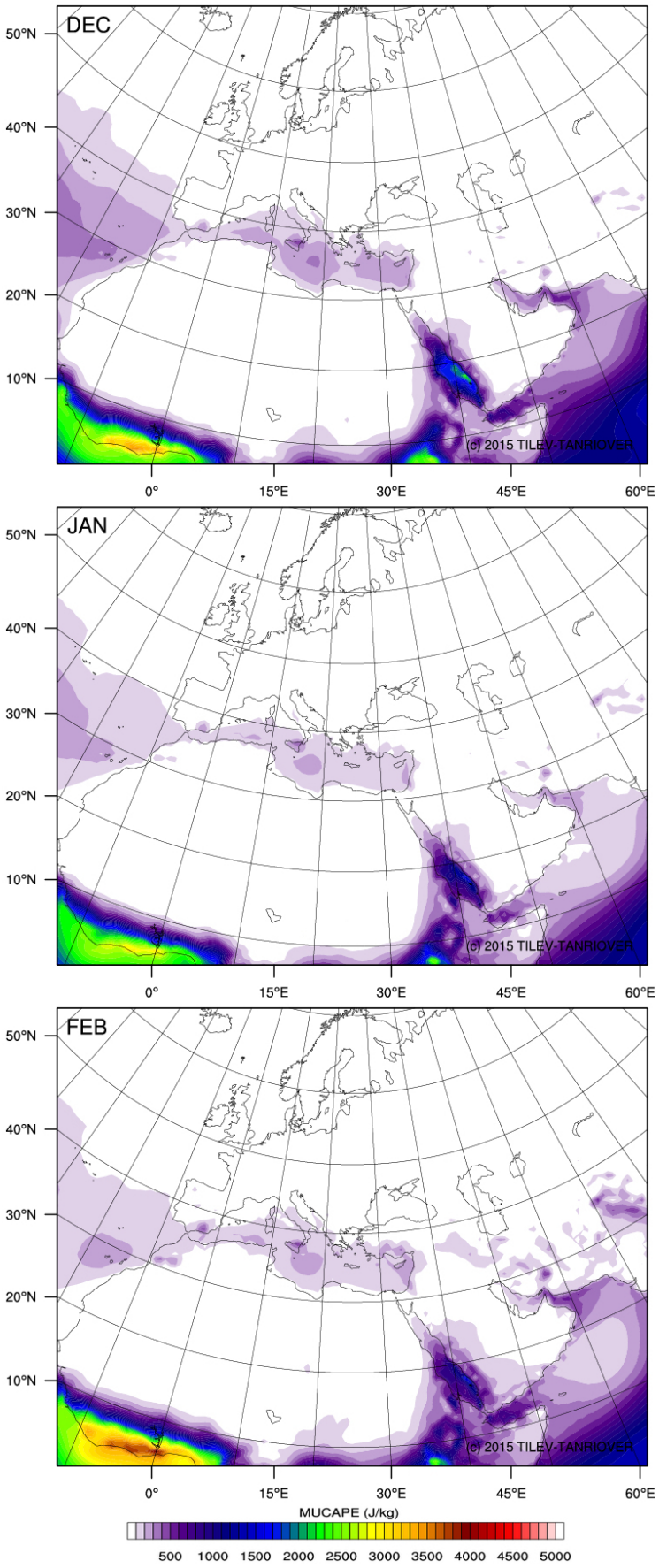

Figure A.9 : Long-term monthly mean maps of MUCAPE for winter: December, January, and February.

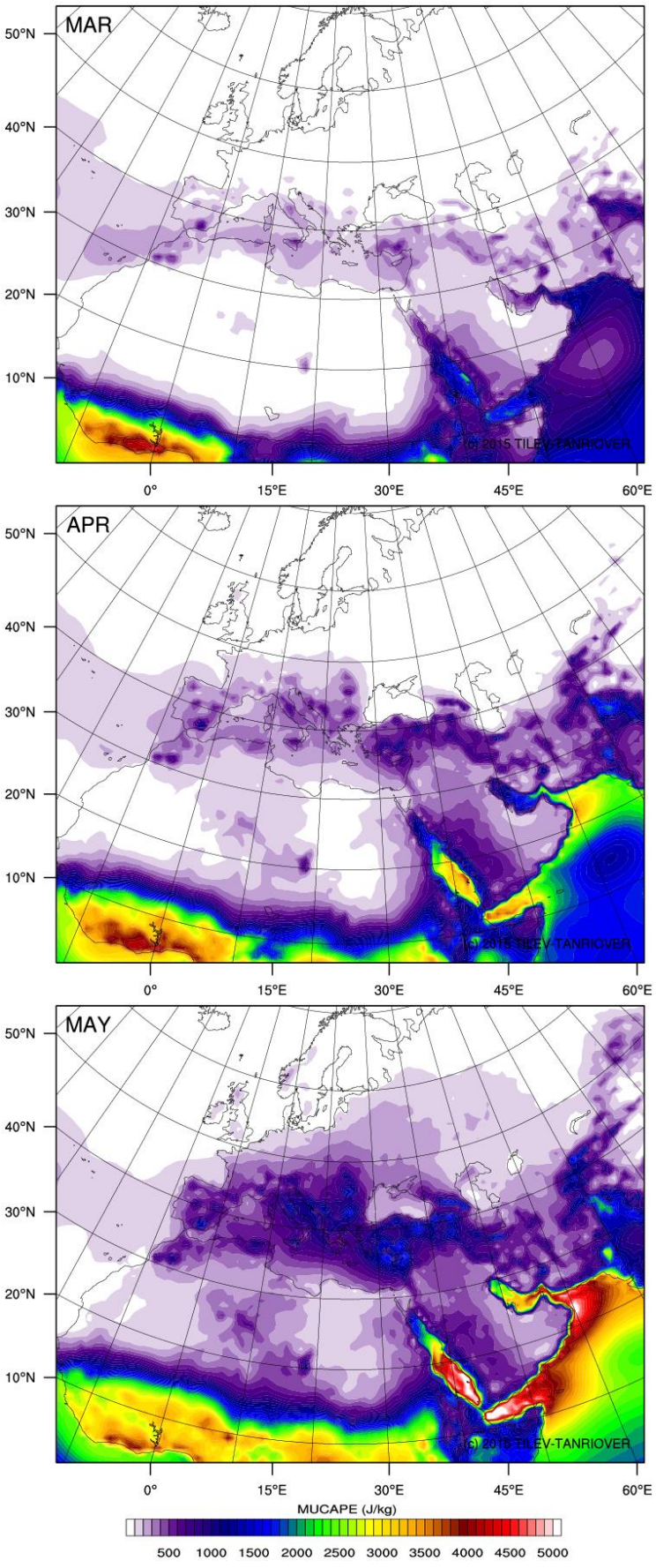

Figure A.10 : Long-term monthly mean maps of MUCAPE for spring: March, April, and May.

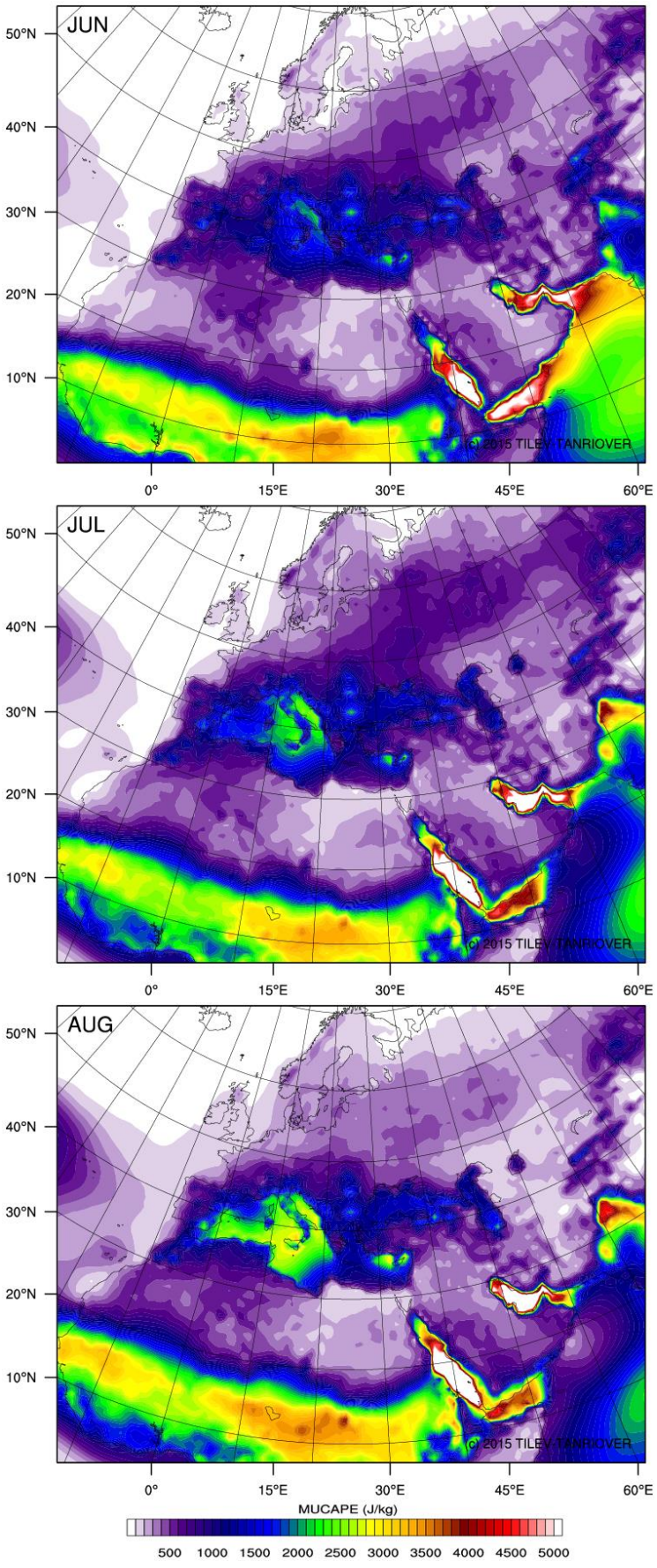

Figure A.11 : Long-term monthly mean maps of MUCAPE for summer: June, July, and August.

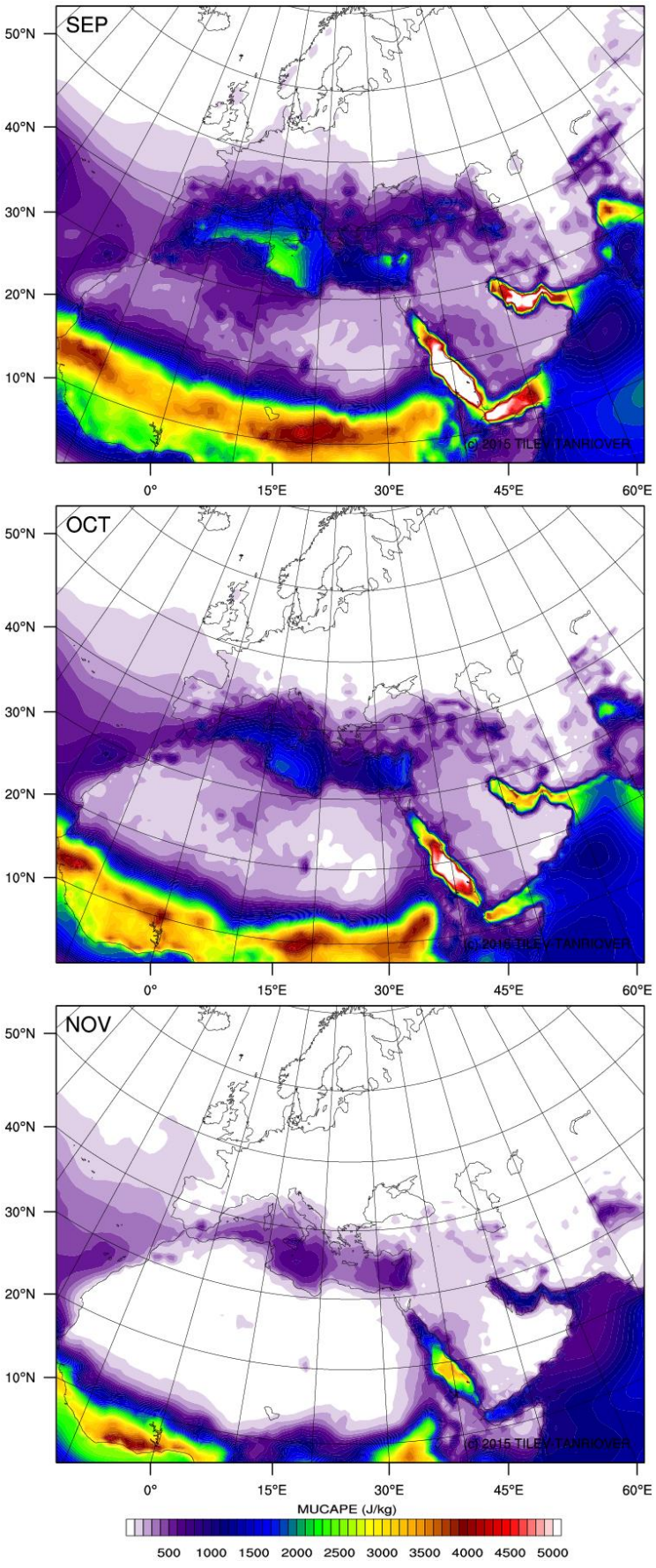

Figure A.12 : Long-term monthly mean maps of MUCAPE for autumn: September, October, and November.

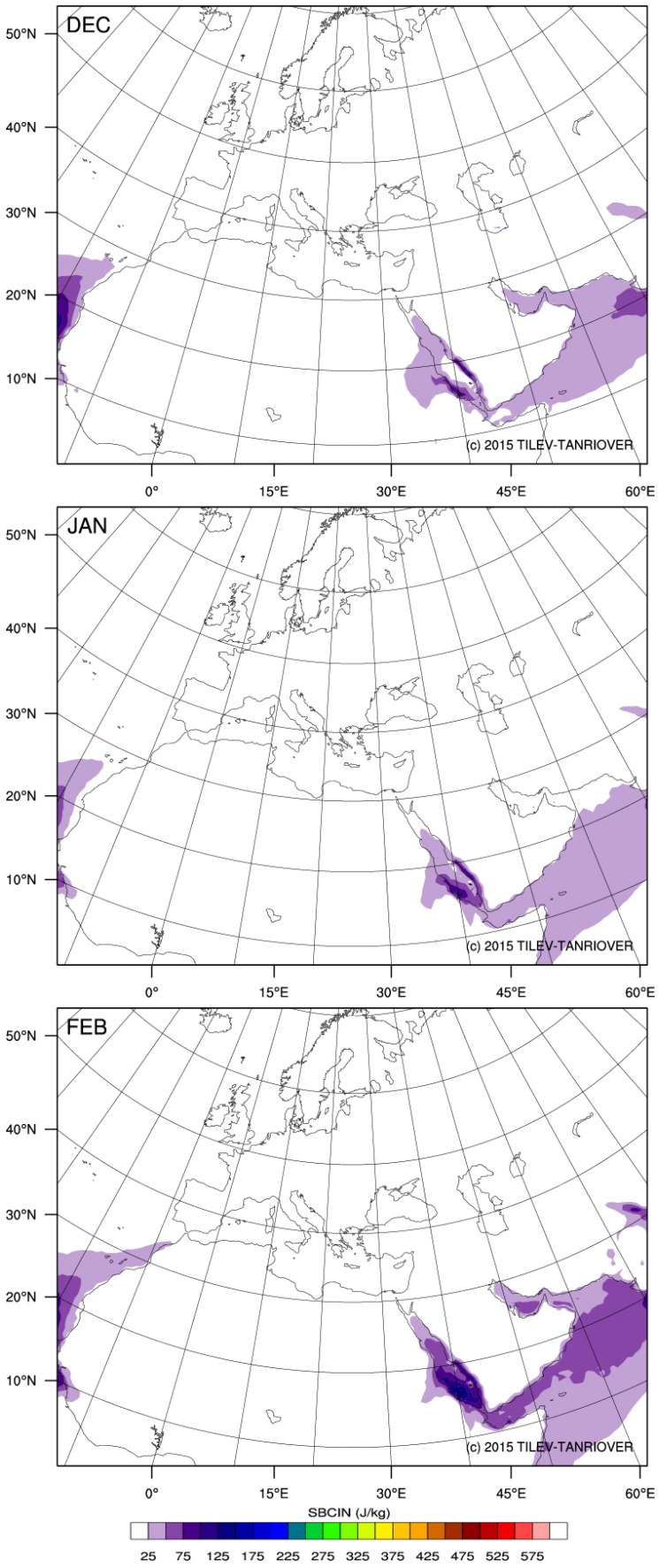

Figure A.13 : Long-term monthly mean maps of SBCIN for winter: December, January, and February.

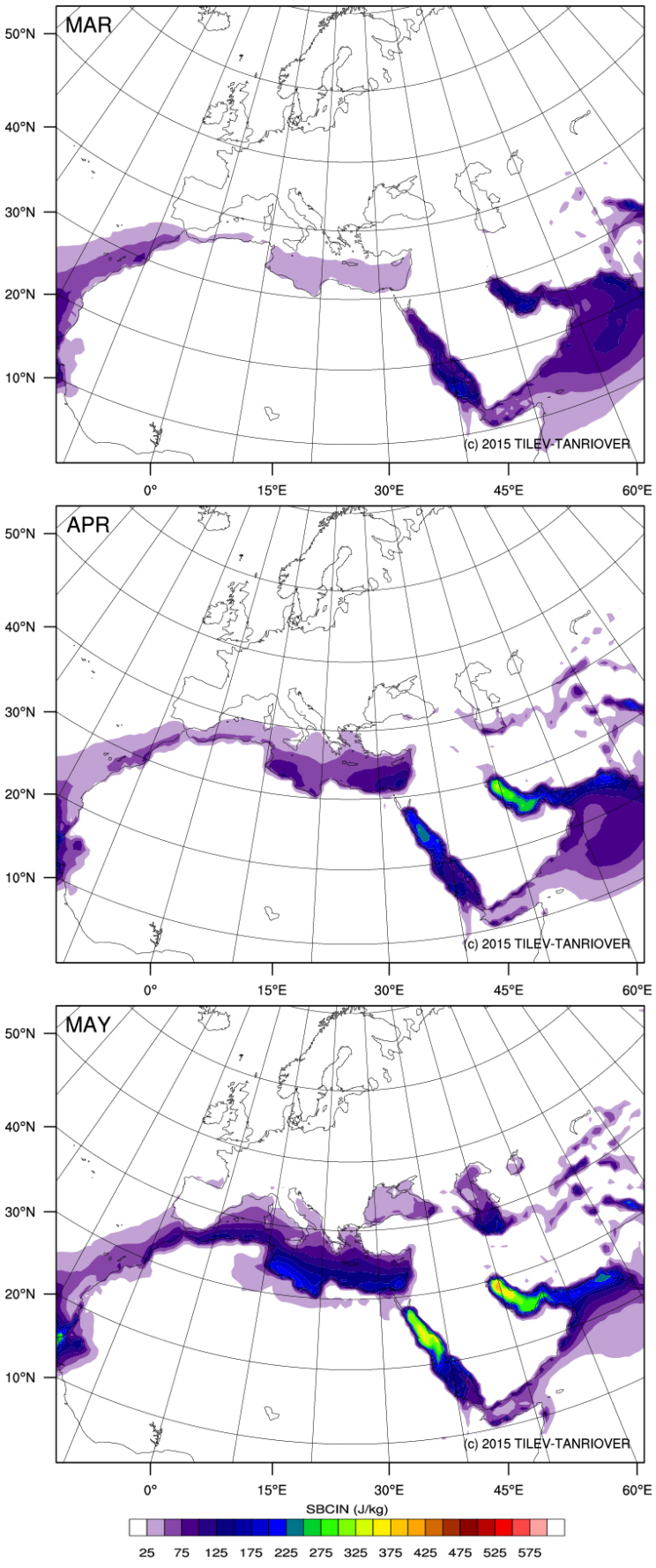

Figure A.14 : Long-term monthly mean maps of SBCIN for spring: March, April, and May.

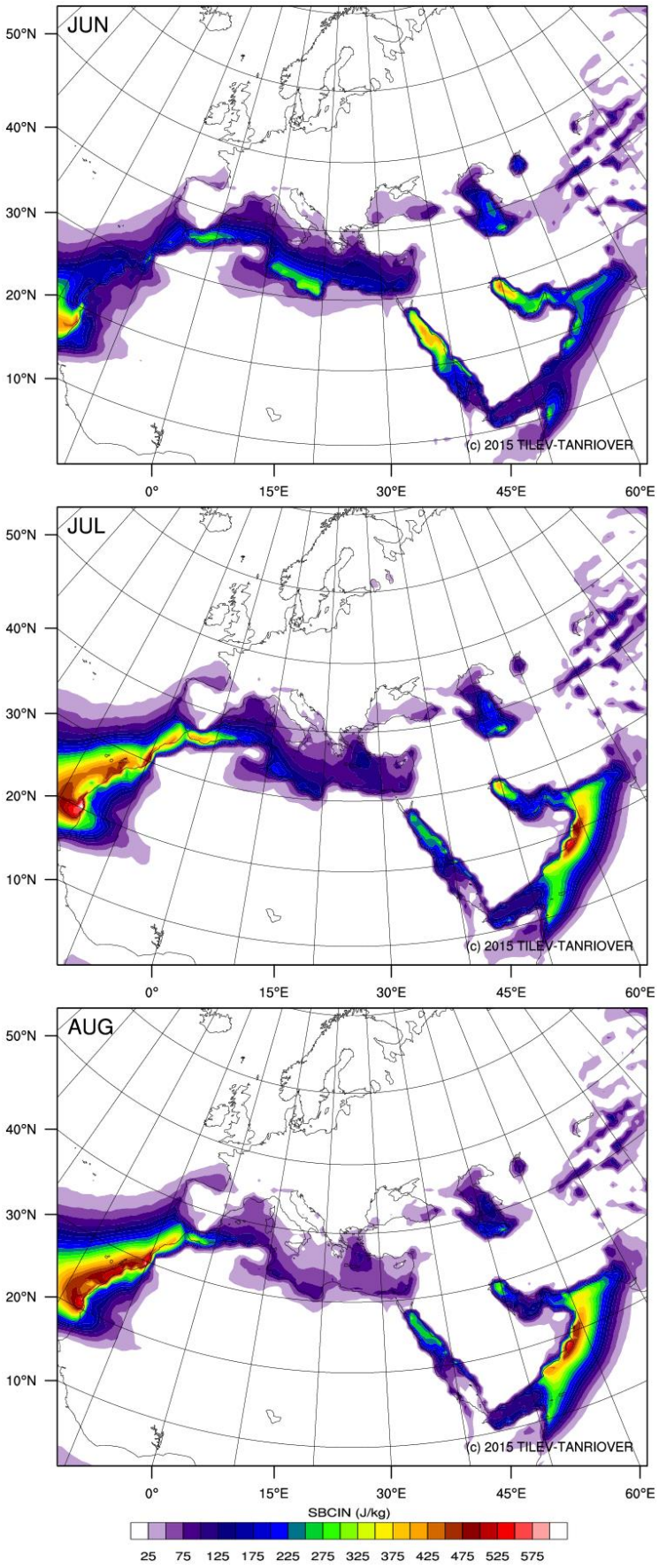

Figure A.15 : Long-term monthly mean maps of SBCIN for summer: June, July, and August.

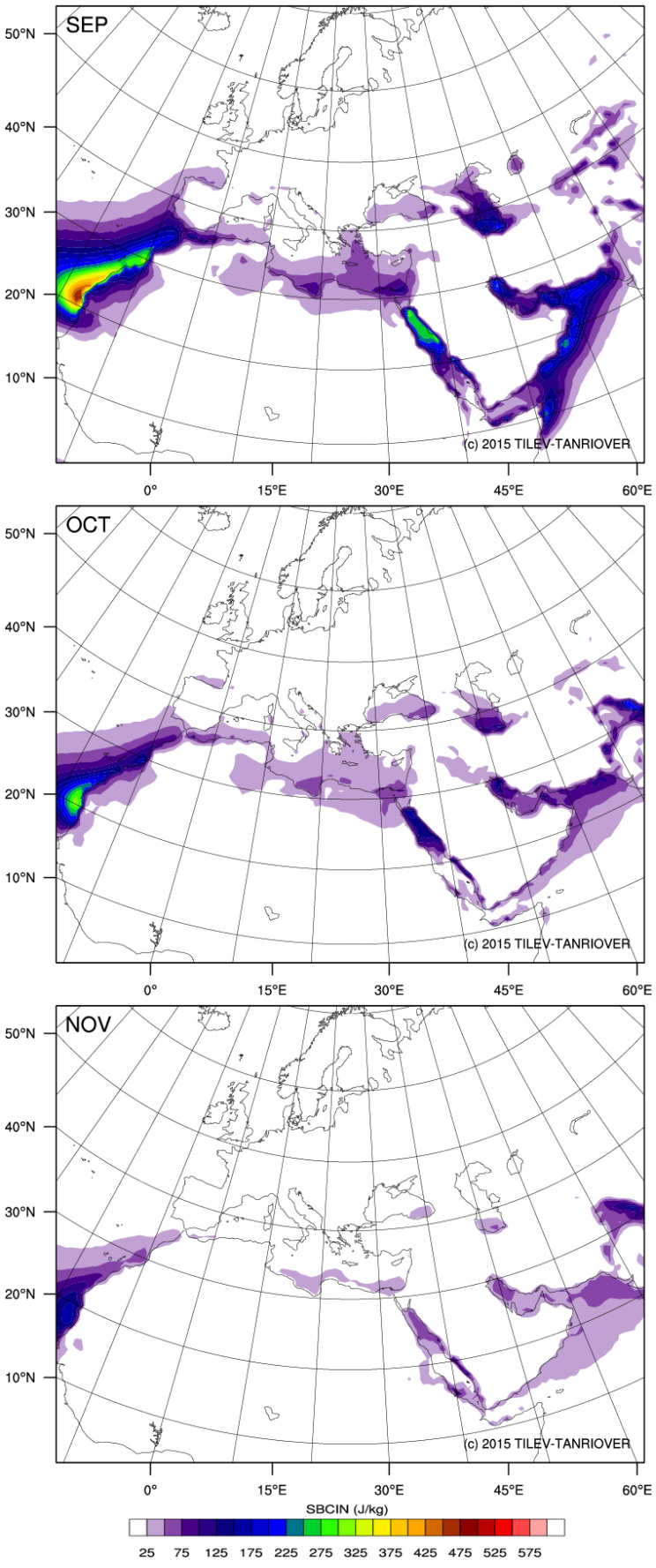

Figure A.16 : Long-term monthly mean maps of SBCIN for autumn: September, October, and November.

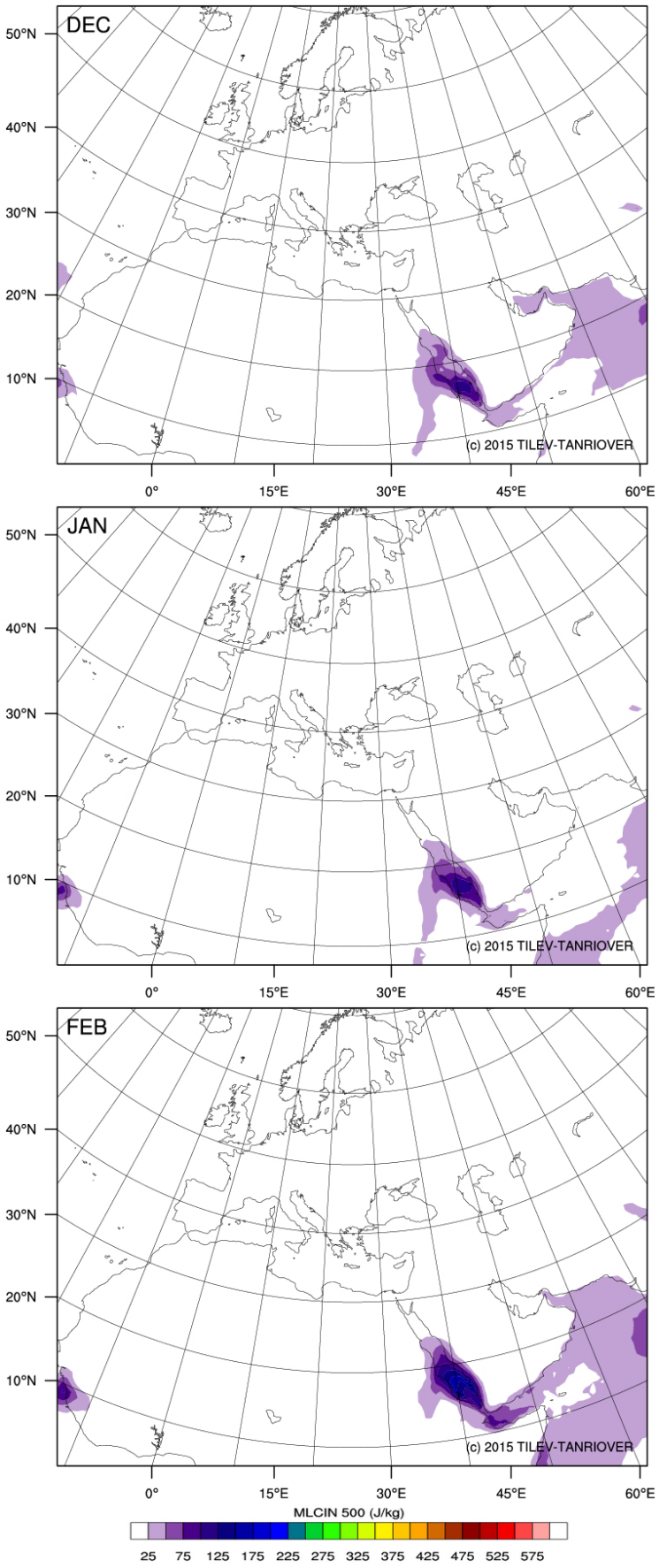

Figure A.17 : Long-term monthly mean maps of MLCIN for winter: December, January, and February.

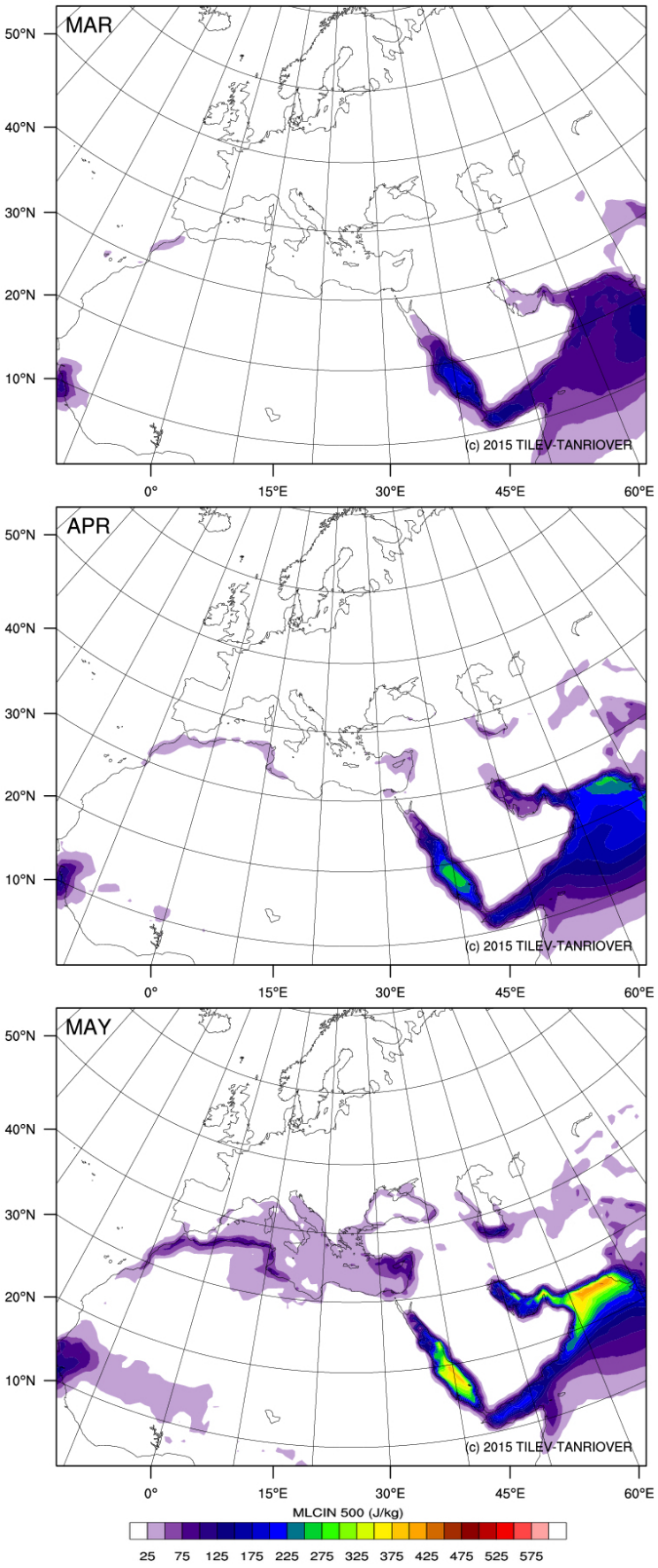

Figure A.18 : Long-term monthly mean maps of MLCIN for spring: March, April, and May.

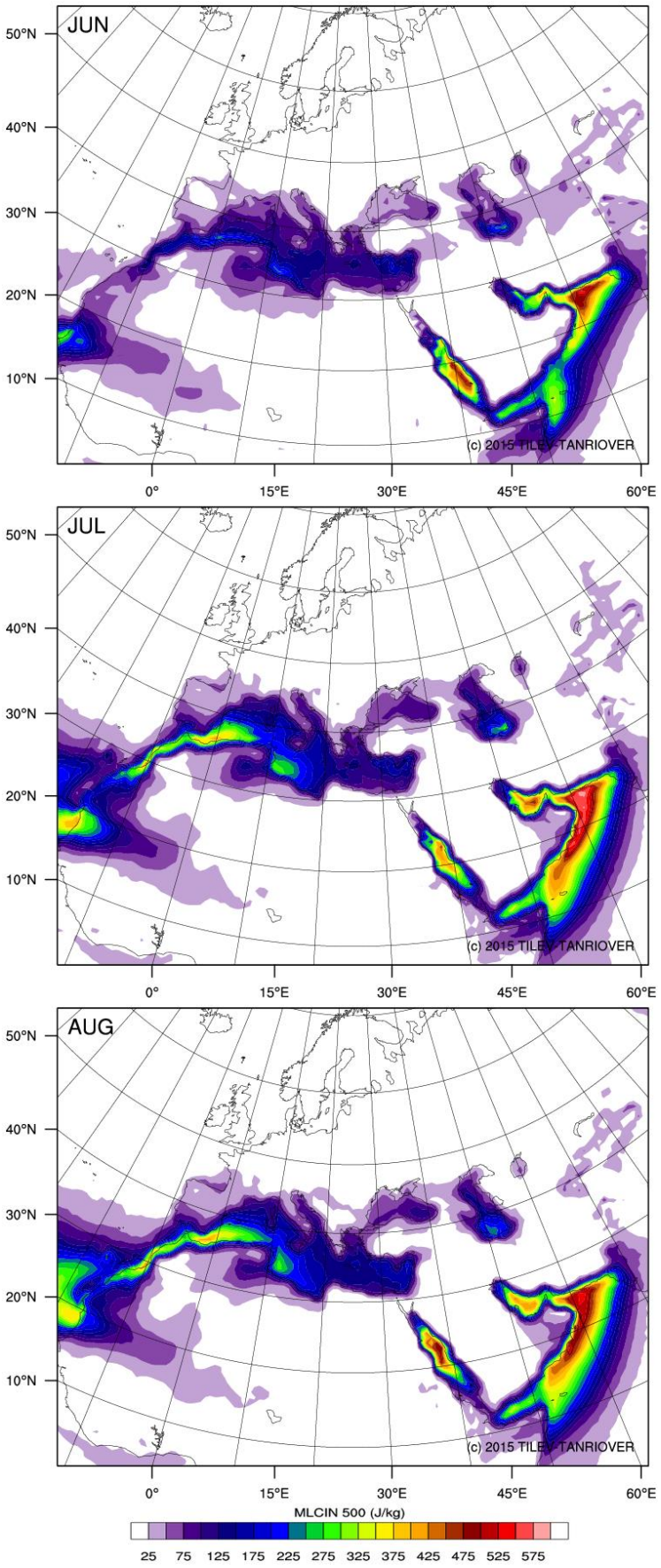

Figure A.19 : Long-term monthly mean maps of MLCIN for summer: June, July, and August.

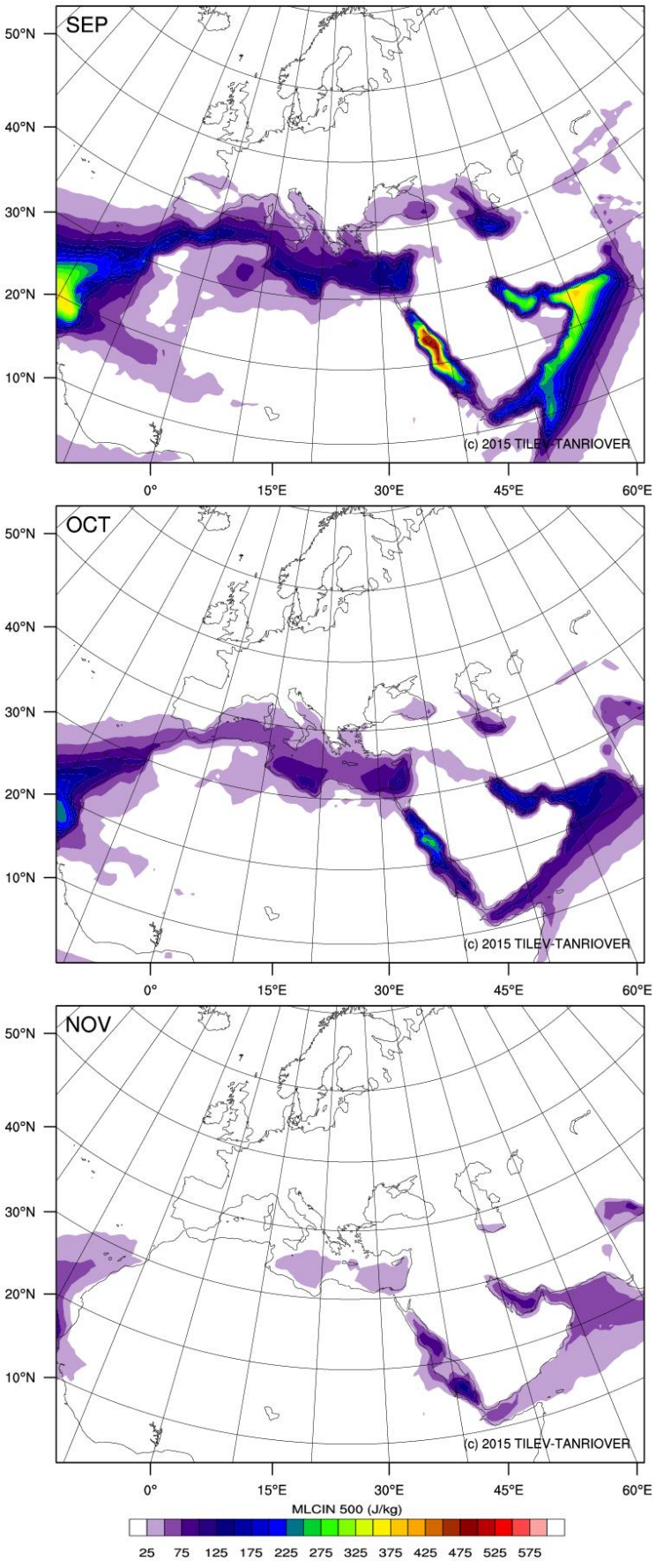

Figure A.20 : Long-term monthly mean maps of MLCIN for autumn: September, October, and November.

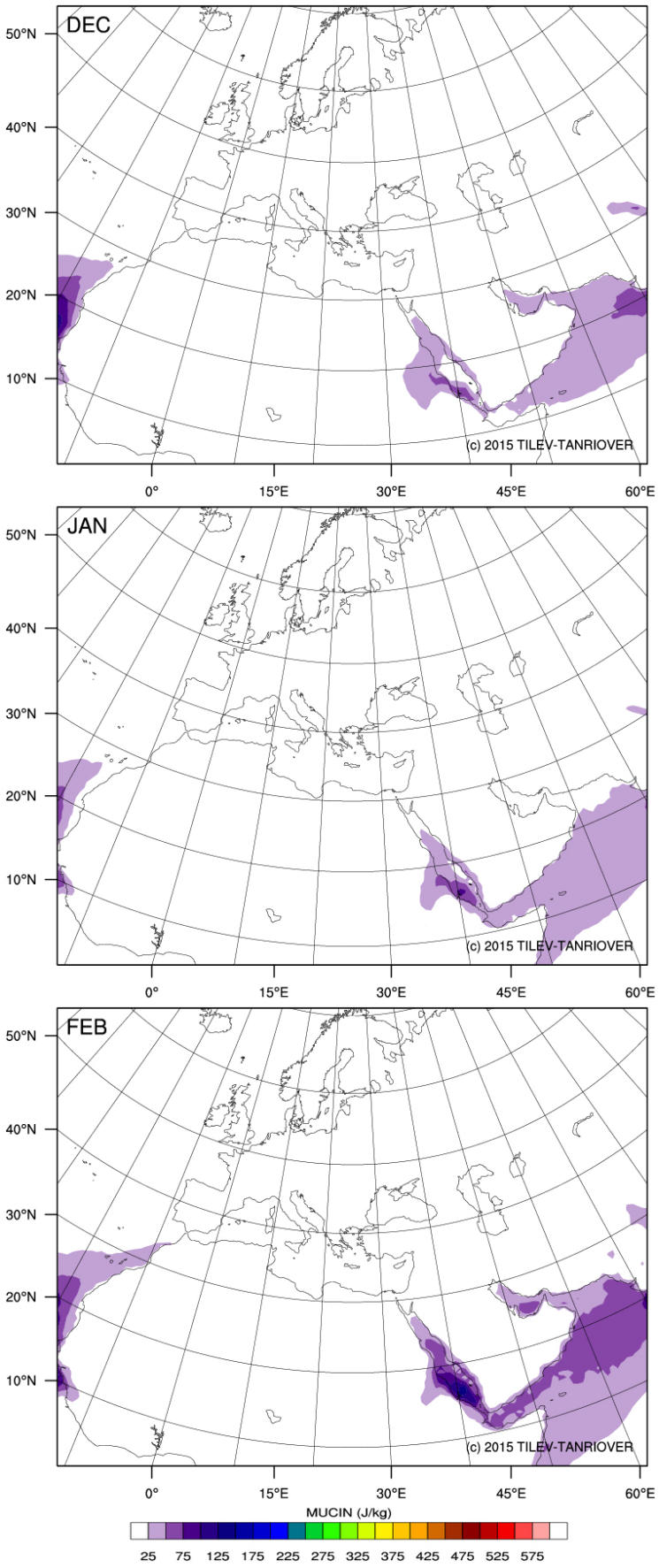

Figure A.21 : Long-term monthly mean maps of MUCIN for winter: December, January, and February.

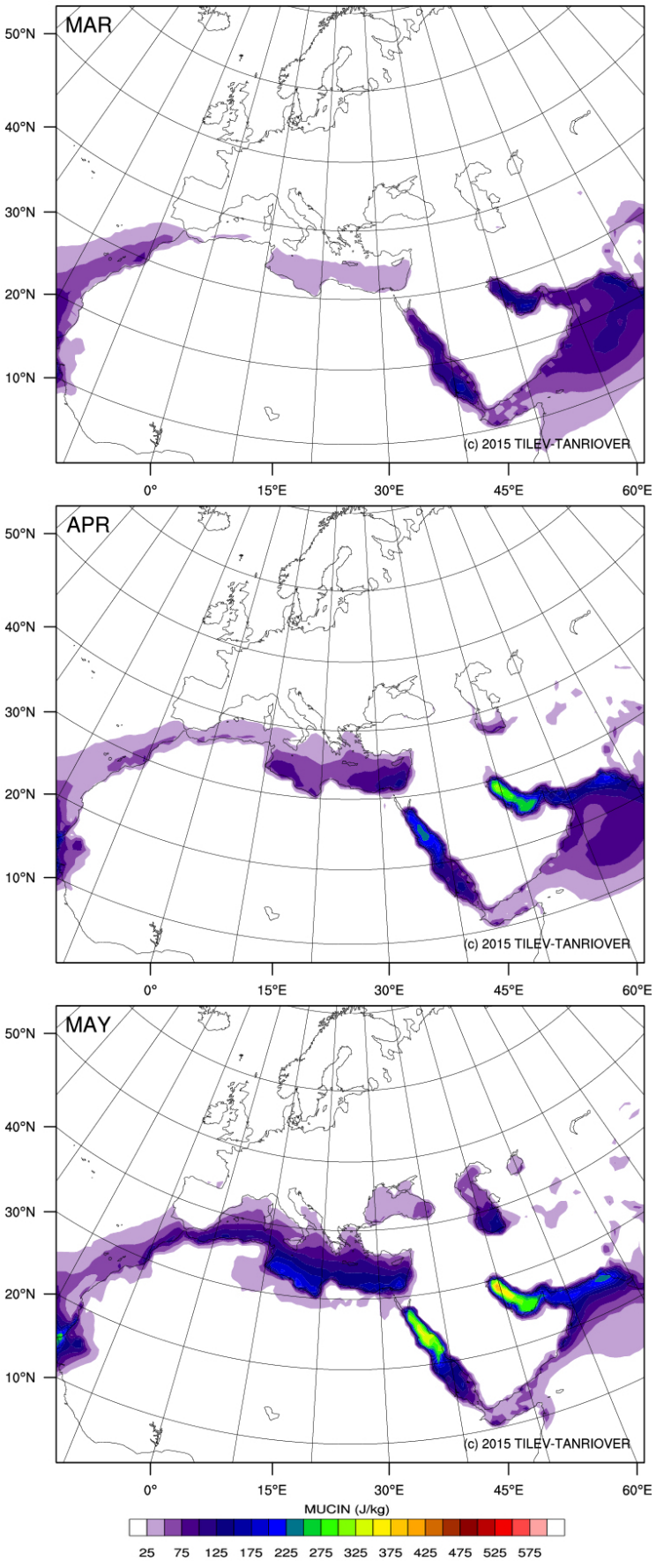

Figure A.22 : Long-term monthly mean maps of MUCIN for spring: March, April, and May.

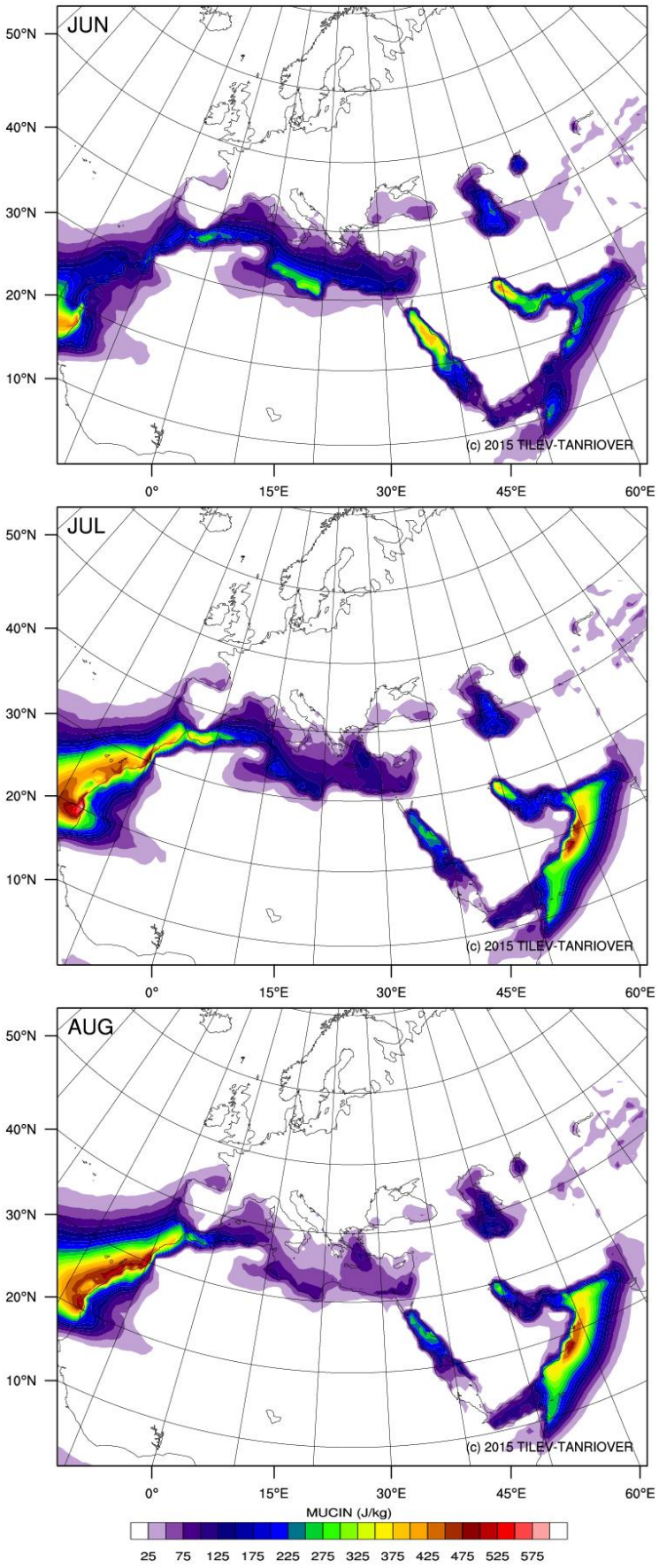

Figure A.23 : Long-term monthly mean maps of MUCIN for summer: June, July, and August.

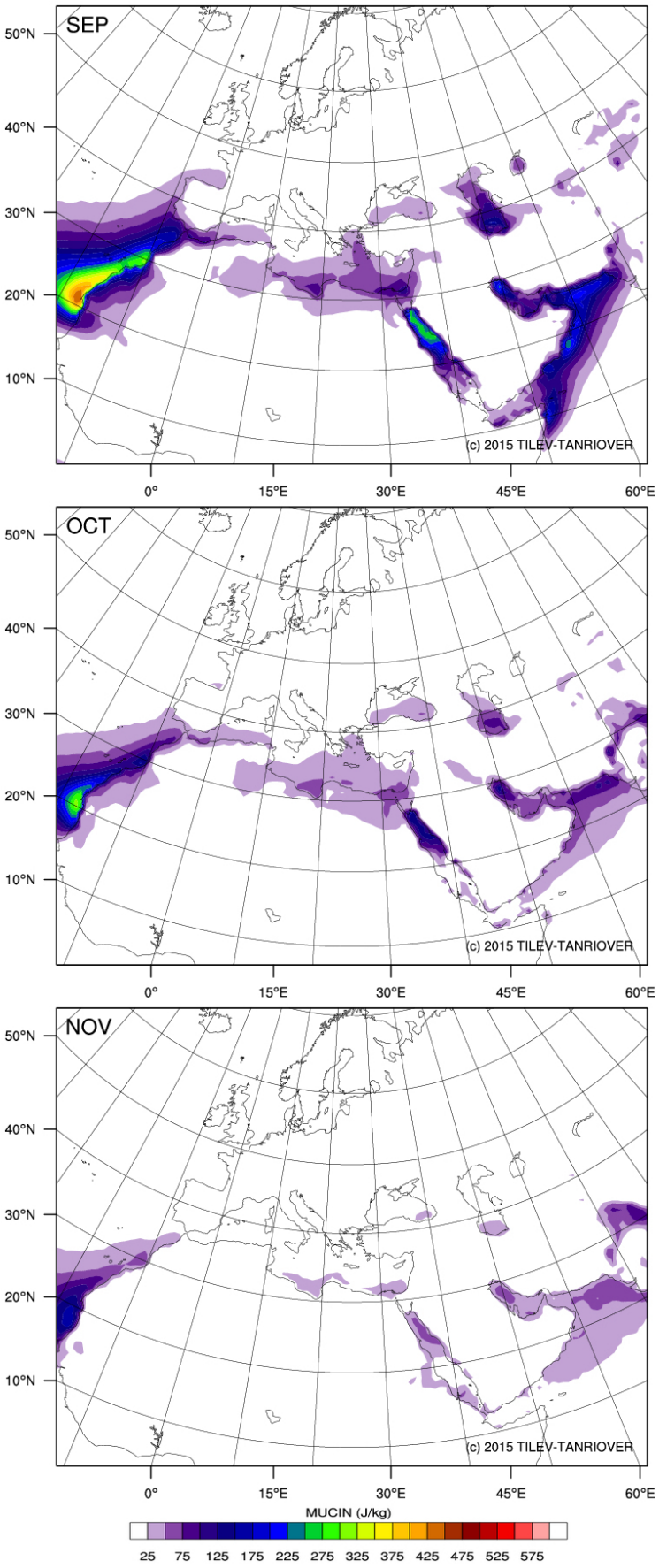

Figure A.24 : Long-term monthly mean maps of MUCIN for autumn: September, October, and November.

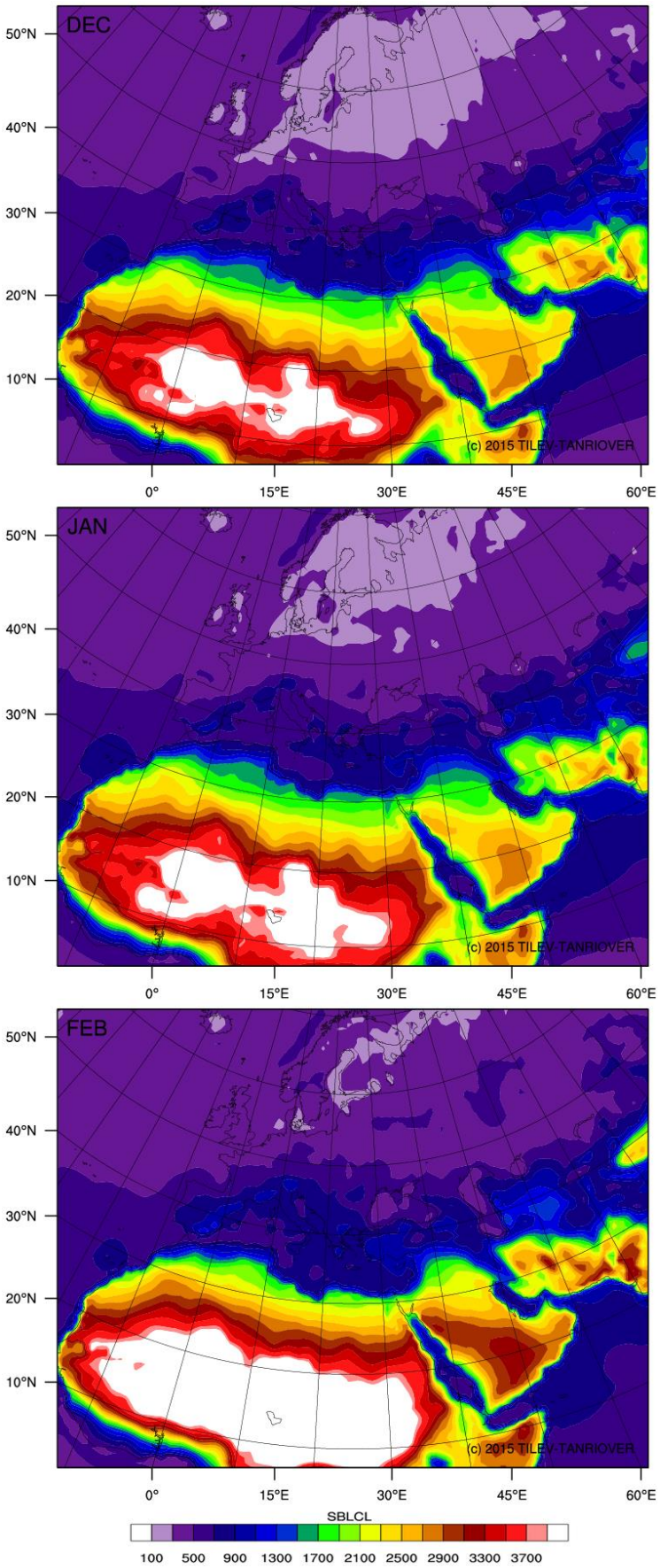

Figure A.25 : Long-term monthly mean maps of SBLCL for winter: December, January, and February.

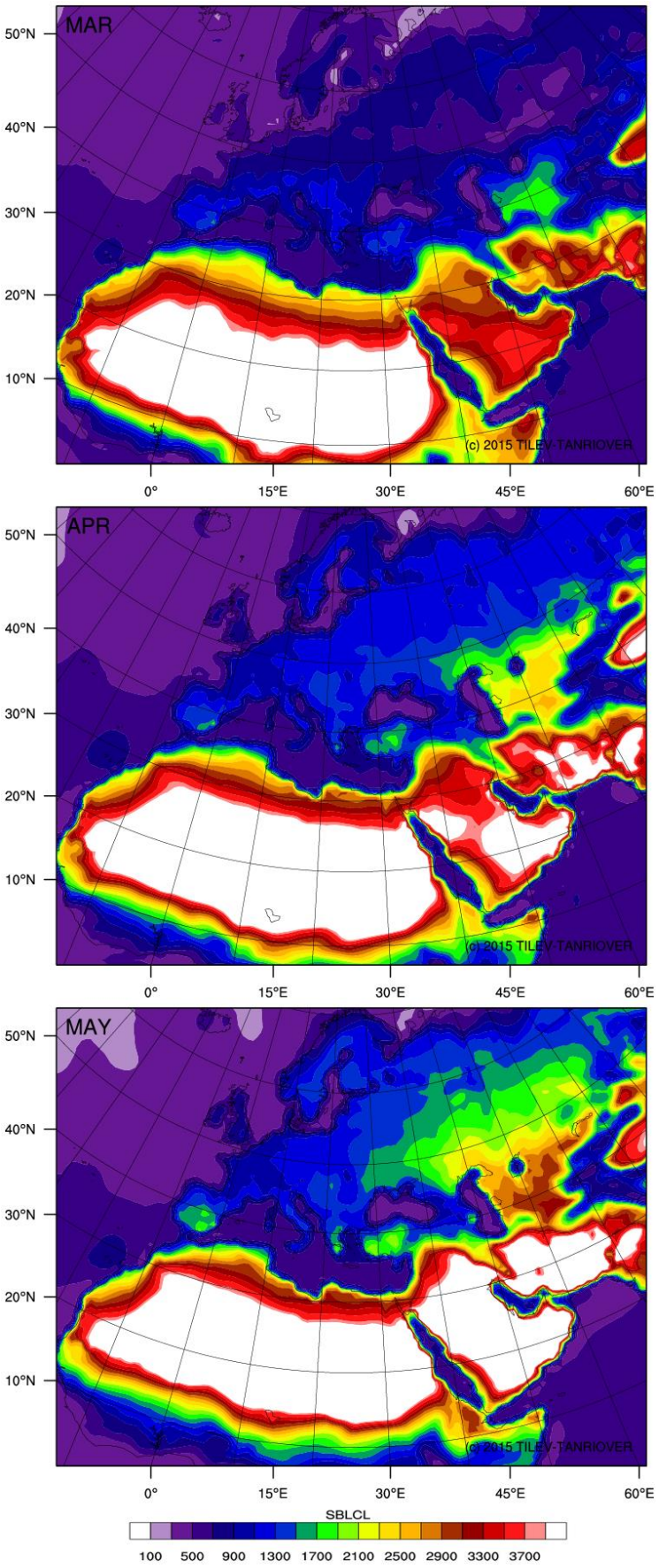

Figure A.26 : Long-term monthly mean maps of SBLCL for spring: March, April, and May.

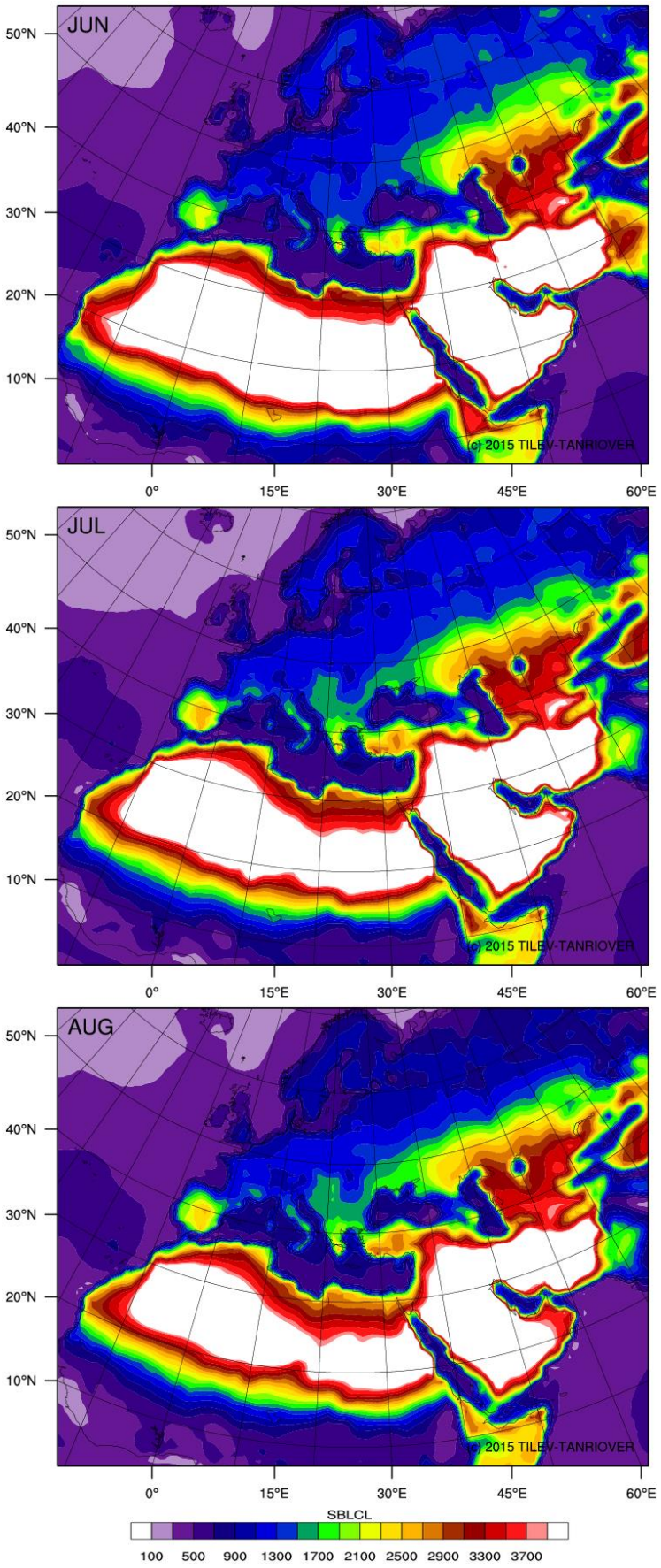

Figure A.27 : Long-term monthly mean maps of SBLCL for summer: June, July, and August.

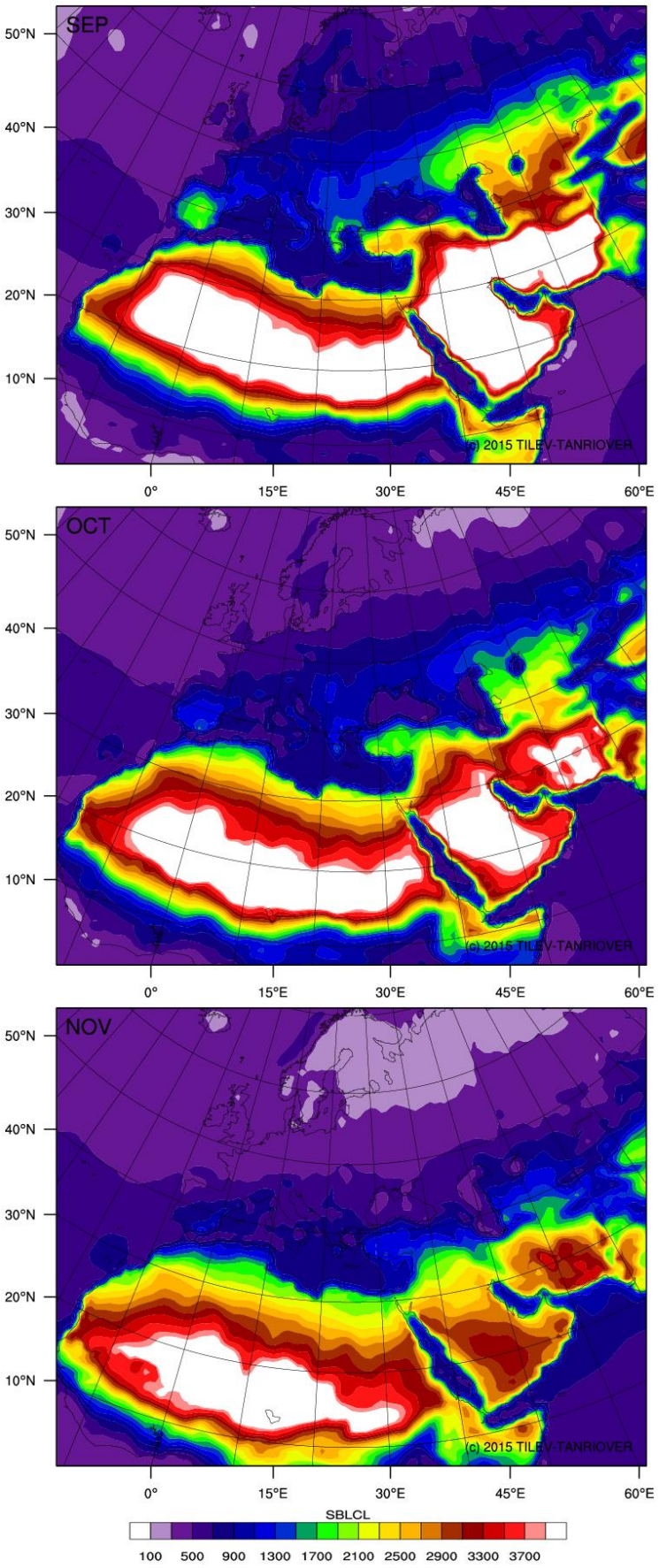

Figure A.28 : Long-term monthly mean maps of SBLCL for autumn: September, October, and November.

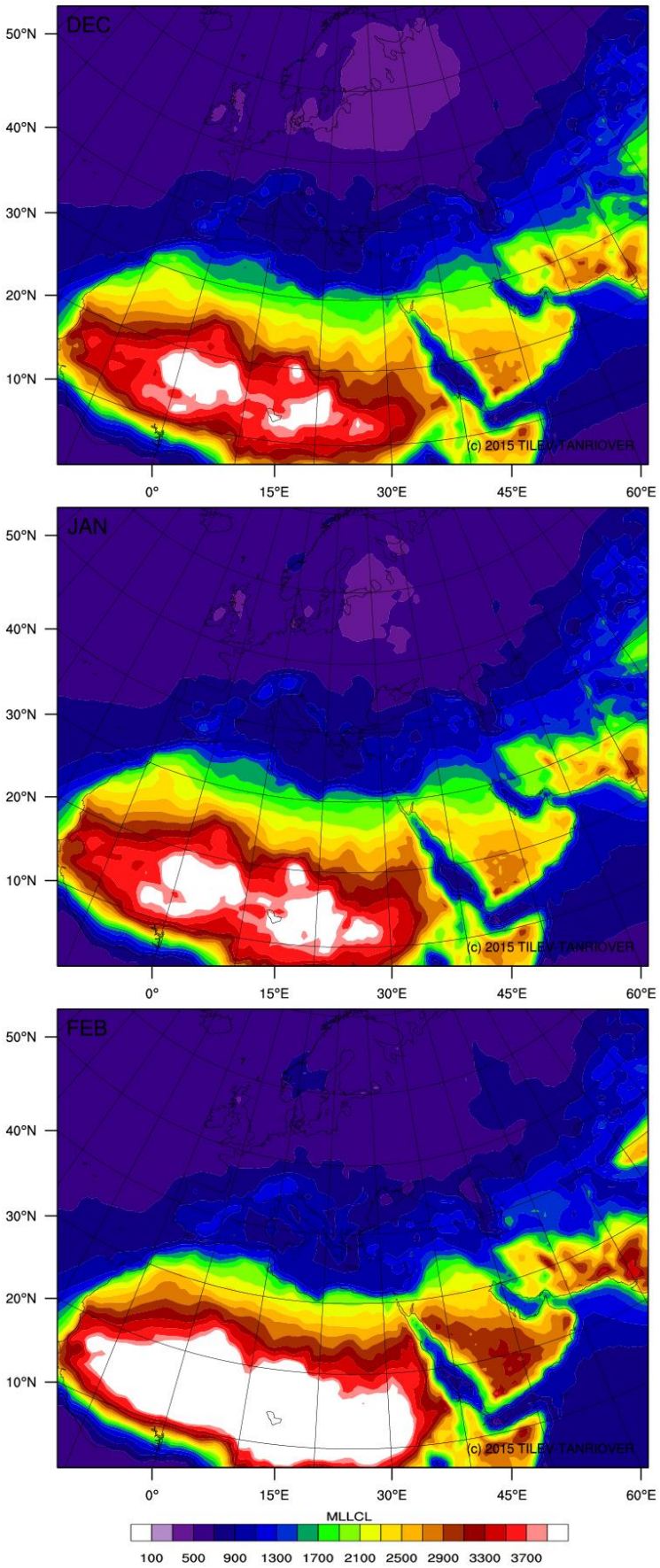

Figure A.29 : Long-term monthly mean maps of MLLCL for winter: December, January, and February.

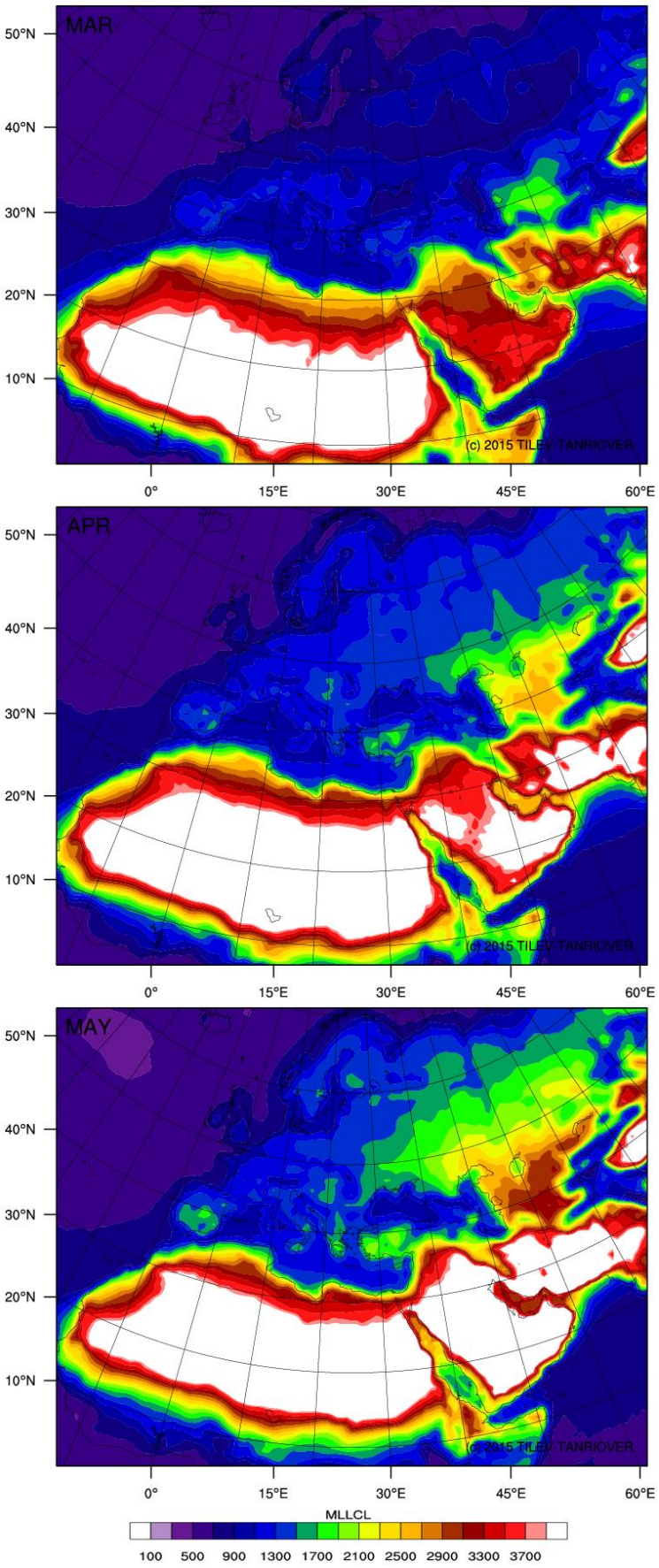

Figure A.30 : Long-term monthly mean maps of MLLCL for spring: March, April, and May.

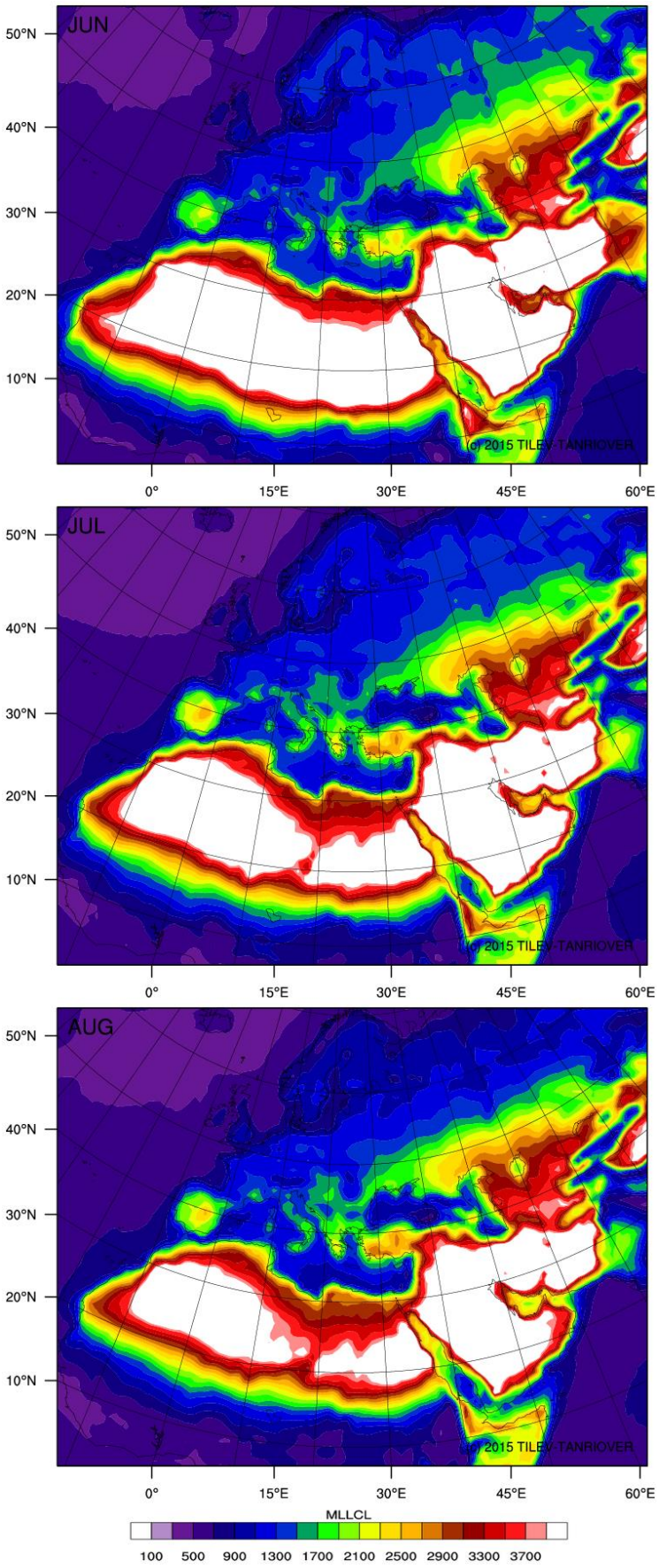

Figure A.31 : Long-term monthly mean maps of MLLCL for summer: June, July, and August.

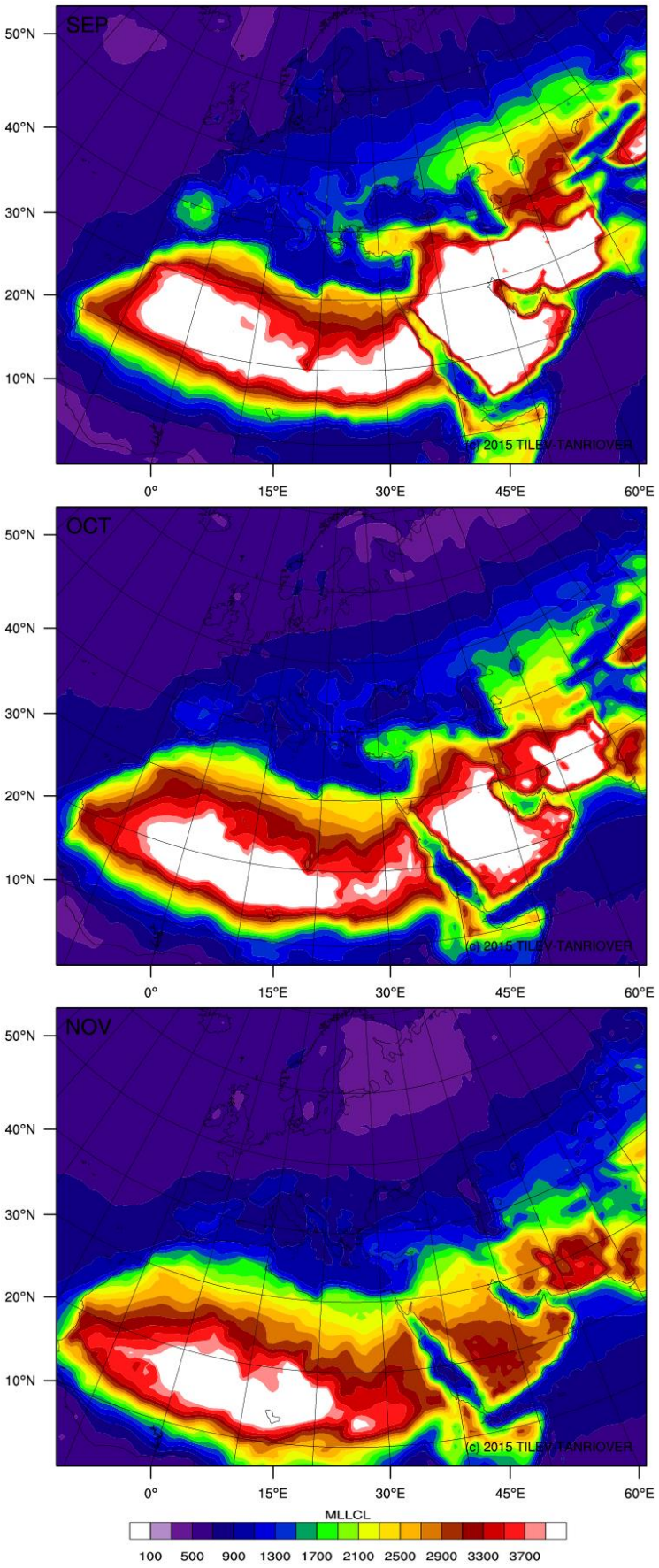

Figure A.32 : Long-term monthly mean maps of MLLCL for autumn: September, October, and November.

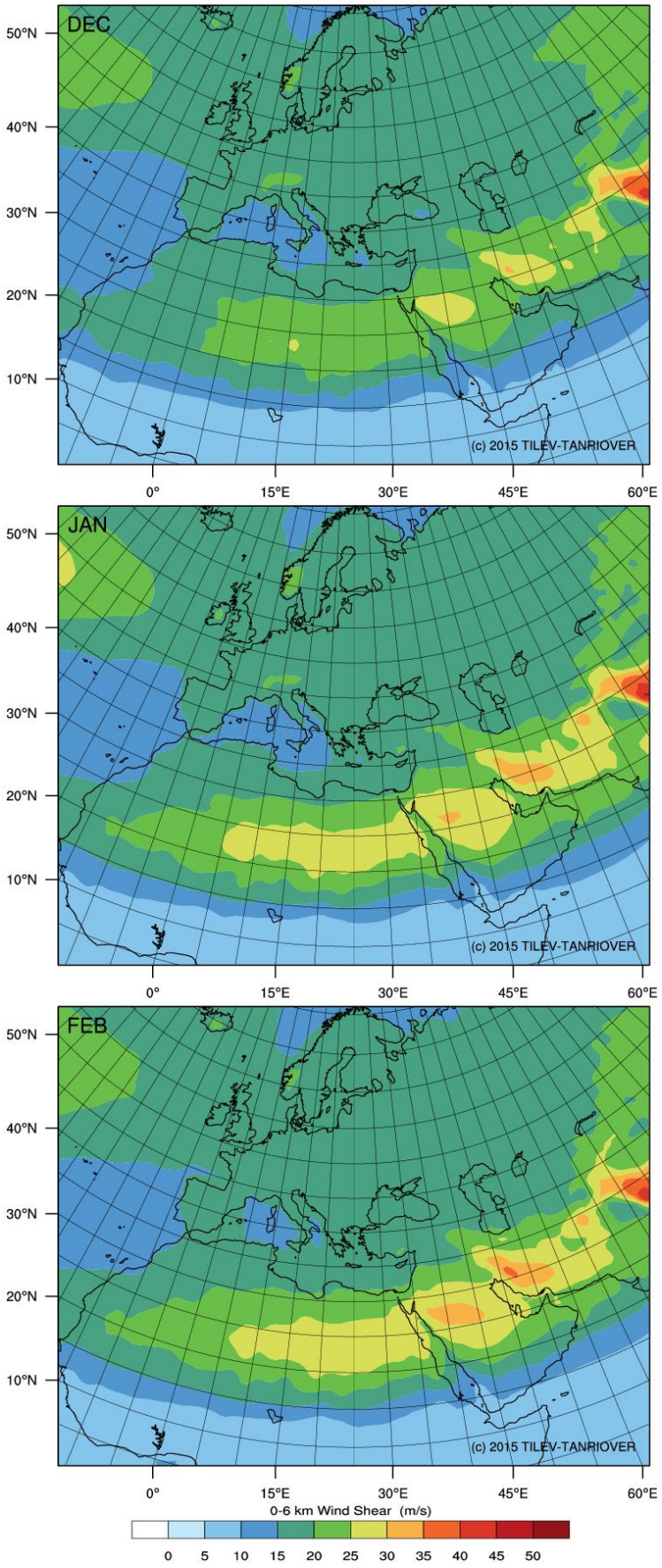

Figure A.33 : Long-term monthly mean maps of 0–6 km wind shear for winter: December, January, and February.

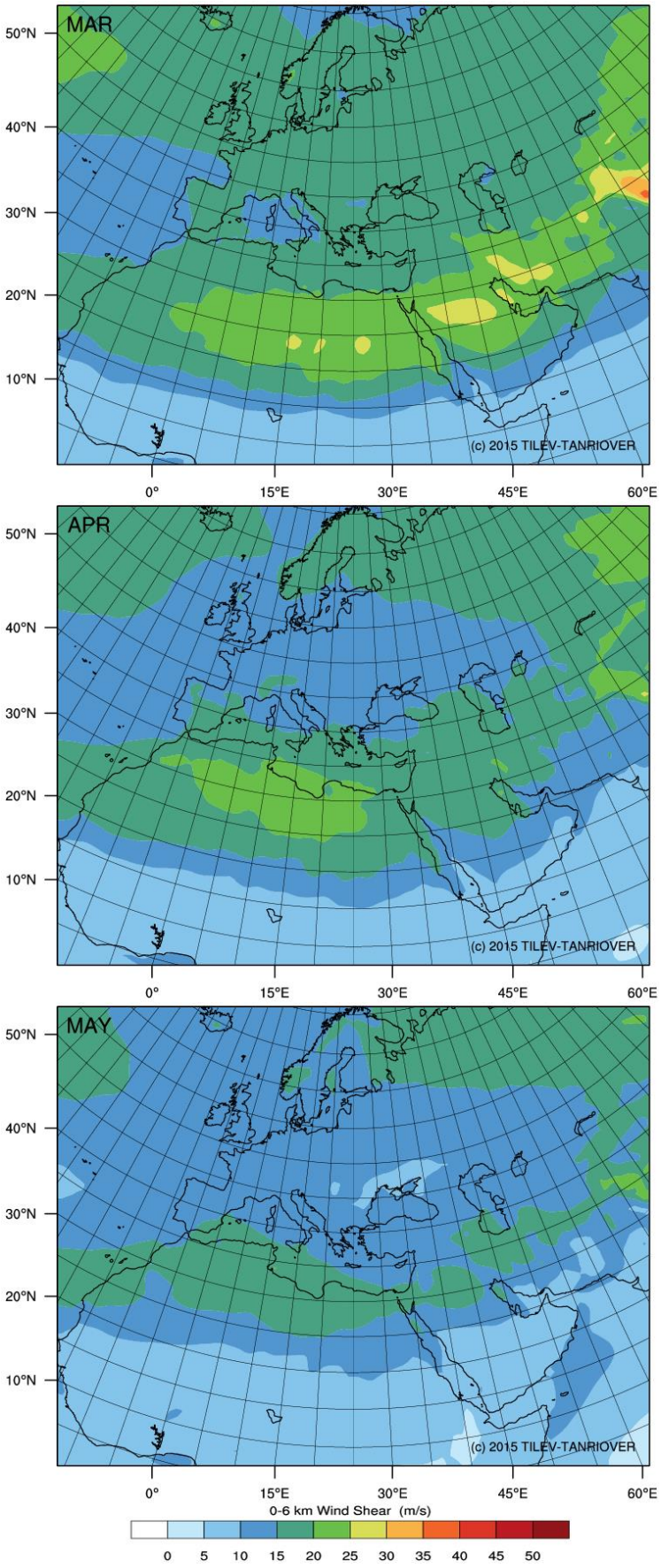

Figure A.34 : Long-term monthly mean maps of 0–6 km wind shear for spring: March, April, and May.

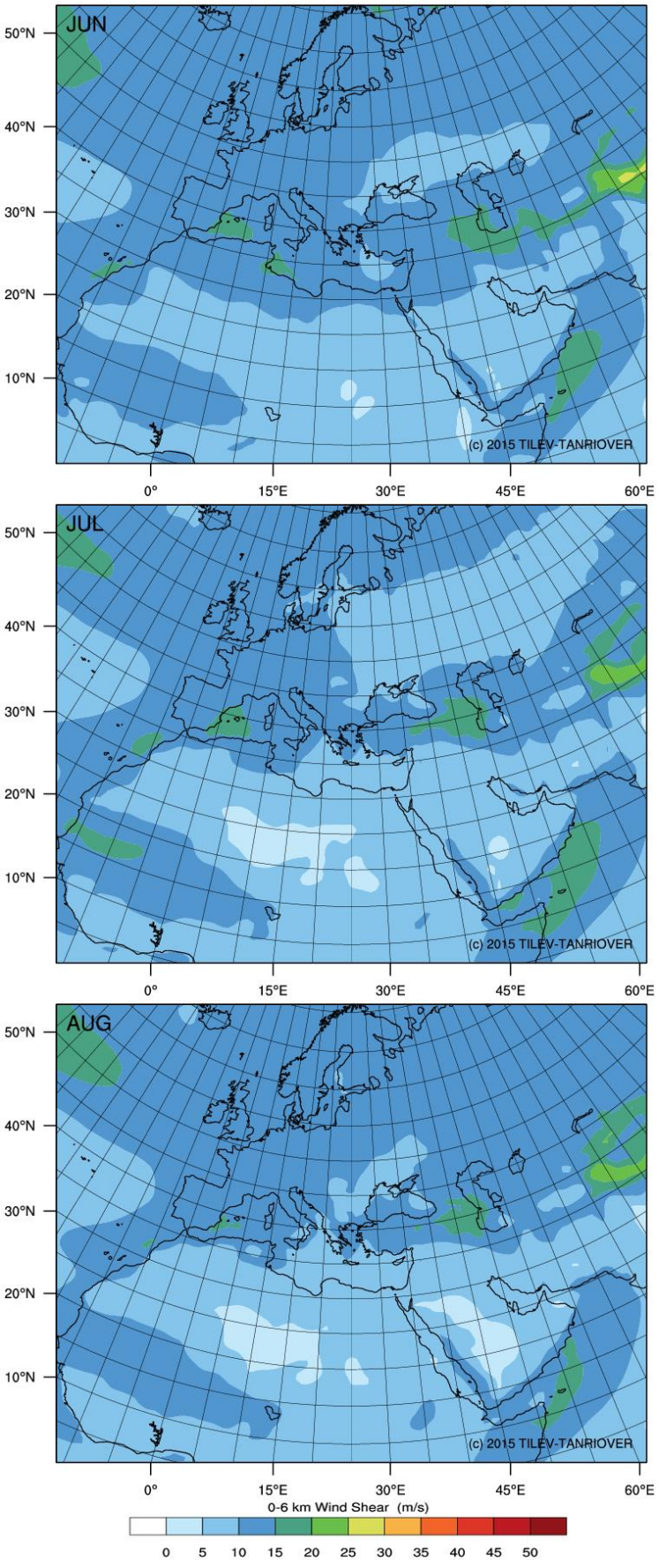

Figure A.35 : Long-term monthly mean maps of 0–6 km wind shear for summer: June, July, and August.

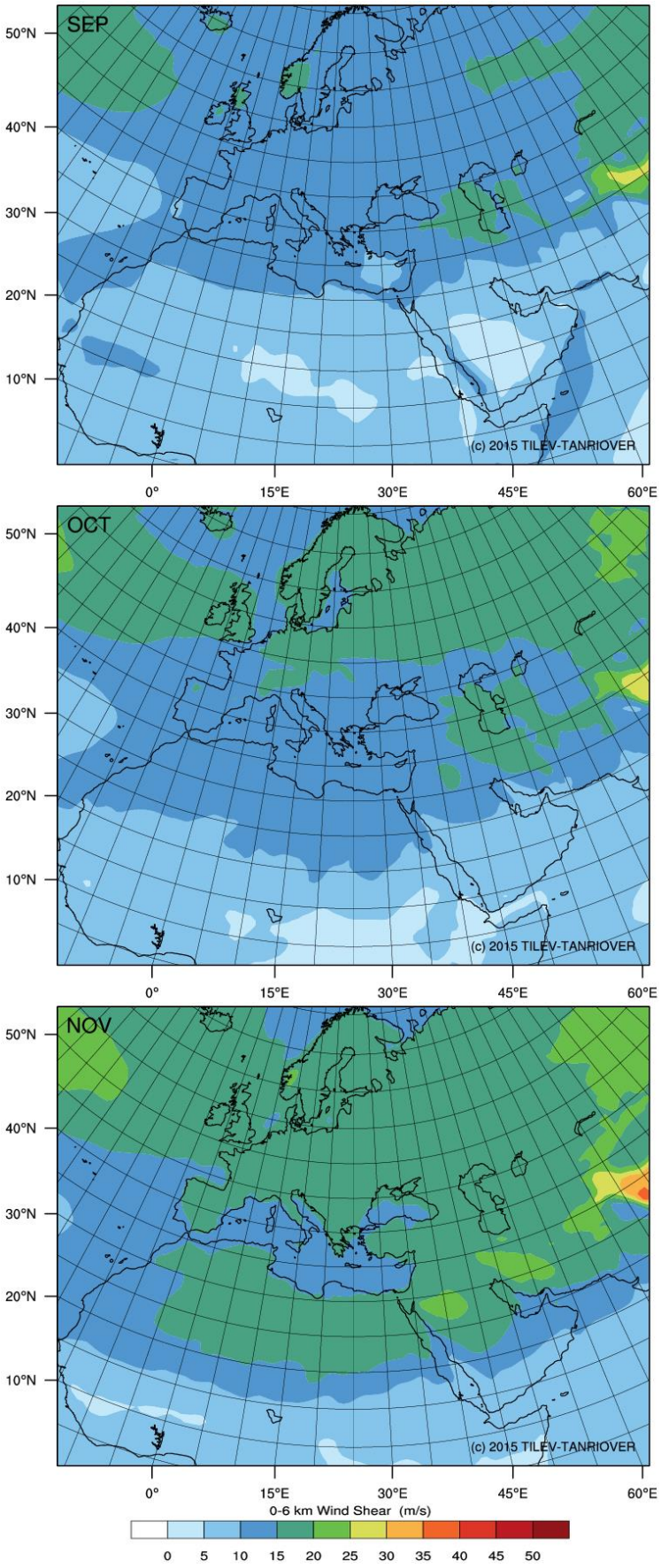

Figure A.36 : Long-term monthly mean maps of 0–6 km wind shear for autumn: September, October, and November.

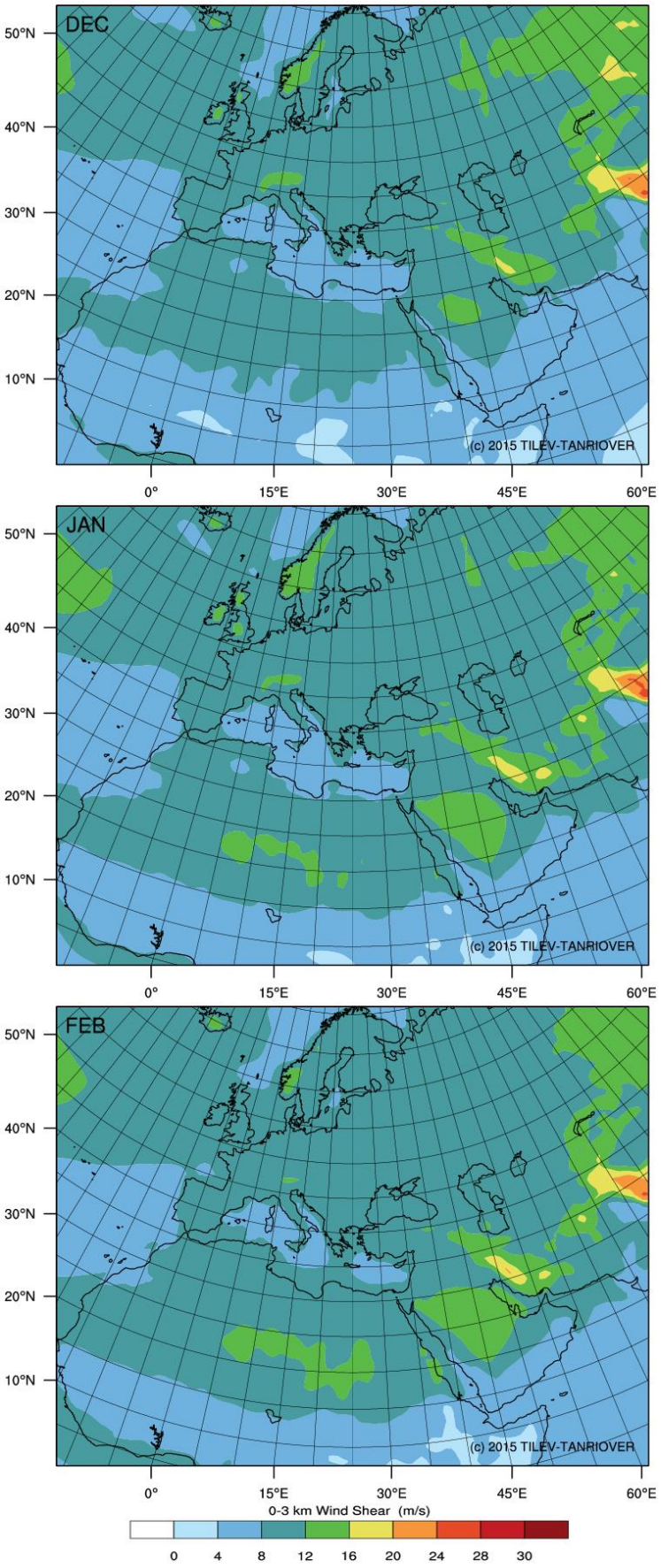

Figure A.37 : Long-term monthly mean maps of 0–3 km wind shear for winter: December, January, and February.

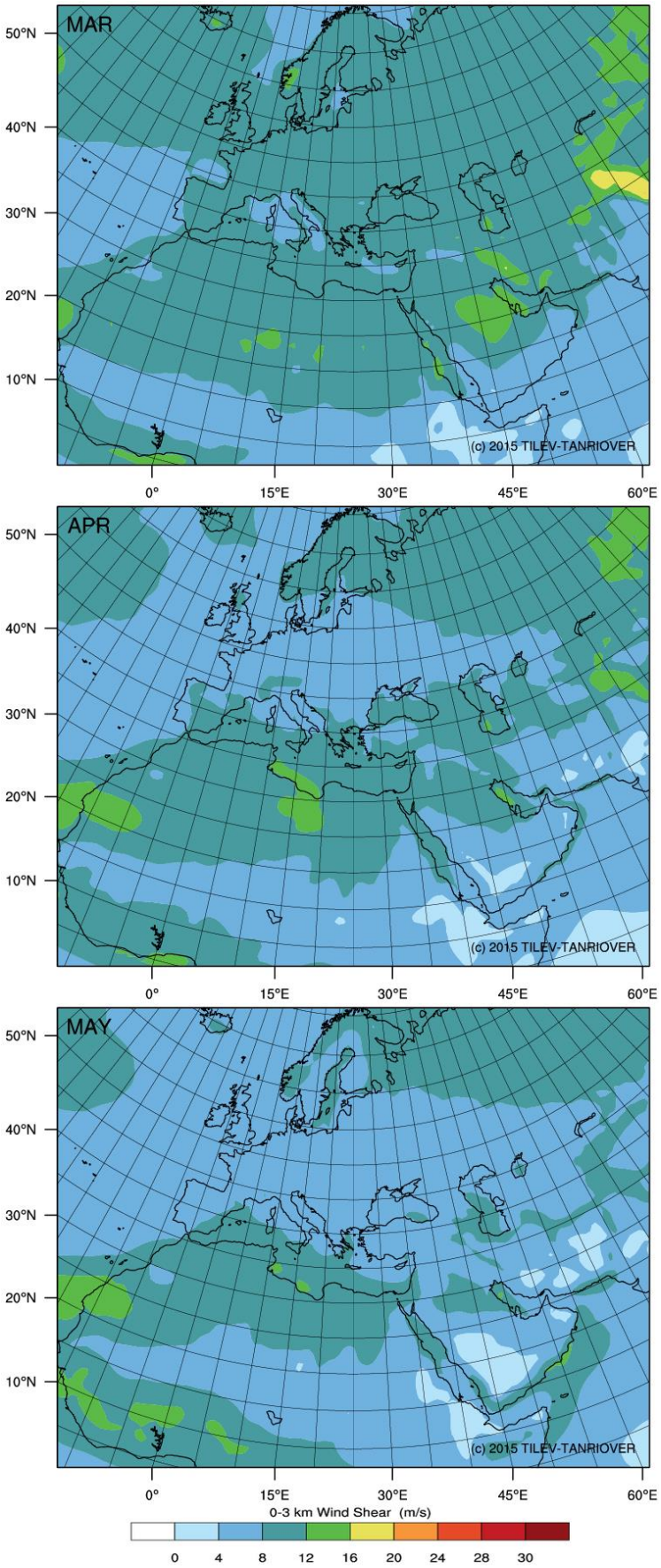

Figure A.38 : Long-term monthly mean maps of 0–3 km wind shear for spring: March, April, and May.

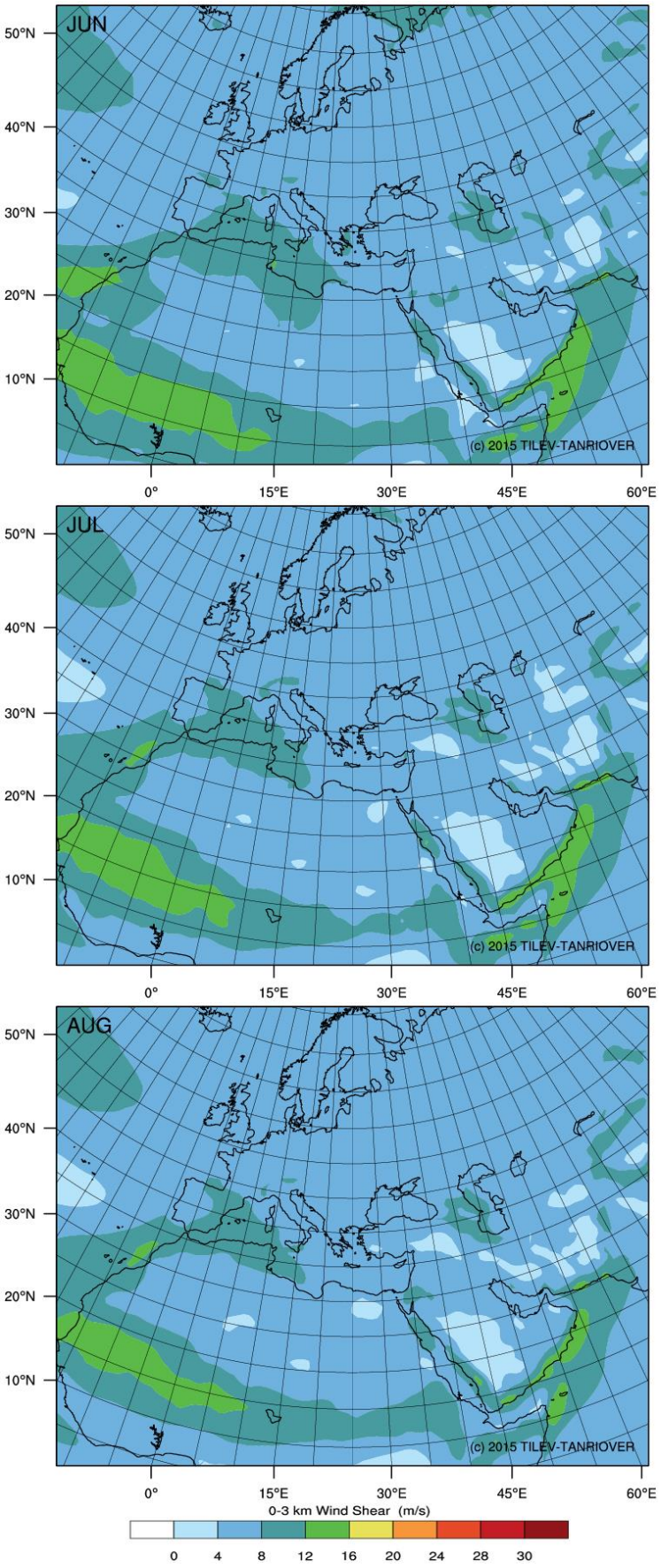

Figure A.39 : Long-term monthly mean maps of 0–3 km wind shear for summer: June, July, and August.

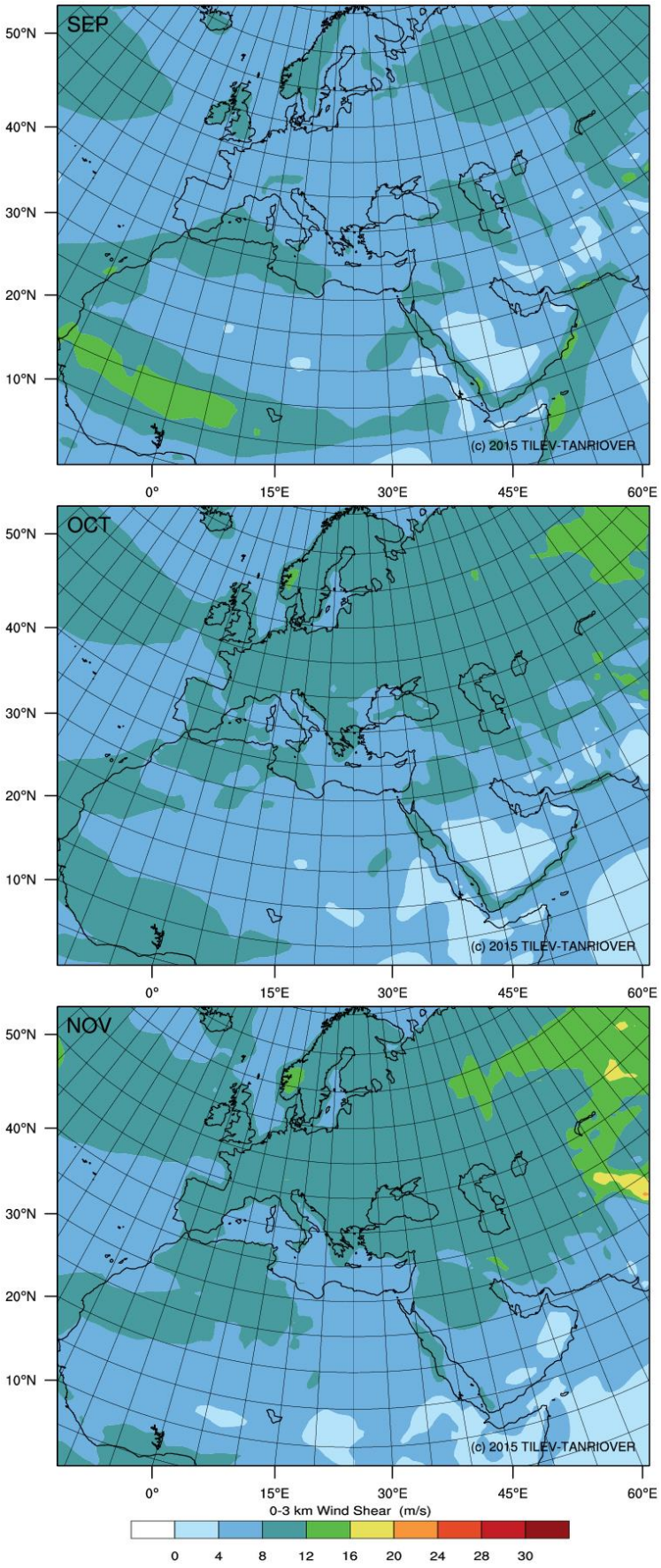

Figure A.40 : Long-term monthly mean maps of 0–3 km wind shear for autumn: September, October, and November.

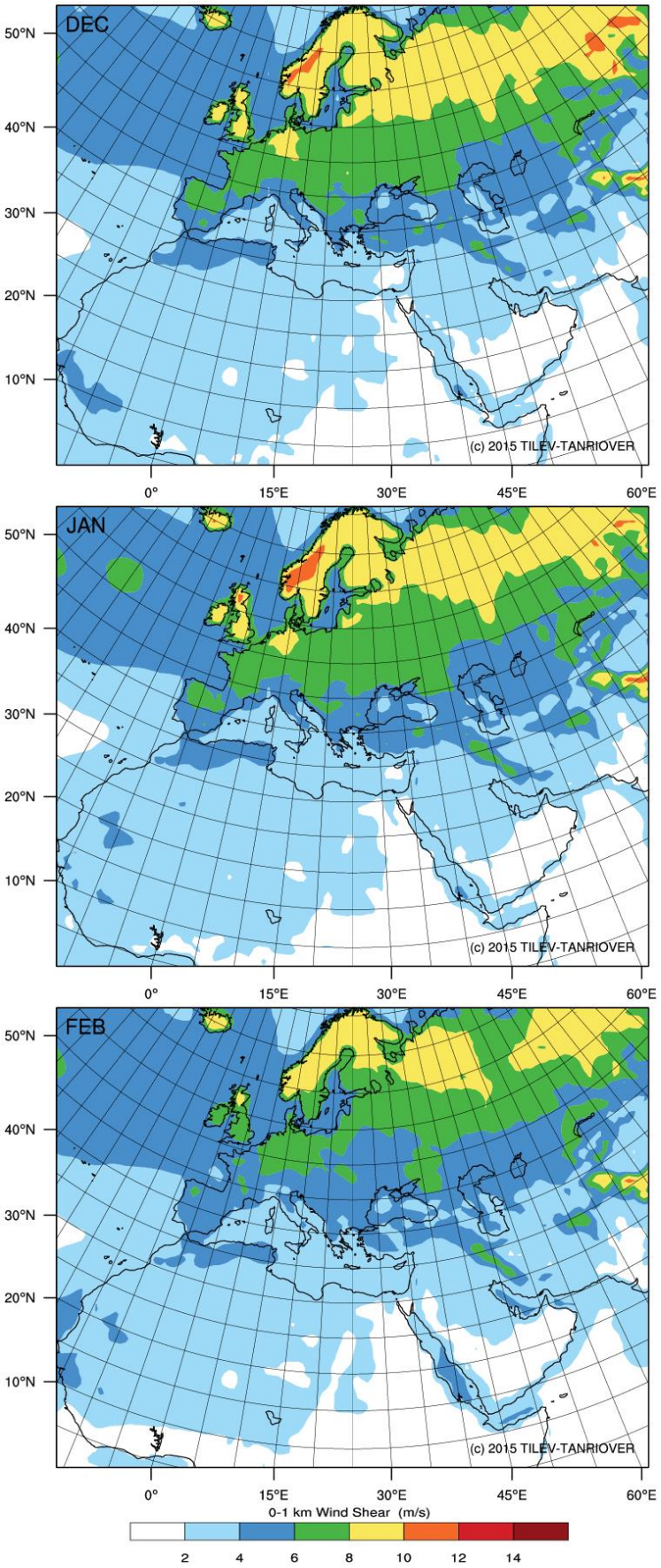

Figure A.41 : Long-term monthly mean maps of 0–1 km wind shear for winter: December, January, and February.

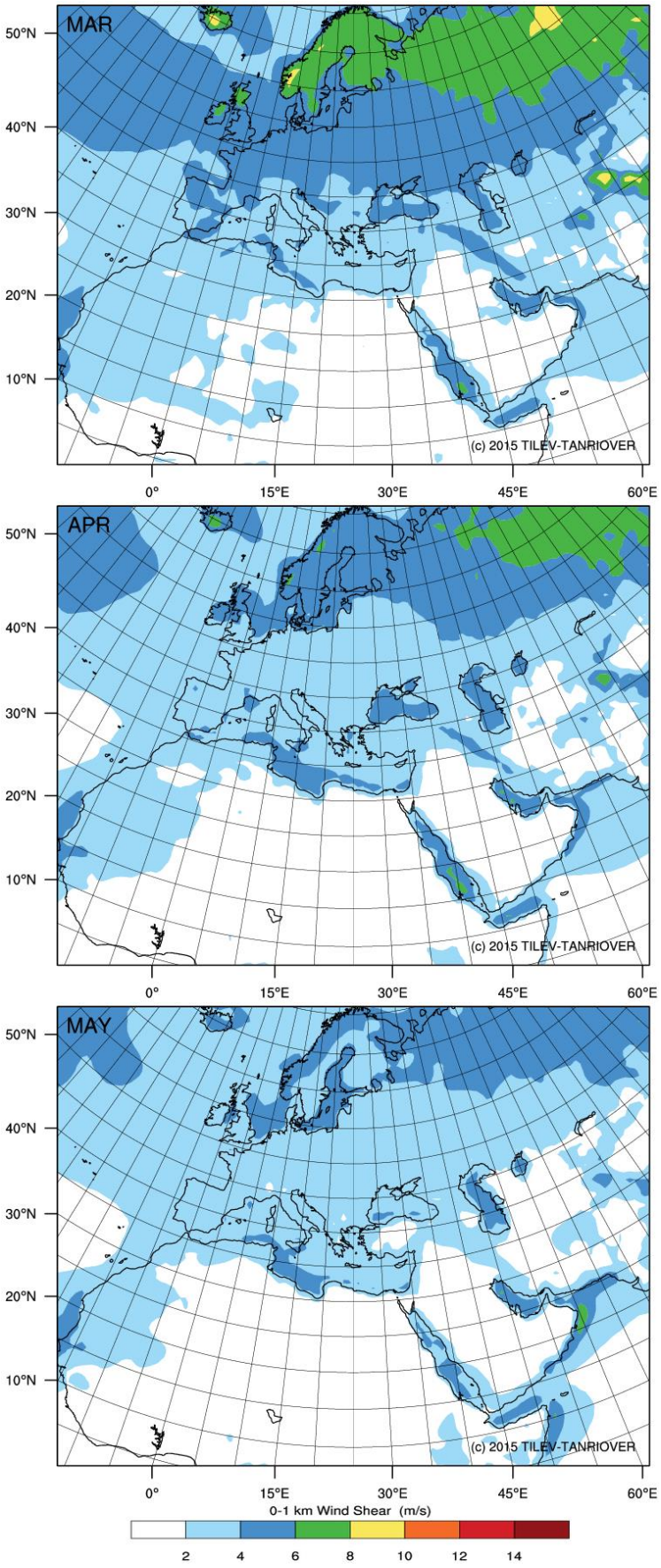

Figure A.42 : Long-term monthly mean maps of 0–1 km wind shear for spring: March, April, and May.

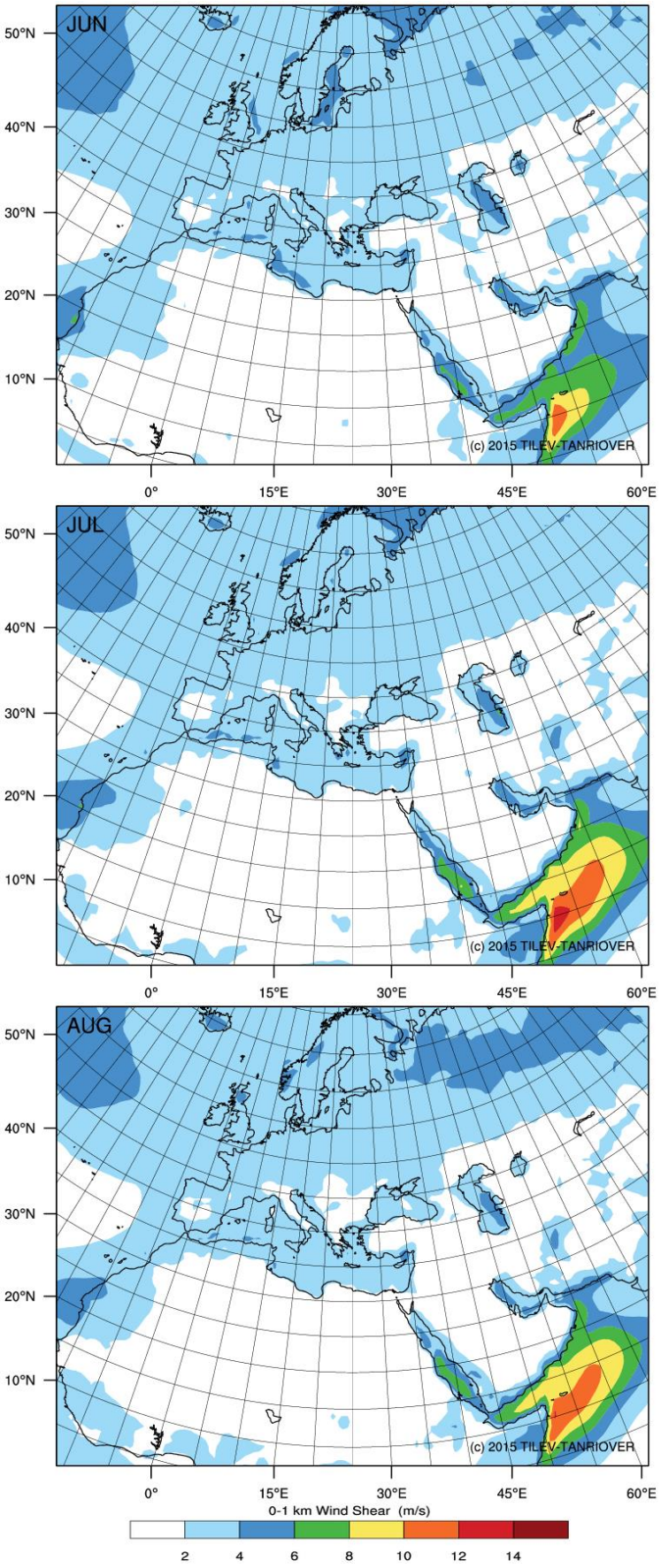

Figure A.43 : Long-term monthly mean maps of 0–1 km wind shear for summer: June, July, and August.

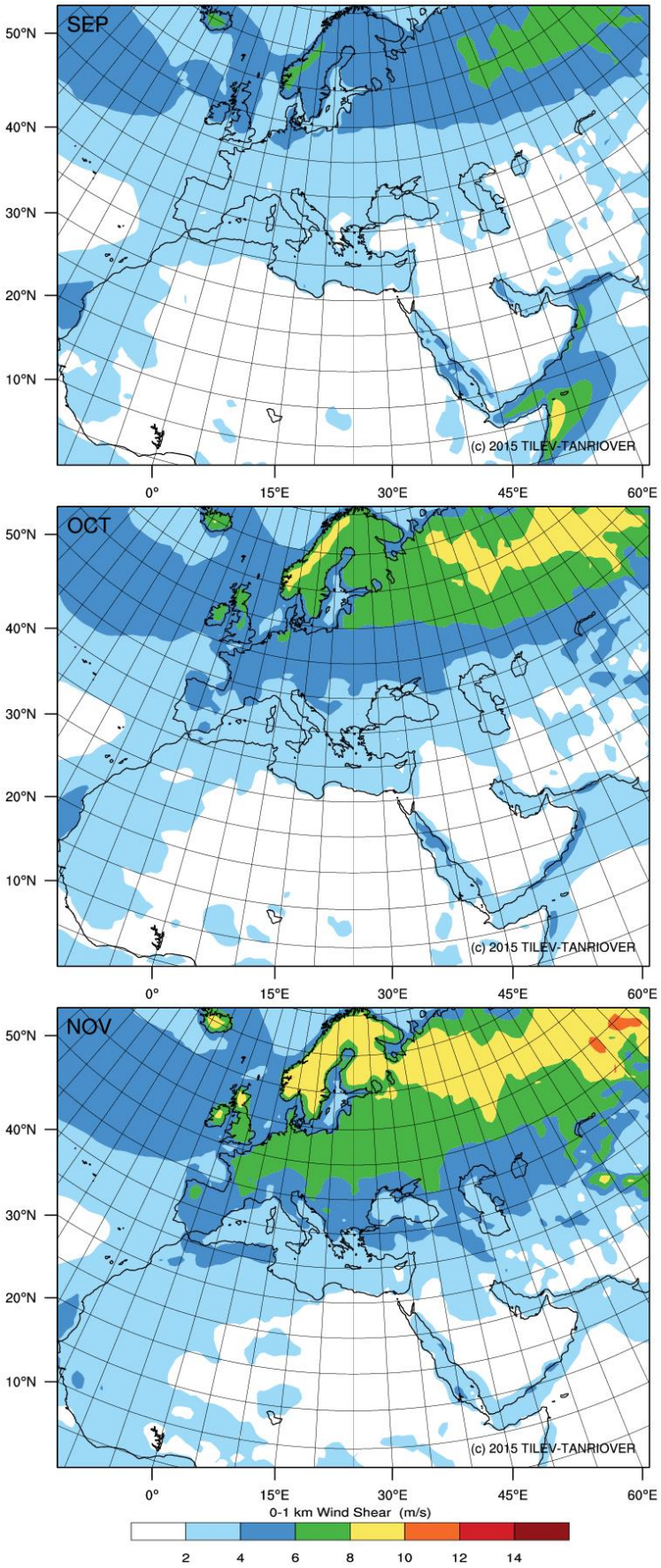

Figure A.44 : Long-term monthly mean maps of 0–1 km wind shear for autumn: September, October, and November.

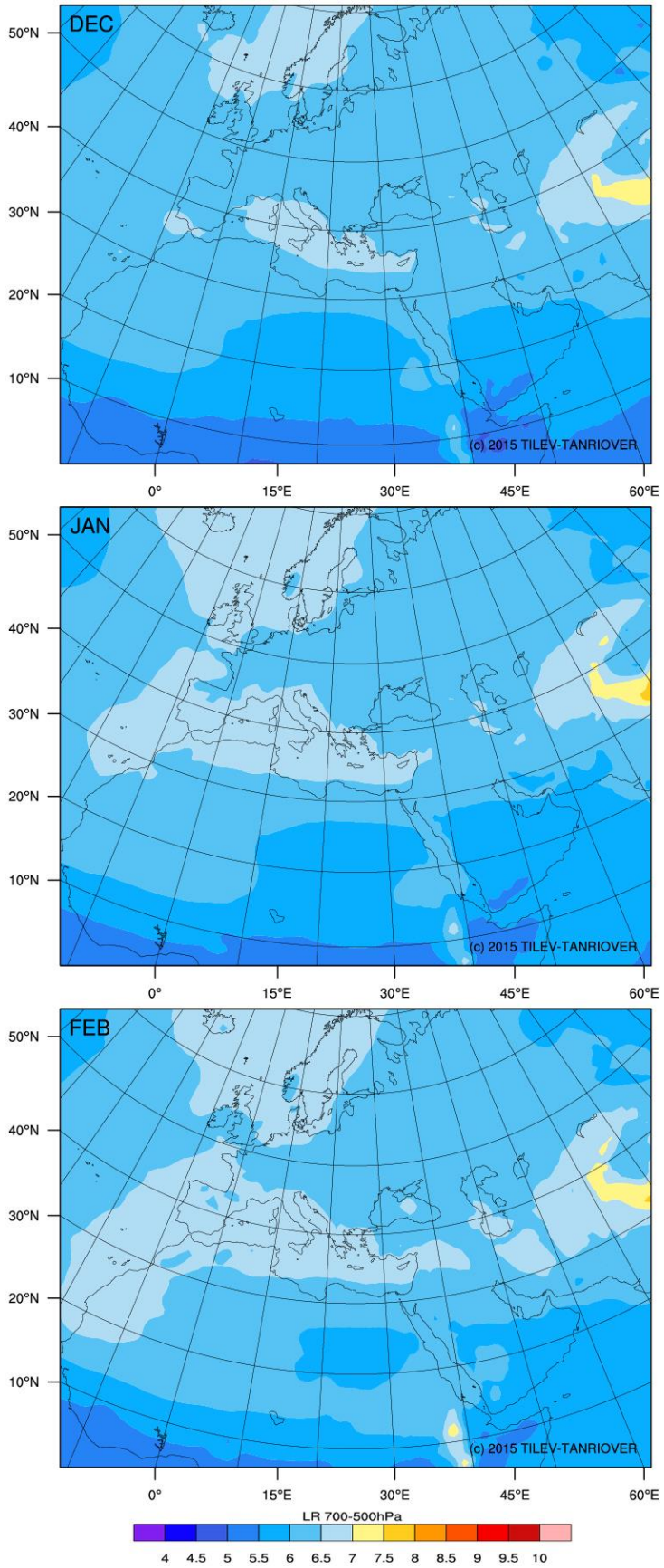

Figure A.45 : Long-term monthly mean maps of mid-tropospheric (700–500-hPa) lapse rates for winter: December, January, and February.

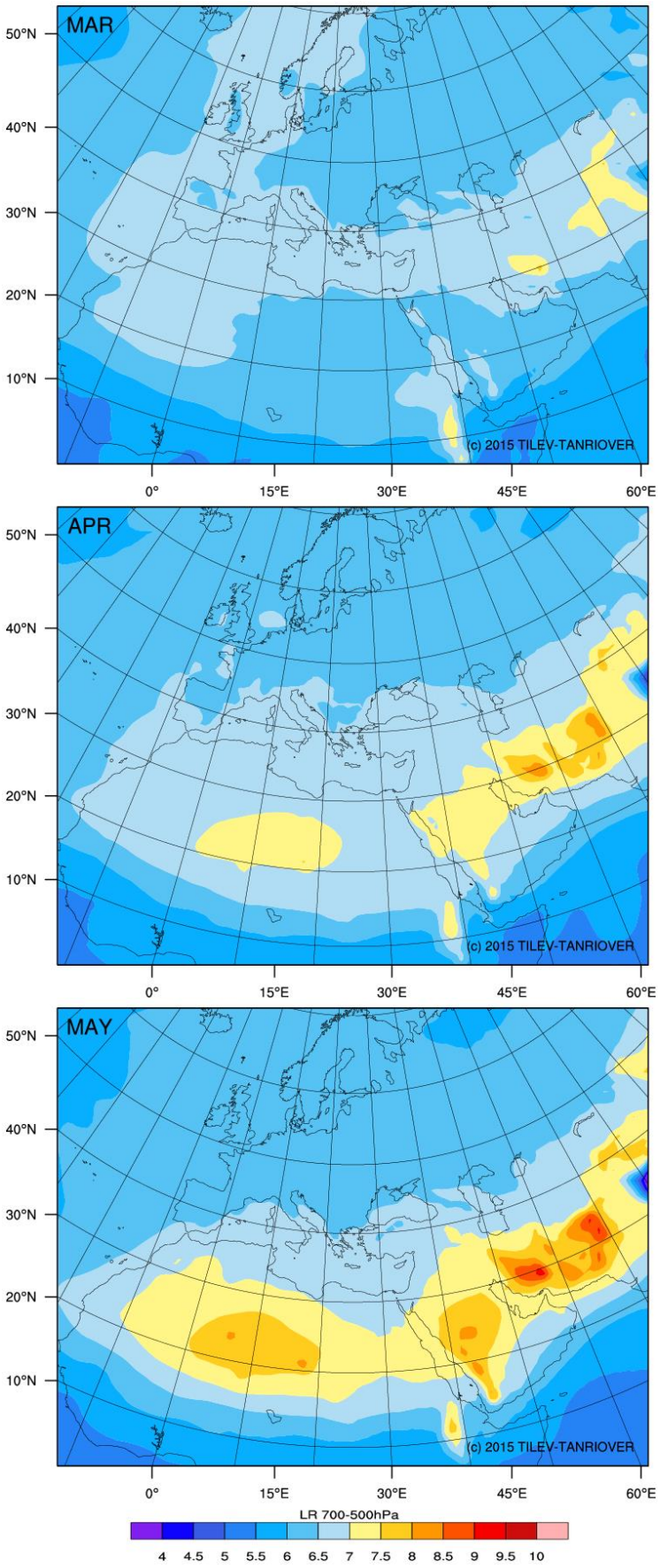

Figure A.46 : Long-term monthly mean maps of mid-tropospheric (700–500-hPa) lapse rates for spring: March, April, and May.

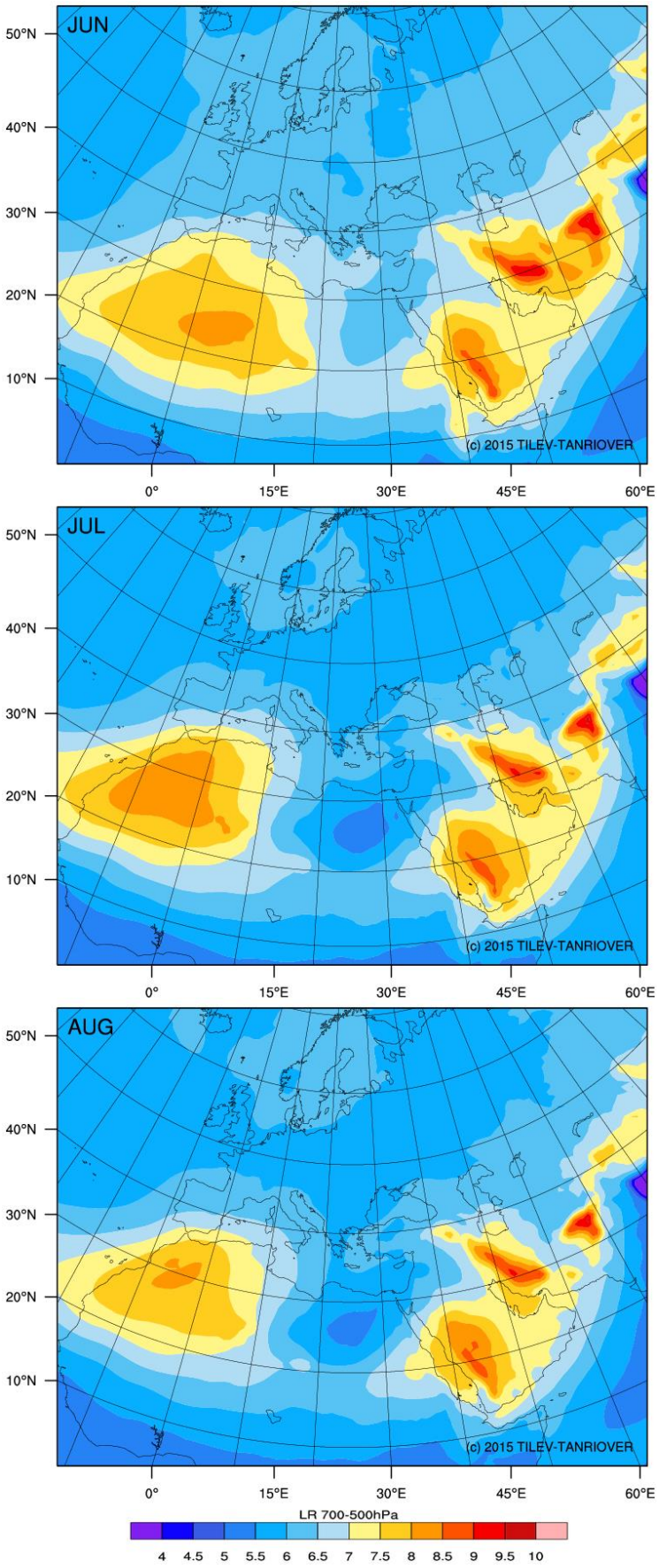

Figure A.47 : Long-term monthly mean maps of mid-tropospheric (700–500-hPa) lapse rates for summer: June, July, and August.

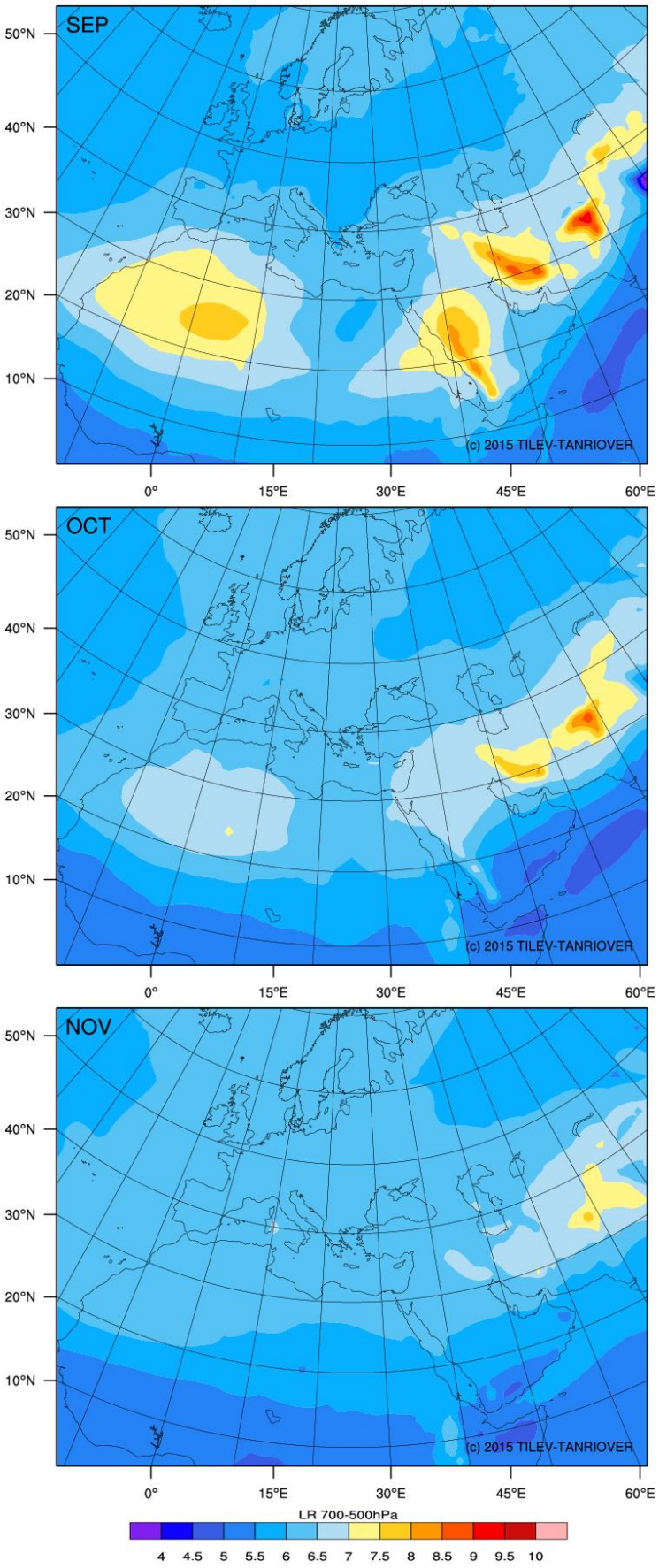

Figure A.48 : Long-term monthly mean maps of mid-tropospheric (700–500-hPa) lapse rates for autumn: September, October, and November.

APPENDIX B

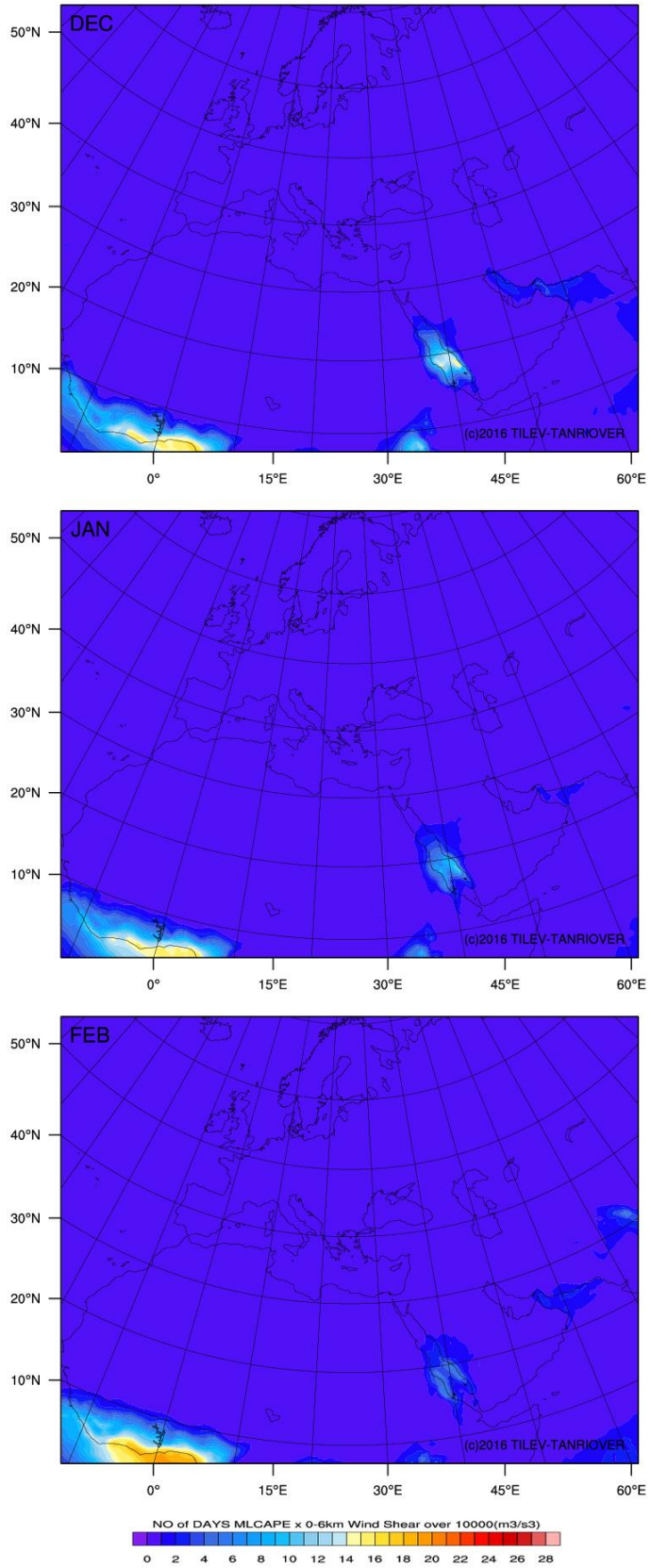

Figure B.1 : Mean number of days with MLCAPE × 0–6 km wind shear values over 10000 m^3/s^3 for winter: December, January, and February.

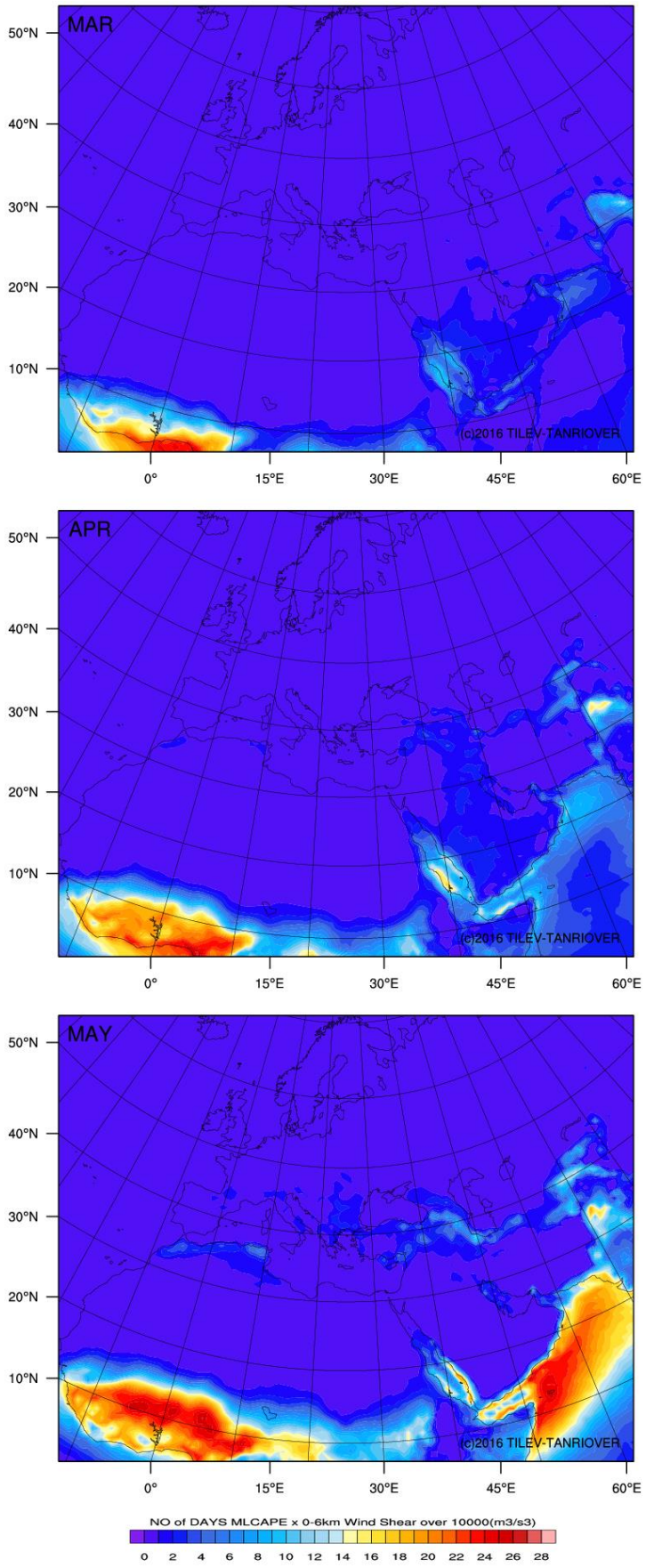

Figure B.2 : Mean number of days with MLCAPE × 0–6 km wind shear values over 10000 m^3/s^3 for winter: December, January, and February.

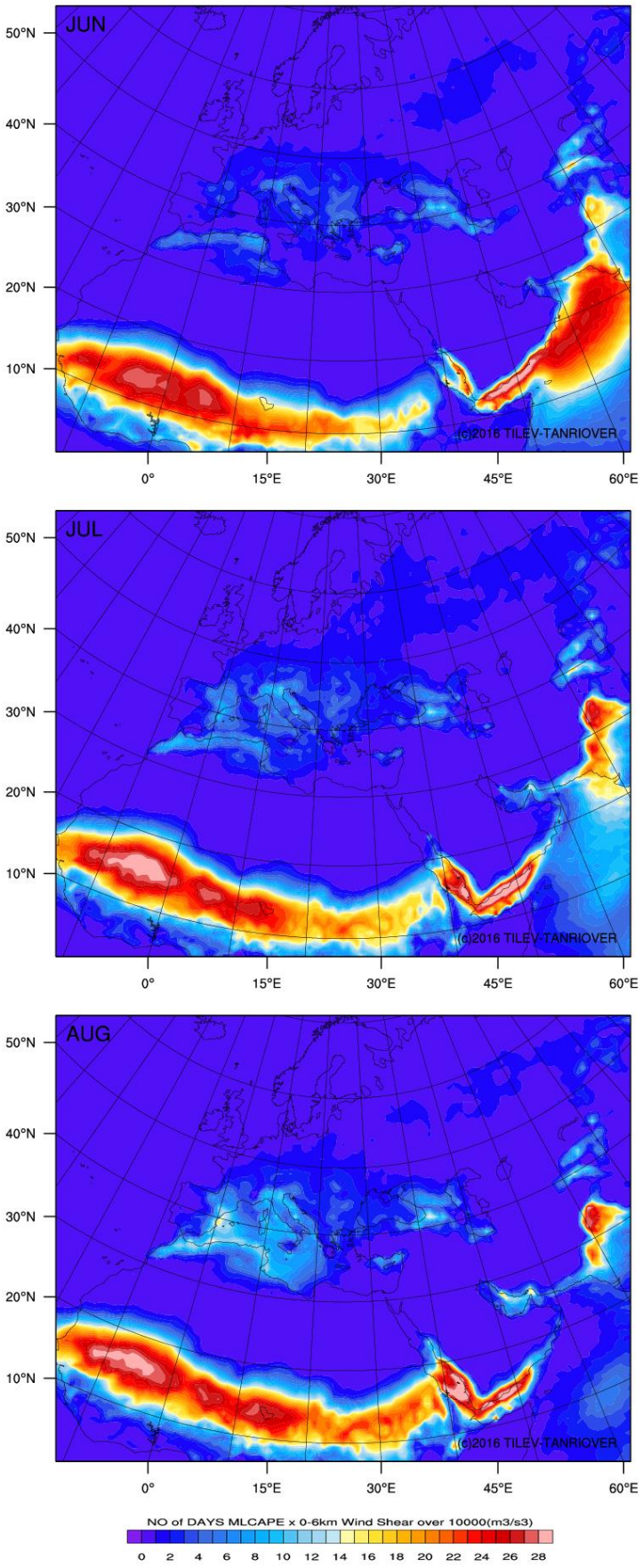

Figure B.3 : Mean number of days with MLCAPE × 0–6 km wind shear values over 10000 m^3/s^3 for summer: June, July, and August.

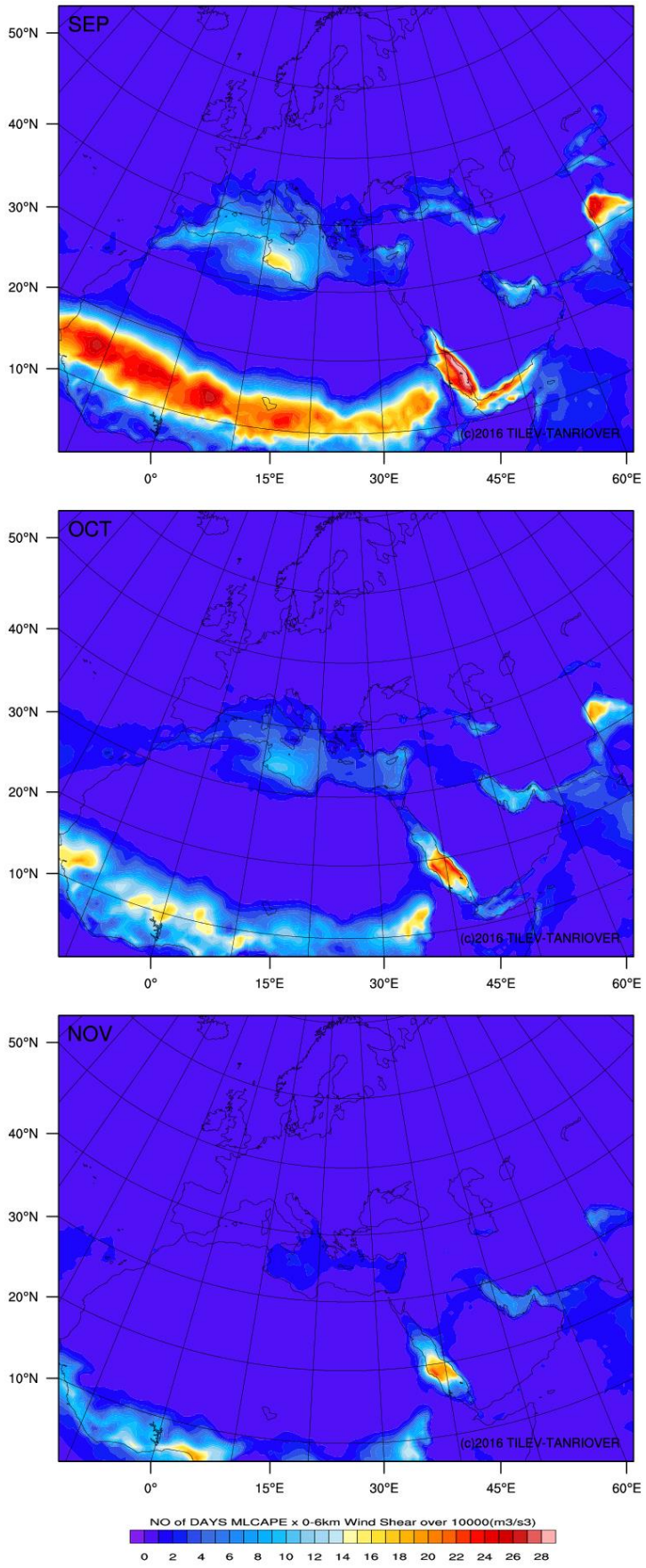

Figure B.4 : Mean number of days with MLCAPE × 0–6 km wind shear values over 10000 m^3/s^3 for autumn: September, October, and November.

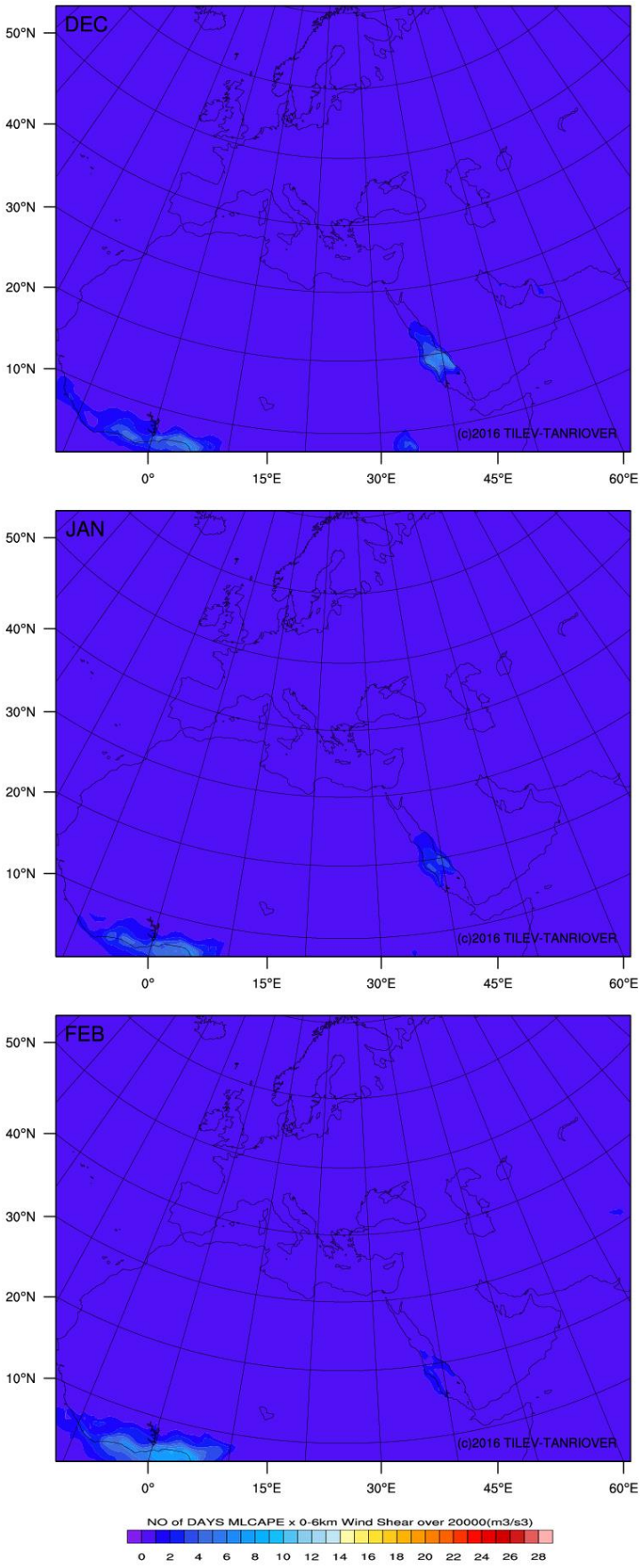

Figure B.5 : Mean number of days with MLCAPE × 0–6 km wind shear values over 20000 m^3/s^3 for winter: December, January, and February.

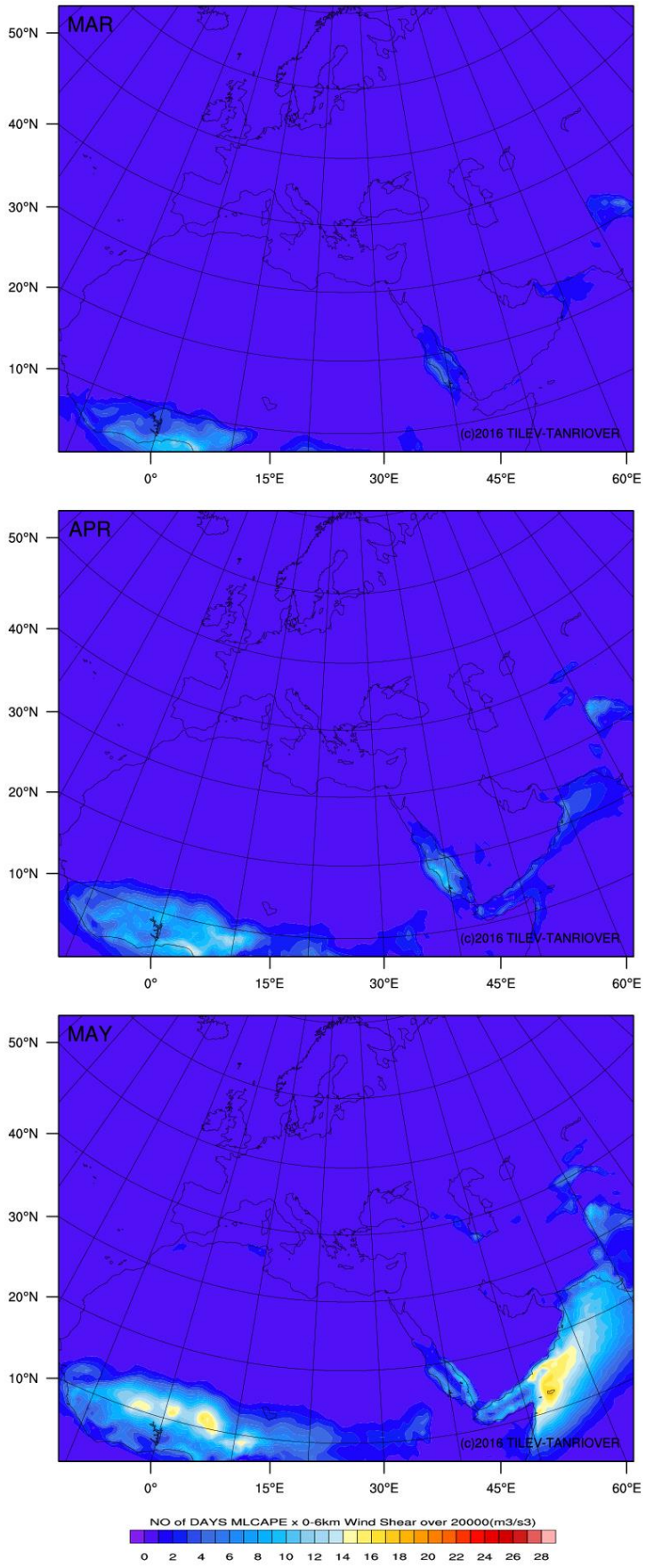

Figure B.6 : Mean number of days with MLCAPE × 0–6 km wind shear values over 20000 m^3/s^3 for spring: March, April, and May.

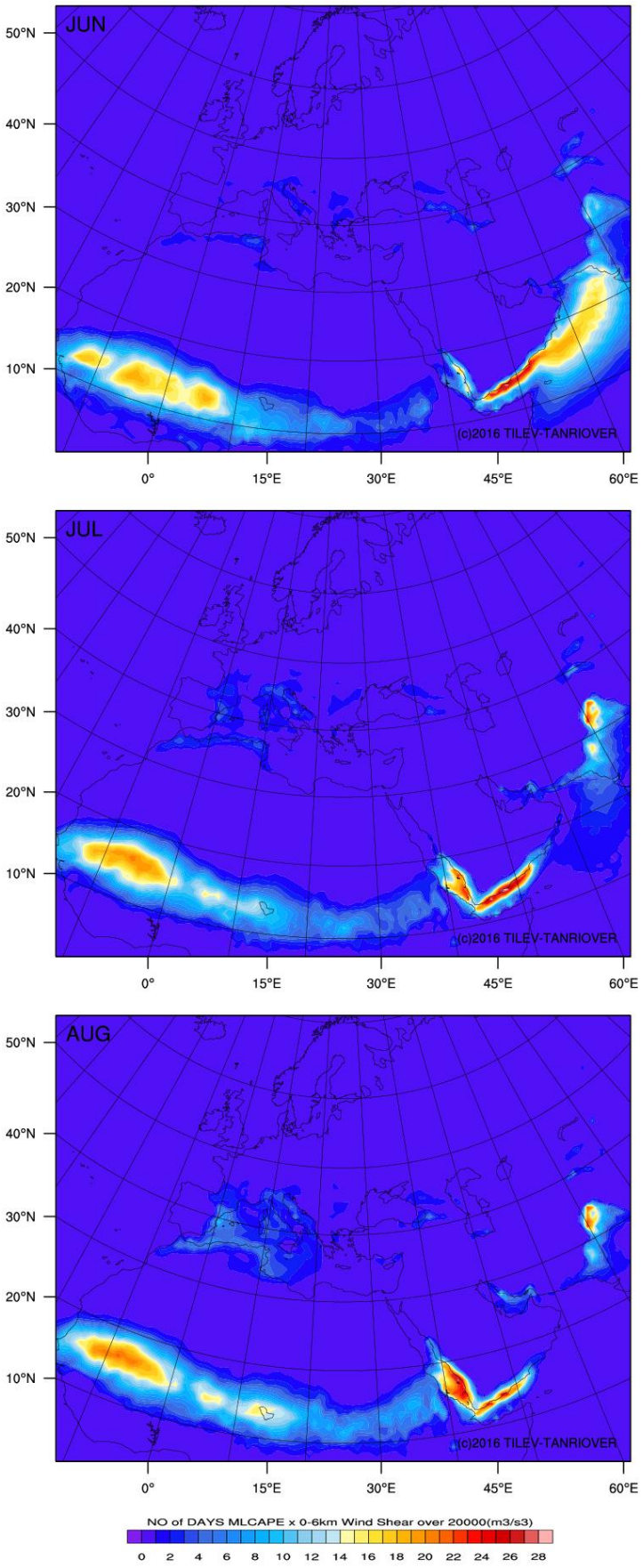

Figure B.7 : Mean number of days with MLCAPE × 0–6 km wind shear values over 20000 m^3/s^3 for summer: June, July, and August.

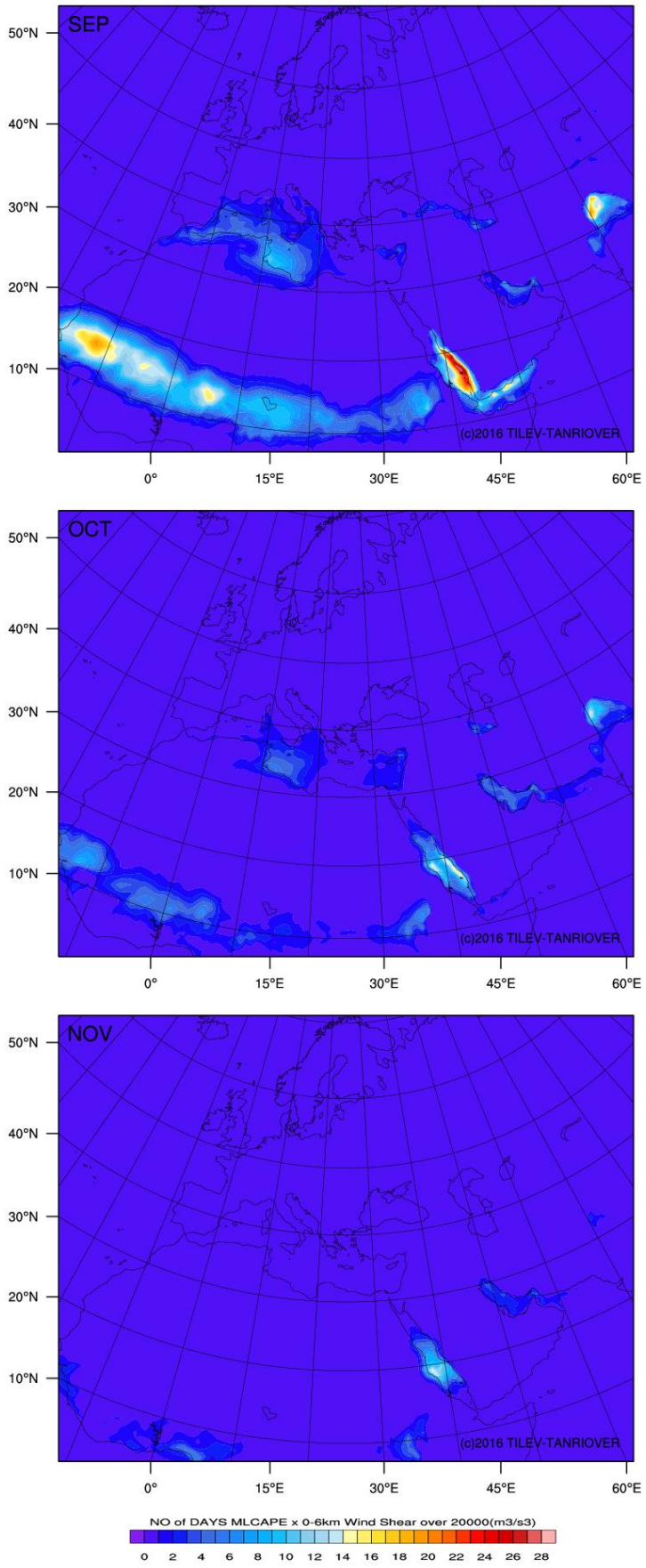

Figure B.8 : Mean number of days with MLCAPE × 0–6 km wind shear values over 20000 m^3/s^3 for autumn: September, October, and November.

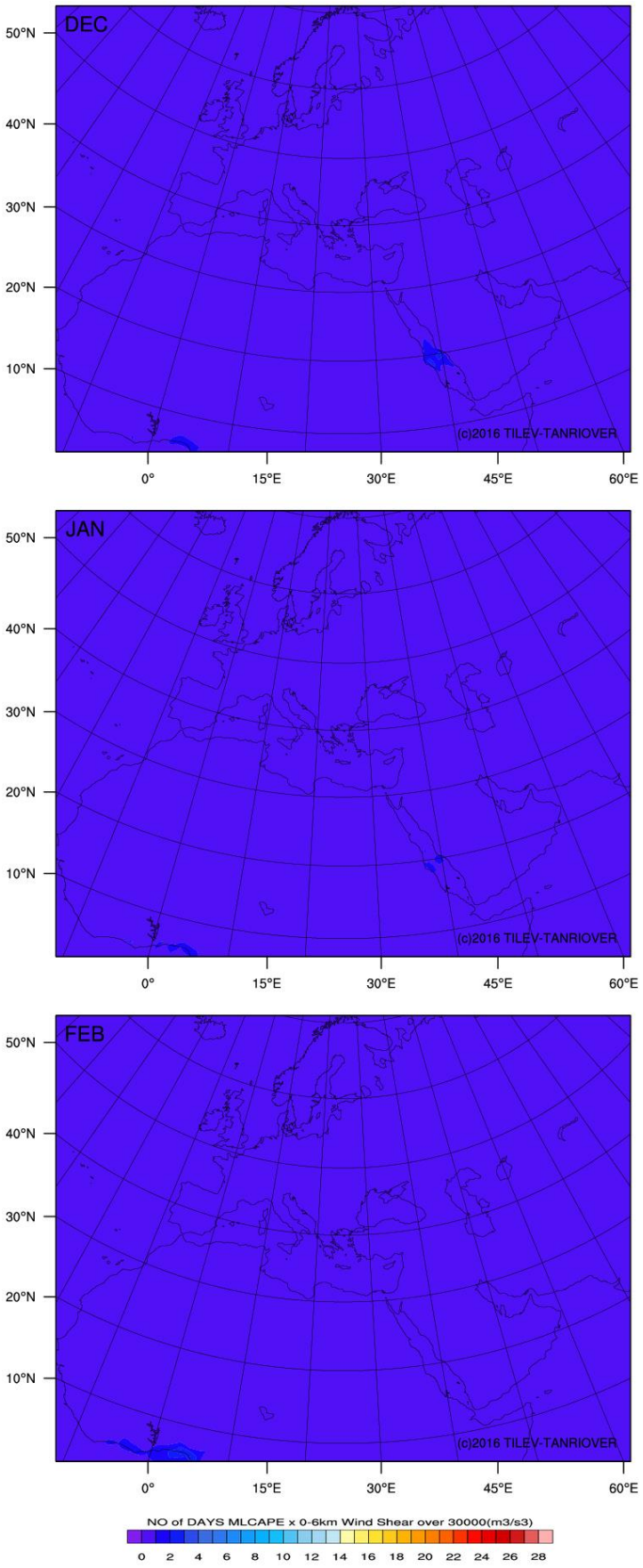

Figure B.9 : Mean number of days with MLCAPE × 0–6 km wind shear values over 30000 m^3/s^3 for winter: December, January, and February.

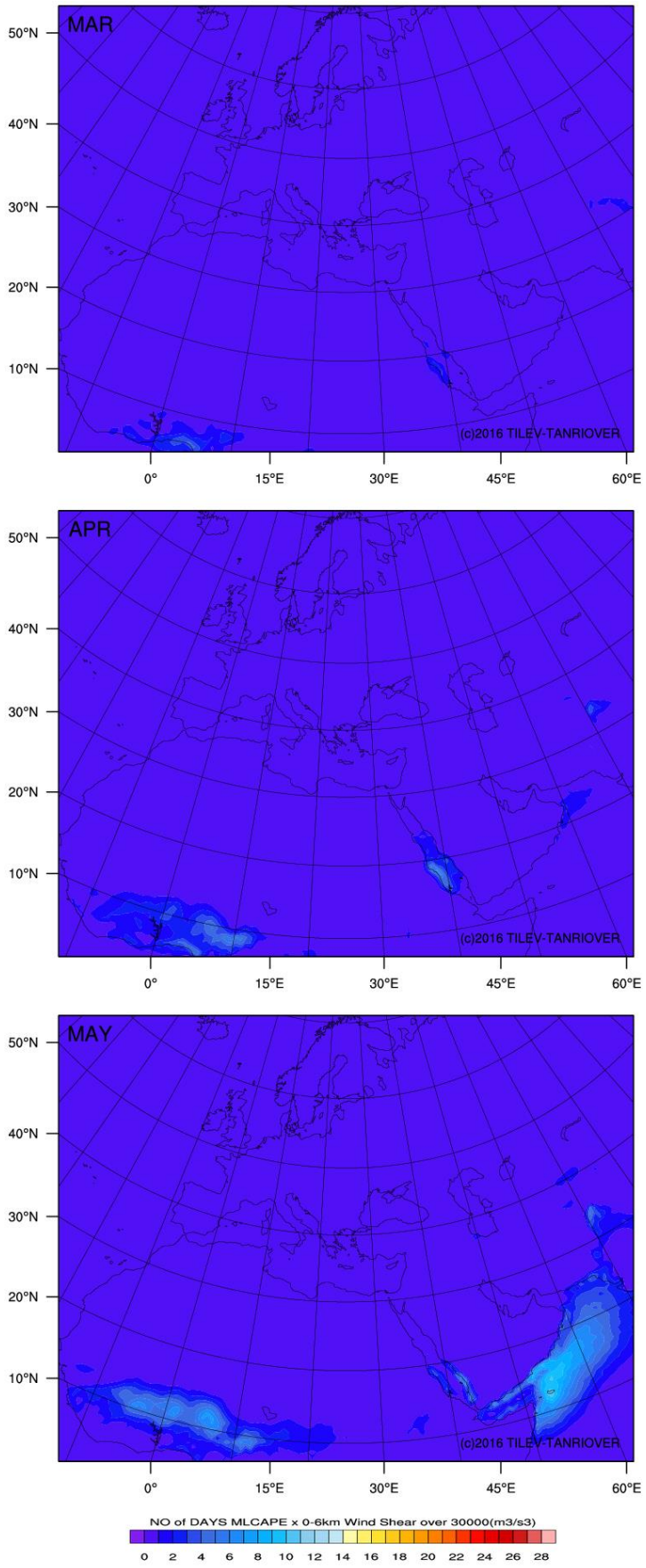

Figure B.10 : Mean number of days with MLCAPE × 0–6 km wind shear values over 30000 m^3/s^3 for spring: March, April, and May.

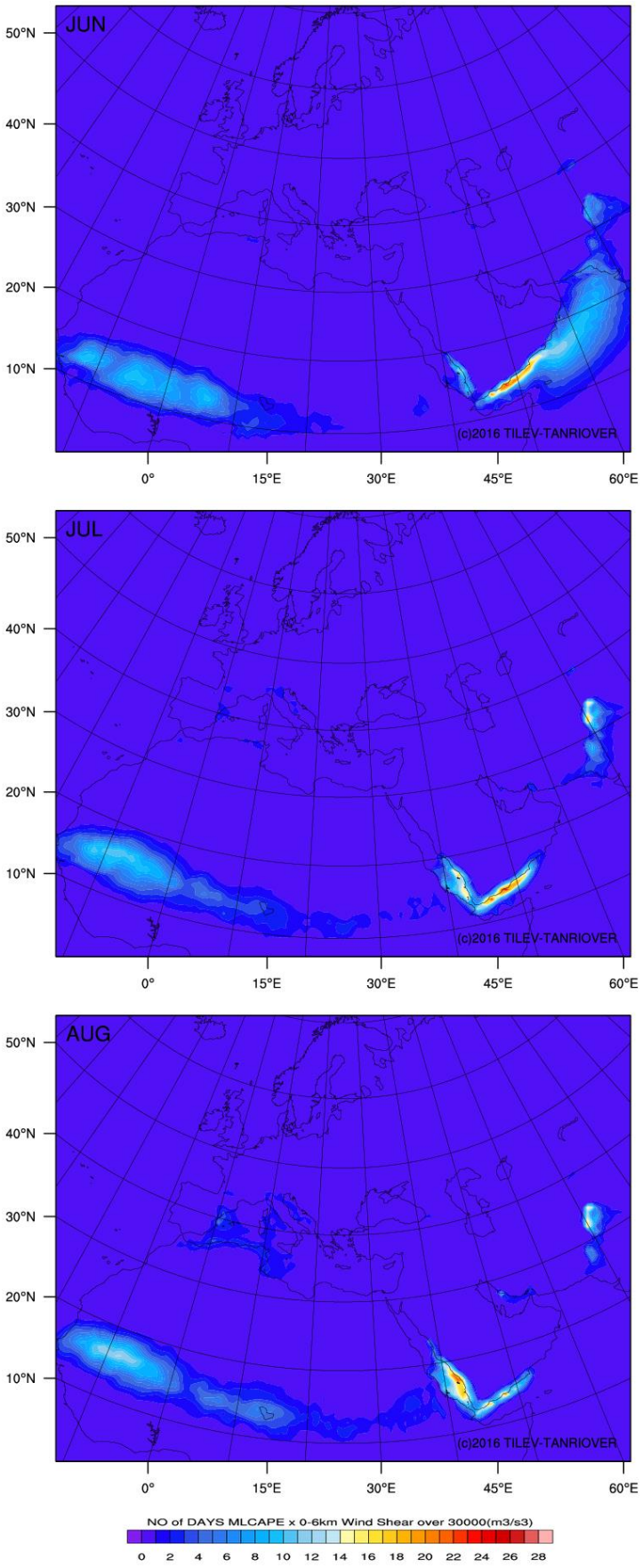

Figure B.11 : Mean number of days with MLCAPE × 0–6 km wind shear values over 30000 m^3/s^3 for summer: June, July, and August.

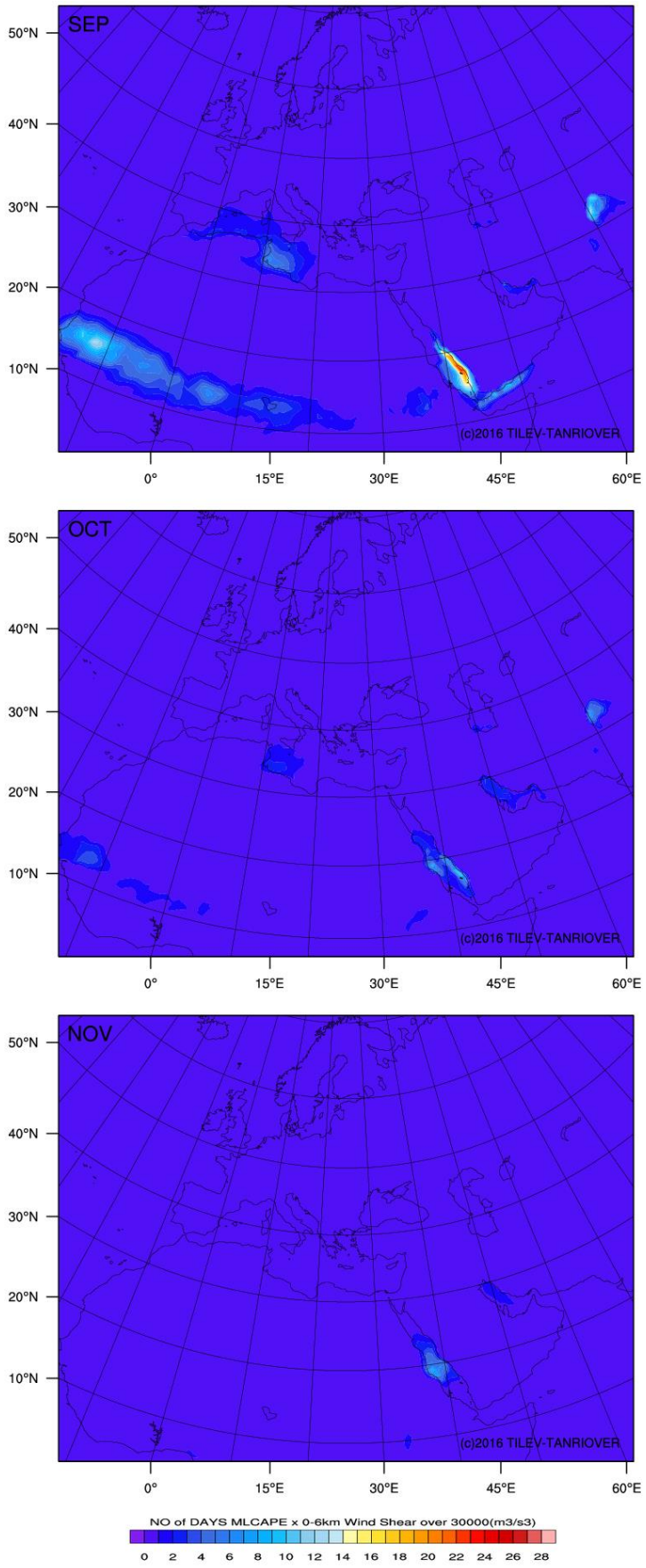

Figure B.12 : Mean number of days with MLCAPE × 0–6 km wind shear values over 30000 m^3/s^3 for autumn: September, October, and November

CURRICULUM VITAE

Name Surname **:** Şeyda TİLEV TANRIÖVER

Place and Date of Birth **:** Kayseri, 1981

E-Mail **:** seydatilev@gmail.com
tanriovers@itu.edu.tr
seyda.tanriover@adpoly.ac.ae

EDUCATION:

- **B.Sc.** **:** 2005, İstanbul Technical University, Faculty of Aeronautics and Astronautics, Meteorological Engineering, GPA: 3.39/4.00 GPA Ranking: 2nd within graduates of 2005
- **M.Sc.** **:** 2009, İstanbul Technical University, Institute of Informatics, Satellite Communication and Remote Sensing Program, GPA: 3.75/4.00

PROFESSIONAL EXPERIENCE AND REWARDS:

- 2015-Cont.: Lecturer, Abu Dhabi Polytechnic, Meteorology Department
- 2014-2015: Academic Visitor, The University of Manchester, UK, School of Earth, Atmospheric and Environmental Sciences
- 2005-2015: Research Assistant, İstanbul Technical University

PUBLICATIONS, PRESENTATIONS AND PATENTS ON THE THESIS:

- **Tilev-Tanriover, Ş.**, Kahraman, A., Kadioglu, M., and Schultz, D.M. (2015), Lightning fatalities and injuries in Turkey, *Nat. Hazards Earth Syst. Sci.*, 3, 1889-1914.

- Kahraman A., **Tilev-Tanriover Ş.**, Kadioğlu M., Schultz D. M. and Markowski P. M. (2014). Severe hail climatology of Turkey, *Monthly Weather Review*, 144, 337–346.
- **Tilev-Tanriover, Ş.**, Schultz, D. M., and Kadioğlu, M. (2015), Climatology of severe convective storm environments from ERA-interim. 8th European Conference on Severe Storms (ECSS), 14-18 September 2015, Wiener Neustadt, Austria.
- **Tilev-Tanriover, Ş.**, Antonescu, B. (2015), Comparison of ERA-interim reanalysis-derived proxy soundings with Collocated Radiosonde Observations. 8th European Conference on Severe Storms (ECSS), 14-18 September 2015, Wiener Neustadt, Austria.
- Kadioglu, M., Coşkun, E., **Tilev Tanriover, S.**, Kahraman, A. (2014), Severe Non-tornadic Winds in Turkey. 9th EGU Alexander von Humboldt International Conference on High Impact Natural Hazards Related to the Euro-Mediterranean Region, Istanbul, Turkey.
- **Tilev Tanriover, S.**, Kahraman, A. (2013), Lightning-related Fatalities and Injuries in Turkey. European Conference of Severe Storms, Helsinki, Finland.

OTHER PUBLICATIONS, PRESENTATIONS AND PATENTS

- **Tilev-Tanriover, Ş.** and Kahraman, A. (2015), Saharan dust transport by Mediterranean cyclones causing mud rain in Istanbul. *Weather*, 70: 145–150. doi: 10.1002/wea.2472
- **Tilev-Tanriover, S.**, Kahraman, A. (2014) Impact of Turkish Ground-based GPS-PW Data Assimilation on Regional Forecast: 8-9 March 2011 Heavy Snow Case. *Atmospheric Science Letters*, Volume: 15, Issue: 3, pp 159-165. doi: 10.1002/asl2.482 (available at http://onlinelibrary.wiley.com/doi/10.1002/asl2.482/full
- **Tilev Tanriover, S.**, Kahraman, A., Incecik, S., Deniz, A., Toros, H., Celebi, H. M., Ozturk, A., and Sezen, I. (2014) Meteorological modeling of the PM10 episode in the creek valley of Golden Horn Harbour, Istanbul under very stable conditions for November 6-9, 2010. A*ir Pollution Modeling and its applications XXII*, NATO Science for Peace and Security Series C: Environmental Security, pp 685-692. doi: 10.1007/978-94-007-5577-2__117
- Barutcu, B., **Tilev Tanriover, S.**, Sakarya, S., Incecik, S., Sayinta, F. M, Caliskan, E., Kahraman, A., Aksoy, B., Kahya, C., Topcu, S. (2015) Improving WRF GHI Forecasts with Model Output Statistics. *Progress in Clean Energy*, Volume 1, pp 291-299. doi: 10.1007/978-3-319-16709-1_20
- Öztaner, Y. B., Kahraman, A., Çalişkan, E., **Tilev Tanrıöver, Ş.**, Kahya, C., Aksoy, B., İncecik, S., Topcu, S., Aslan, Z., Barutçu, B., Sezen, İ., Sakarya, S., Deniz, A. (2014) Açık Gökyüzü Şartlarında Güneş Radyasyonun WRF Modeli ile Kısa Vadeli Tahmininde Aerosol Etkisinin Değerlendirilmesi. *Hava Kirliliği Araştırmaları Dergisi,* Cilt 3, Sayı 1, Sayfa 2-11.
- İncecik S., B. Barutcu, S. Sakarya, S. Topcu, B. Aksoy, M. Sayinta, C. Kahya, **S. Tilev**, E. Caliskan, A. Kahraman, Z. Aslan (2015) A Neural Network Post-

Processing Approach for Improving WRF Global Horizontal Solar Radiation Forecasts in Turkey. AOGS 2015, Singapore.

- İncecik S., **Tilev-Tanriover, S.**, Kahraman, A., Topcu, S., Caliskan, E., Aksoy, B., Kahya, C. (2014) Evaluation of the Global Horizontal Irradiance Forecasts Based on WRF-ARW Mesoscale Meteorological Model in Turkey. AOGS, Sapporo, Japan.
- Barutcu, B., **Tilev Tanriover, S.**, Sakarya, S., Incecik, S., Sayinta, F. M. , Caliskan, E., Kahraman, A. Aksoy, B., Kahya, C., Topcu, S. (2014) Improving WRF GHI Forecasts with Model Output Statistics, International Conference on Clean Energy 2014, Istanbul, Turkey.
- Kadıoglu, M., Cakir, S., **Tilev Tanriover, S.**, Kahraman, A., 2014. Wind analyses for European side of Istanbul. İstanbul Teknik Üniversitesi Rektörlüğü Döner Sermaye İşletmeleri Projesi
- Kadıoglu, M., Cakir, S., **Tilev Tanriover, S.**, (2013). Meteorological and Climatological Analyses of Istanbul 3. Airport Region. İstanbul Teknik Üniversitesi Rektörlüğü Döner Sermaye İşletmeleri Projesi
- **Tilev Tanriover, S.**, Kahraman, A., Çalışkan, E., Incecik, S., Kahya, C., Topçu, S., Aksoy, B. (2013) The performance analysis of WRF on GHI prediction in two different regions of Turkey. UTES 13, 9. Ulusal Temiz Enerji Sempozyumu Bildiriler Kitabı, pp 436-449.
- Öztaner, B., Kahraman, A., Çalışkan, E., **Tilev Tanrıöver, Ş.**, Kahya, C., Aksoy, B., İncecik, S., Topçu, S., Aaslan, Z., Barutçu, B., Sezen, S., Sakarya, S., Deniz, A. (2013) WRF modeli ile güneş radyasyonu öngörüsünde aerosol etkisinin değerlendirilmesi. 5. Hava Kirliliği ve Kontrolü Sempozyumu, Eskişehir, Türkiye.
- Acar, M., Ballı, C., Tan, E., Karan, H., Aksoy, A., Çağlar, F. Önol, B., Kahraman, A., **Tilev Tanrıöver, Ş.**, Demir, F. and Ünal, Y. (2013) Lagrangian model forecast of the transport and dispersion of toxic gases/particles over İstanbul. 6th Atmospheric Science Symposium - ATMOS 2013, İstanbul, Türkiye.
- **Tilev Tanrıöver, Ş.**, Kahraman, A. (2013) Improvement of forecast skills with cycling mode 3DVAR assimilation: evolution of a mediterranean cyclone. 6th Atmospheric Science Symposium - ATMOS 2013, İstanbul, Türkiye.
- **Tilev Tanriover, S.**, Kahraman, A. (2013) Heavy Rain Forecast Improvement with Radar Data Assimilation. European Conference of Severe Storms, Helsinki, Finland.
- **Tilev-Tanriover S.**, Kahraman, A., Caliskan, E., Incecik, S., Aksoy, B., Kahya, C., Topcu, S. (2013) The Performance Analysis of the WRF Model GHI Forecasts Using five Different Configurations Session 4 of the WIRE Status Workshop, Oct. 10th 2013 Budapest, Hungary.
- **Tilev Tanriover, S.**, Kahraman, A., Incecik, S., Deniz, A., Toros, H., Celebi, H. M., Ozturk, A., and Sezen, I (2012) Meteorological Modeling Of The Pm10 Episode In The Creek Valley Of Golden Horn Harbour, Istanbul Under Very Stable Conditions For November 6-9, 2010. 32st NATO/SPS International Technical Meeting on Air Pollution Modelling and its Application, Utrecht, Netherlands.

- **Tilev Tanriover, S.**, Kahraman, A., Kadioglu, M. (2012) A Case Study On Cycling Mode 3D-Var Assimilation of GPS-PW Data into a Mesoscale Atmospheric Model. AOGS - AGU (WPGM) Joint Assembly, Sentosa, Singapore.
- Kahraman A., **Tilev Tanriover S.**, Kadioglu M. (2011) Severe Hail Climatology of Turkey, 6th European Conference on Severe Storms (ECSS) Palma de Mallorca, Spain.
- **Tilev Tanriover S.**, Kahraman A., and Kadioglu M., (2011) Assimilation of Turkish Ground-based GPS Network Data with WRF 3DVAR: A case study of a heavy snow event in March 2011, 11th EMS Annual Meeting, Berlin, Germany.
- Kahraman A., **Tilev Tanriover S.**, Incecik S., Deniz A., Toros H., Celebi H. M., Ozturk A., and Sezen I. (2011) Analyses and Forecasting of Urban PM10 Air Pollution Episode in Very Stable Conditions in Istanbul, Turkey on 6-9 November 2010, 11th EMS Annual Meeting, Berlin, Germany.
- Efe B., Mentes S. S., Akcan D., Tan E., Unal Y.S., Onol B., **Tanriover S.**, Rustemoglu S., Anbarci K., Oner E., and Incecik S. (2011) Preliminary Results of Short Term Wind Energy Prediction System (SWEPS) for The Northwestern Region of Turkey, 11th EMS Annual Meeting, Berlin, Germany.
- Kahraman A., **Tanriover S.** (2011), Forecast Skills of ARW vs GFS for two cases over Turkey. WRF in the Middle East Worskhop, Nicosia, Southern Cyprus.
- Akcan, D., Efe, B., Menteş, S., Unal, Y., TAN, E., Onol, B., Incecik, S., **Tanriover, S.**, Barutcu, B., Anbarcı, K., Oner, E. (2011) Preliminary results of short term wind energy prediction system (sweps) for Soma, Manisa in Turkey, EGU General Assembly, Vienna, Austria.
- Kahraman A., **Tanriover, S.**, (2010), Heavy rain over Marmara region due to a cut-off cyclone. EMS Annual Meeting, Zurich, Switzerland.
- **Tanriover, S.**, Kahraman A., (2010), Saharan dust transport by Mediterranean cyclones causing dust rain in Istanbul. EMS Annual Meeting, Zurich, Switzerland.
- Kahraman A., **Tanriover, S.** (2009), Sensitivity and predictability analysis of Advanced Research WRF Model (WRF-ARW) in Eastern Mediterranean Region. EGU General Assembly, Vienna, Austria
- **Tanriover, S.**, Kadıoğlu, M., (2009), Assimilation of GPS-RO Atmospheric Profile Data: A Case Study of A Mediterranean Low Pressure System. EGU General Assembly, Vienna, Austria.